AD-A173 511 FUNDAMENTAL STUDIES AND DEVICE DEVELOPMENT IN BETA SILICON CARBIDE(U) NORTH CAROLINA STATE UNIV AT RALEIGH DEPT OF MATERIALS ENGINEERING R F DAVIS 31 JAN 85 1/2

UNCLASSIFIED 243-043-000 N00014-82-K-0182 F/G 20/12 NL

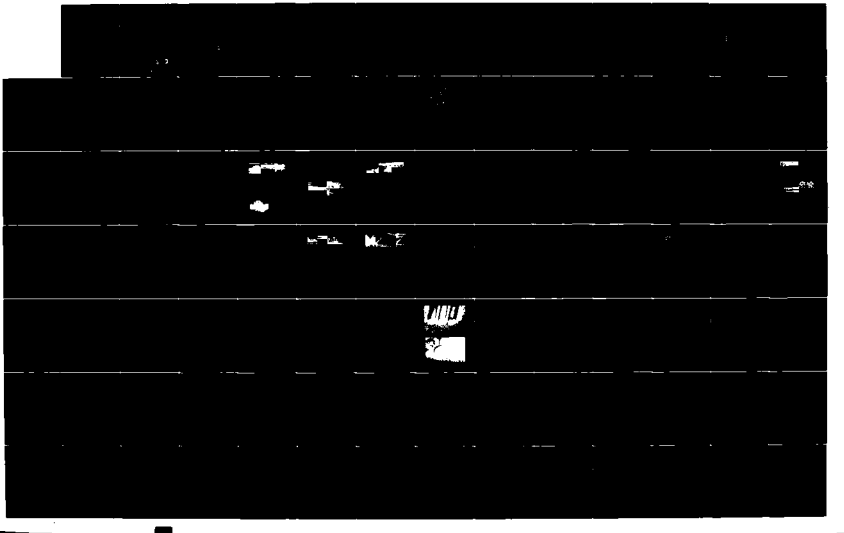

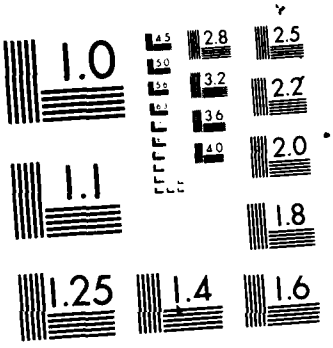

(2)

Annual Letter Report

on

# FUNDAMENTAL STUDIES AND DEVICE DEVELOPMENT IN BETA SILICON CARBIDE

Supported by ONR Under Contract N00014-82-K-0182 P0005

For the Period February 1, 1985 - January 31, 1986

Annual Letter Report

on

# FUNDAMENTAL STUDIES AND DEVICE DEVELOPMENT IN BETA SILICON CARBIDE

Supported by ONR Under Contract N00014-82-K-0182 P0005

For the Period February 1, 1985 - January 31, 1986

SECURITY CLASSIFICATION OF THIS PAGE (When Data Entered)

| REPORT DOCUMENTATION PAGE | | READ INSTRUCTIONS BEFORE COMPLETING FORM |
|---|---|---|
| 1. REPORT NUMBER<br>243-043-008 | 2. GOVT ACCESSION NO.<br>ADA173511 | 3. RECIPIENT'S CATALOG NUMBER |
| 4. TITLE (and Subtitle)<br>Fundamental Studies and Device Development in Beta Silicon Carbide | | 5. TYPE OF REPORT & PERIOD COVERED<br>Annual Letter<br>2/1/85 - 1/31/86<br>6. PERFORMING ORG. REPORT NUMBER |
| 7. AUTHOR(s)<br>Robert F. Davis | | 8. CONTRACT OR GRANT NUMBER(s)<br>N00014-82-K-0182 P0005 |
| 9. PERFORMING ORGANIZATION NAME AND ADDRESS<br>North Carolina State University<br>Dept. of Materials Engineering<br>Box 7907, Raleigh, NC 27695-7907 | | 10. PROGRAM ELEMENT, PROJECT, TASK AREA & WORK UNIT NUMBERS<br>PE 61153N<br>RR 021-02-03<br>NR 243-027 |
| 11. CONTROLLING OFFICE NAME AND ADDRESS<br>ONR-414<br>Arlington, VA 22217 | | 12. REPORT DATE<br>January 31, 1985<br>13. NUMBER OF PAGES<br>58 |
| 14. MONITORING AGENCY NAME & ADDRESS(if different from Controlling Office) | | 15. SECURITY CLASS. (of this report)<br>Unclassified<br>15a. DECLASSIFICATION/DOWNGRADING SCHEDULE |

16. DISTRIBUTION STATEMENT (of this Report)

Approved for public release; distribution unlimited

17. DISTRIBUTION STATEMENT (of the abstract entered in Block 20, if different from Report)

18. SUPPLEMENTARY NOTES

ONR Scientific Officer; Tel: (202) 696-4218

19. KEY WORDS (Continue on reverse side if necessary and identify by block number)

Silicon carbide
chemical vapor deposition
electronic materials
in situ doping
dry etching
ion implantation
electron microscopy
secondary ion mass spectroscopy
electrical properties
Rutherford Back-scattering
oxidation
p-n junction

20. ABSTRACT (Continue on reverse side if necessary and identify by block number)

The research of this reporting period has involved the growth of large area thin films of β-SiC and an investigation regarding the improvement of thickness uniformity of the films in a given run. Additional research, described in pre-prints derived from recent presentations and included in this document, include ion implantation, amorphization, rapid thermal annealing, electrical properties, oxidation, reactive ion etching and device fabrication. Finally, the highlights of and program and abstracts from the 1985 SiC Conference are included in this document.

DD FORM 1 JAN 73 1473 EDITION OF 1 NOV 65 IS OBSOLETE
S/N 0102-014-6601

Enclosure (1)

SECURITY CLASSIFICATION OF THIS PAGE (When Data Entered)

TABLE OF CONTENTS

# I. INTRODUCTION

Silicon carbide is the only compound species that exists in the solid state in the Si-C system and can occur in the cubic (C), hexagonal (H) or rhombohedral (R) structures. It is also classified as existing in the beta and alpha modifications. The beta, or cubic, form crystallizes in the zincblende or sphalerite structure; whereas, a large number (approximately 140) of the alpha occur in the hexagonal or rhombohedral forms known as polytypes.

Because of the emerging need for high temperature, high frequency and high power electronic devices, blue L.E.D.'s, Schottky diodes, U. V. radiation detectors, high temperature photocells and heterojunction devices, silicon carbide is being examined throughout the world for employment as a candidate material in these specialized applications. The electron Hall mobility of high purity updoped β-SiC has been postulated from theoretical calculations to be greater than that of the α-forms over the temperature range of 300-1000K because of the smaller amount of phonon scattering in the cubic material. The energy gap is also less in the β-form (2.3 eV) compared to the α-forms (e.g., 6H = 2.86 eV). Thus, the β-form is now considered more desirable for electronic device applications, and therefore, improvements in the growth and the characterization if thin films of this material and device development from this material constitute principal and ongoing objectives of this research program.

The research of this reporting period has involved the systematic study of various CVD equipment parameters and their effect on growth and quality of the β-SiC films, growth of large area films, amorphization and recrystallization process as a result of dopant ion implantation and rapid thermal annealing, respectively, wet and dry oxidation and dry etching of these β-SiC films. The presentation of this material in this report will, for

the most part, deviate from that used previously. With the exception of the description of the growth studies and the report of the National SiC Review Meeting (see Appendix I), the remaining subjects will be in the form of preprints of papers presented at (1) the November, 1985 Materials Research Society meeting in Boston on the subjects of ion implantation, amorphization, rapid thermal annealing, recrystallization, electrical properties and oxidation and (2) the October meeting of the American Vacuum Society on the topic of reactive ion etching. These papers not only summarize the work for 1985 in precise and concise form but also provide to the reader early access to these forthcoming papers.

# II. BETA SILICON CARBIDE GROWTH RESEARCH

## A. Introduction

Considerable effort has been expended during the latter part of this year to improve the quality of the β-SiC grown on Si(100) wafers. The primary objectives of this research have been the improvement of the thickness uniformity across each film and among the films in a given run and the achievement of higher resistivity films which have similar values of this parameter in a given run.

At the outset of this study it was reasoned that three factors contributed to both the nonuniformity in thickness and the variation in electrical properties among the films: (1) nonuniform magnetic field which caused the various samples to be at different temperatures during a growth run, (2) nonuniform gas flow and (3) poor and nonuniform seating of the Si wafers in the sample locations in the susceptor.

The following paragraphs detail the experimental procedures and the results of this work regarding the solutions to the above problems including the alteration of the susceptor to allow growth on larger substrates.

## B. Susceptor Rotation and its Effect on the Film Character

### 1. General

Since the rf coil is wound such as to be as uniform as possible and is situated such that the susceptor resides in the center of the coil, both in terms of radial and vertical positioning, the only remaining alteration in the process is the rotation of the susceptor. Similarly, the gas distribution tube and dispersing unit are located in the center of the growth chamber, directly over the susceptor and allow an even radial flow into the chamber. Thus, to improve the uniformity of the gas - silicon wafer reaction, rotation of the susceptor is again the obvious next step. The following subsections describe

the effects on film character of this additional procedure.

2. Occurrence of a Second Phase

The results of this research support the findings of a much more abbreviated study regarding the rotation of the susceptor in that the introduction of this procedure causes an increase in deposition of small black particles. These particles have been found to be either SiC or C, depending on the Si/C ratio in the gas phase. They are believed to be homogeneously nucleated in the gas phase. Furthermore, they are inhomogeneously distributed of the surface of the films, with a majority occurring in the upper half of each sample.

Since the Si/C ratio remains the same as that employed using an unrotated susceptor (wherein no black particles occur), the occurrence of these particles indicates that rotation causes changes in the gas transport process. The most likely areas of change are in the gas flow pattern and boundary thickness which, in turn, cause a change in the Si/C ratio near the substrate surface.

In order to eliminate these black particles and still maintain the desired susceptor rotation, the obvious experimental procedure of altering the Si/C ratio was employed. It was subsequently found that increasing the ratio by ≅5% markedly reduced the concentration of this unwanted phase. In most samples, they could be eliminated completely.

It should also be noted that the above description of the elimination of the second phase was achieved using a relatively new SiC-coated susceptor and a used tank of $C_2H_4$. It has also been found that as SiC is continually coated on the susceptor, the particles which form apparently act to disturb the flow or remove extra Si from the gas stream or assist nucleation of the black particles which subsequently fall on the film. In any event, there is always

an increase in this second phase which can be correlated with the age of the susceptor. Furthermore, the introduction of a new cylinder of $C_2H_4$ always causes an increase in these particles for seven-to-ten runs. The exact reason for this is unknown.

3. Surface Smoothness

Rotation of the susceptor invariably improves the smoothness of the sample surface. Pits of all dimensions are greatly reduced in number for essentially all samples. A typical surface of a rather thick film grown over an 8 hour period is shown in Figure 1.

4. Thickness uniformity in a Given Growth Run

The principal problem and cause of the nonuniformity of thickness in the present growth chamber is the unequal heating which the collection of Si wafers receive as a result of variation in the excellence of the contact between a given wafer and the susceptor. If a wafer fails to make good contact, the wafer will be nonuniform; if the contact interface varies between wafers so will the thickness.

We have learned from this study that (1) all wafers must be carefully and completely situated in the susceptor depressions. Furthermore, the contact between the bottom of each depression and the back of each wafer must e ery good. Otherwise, a pocket of gas is trapped at this interface which will partially dislodge the wafer during initial evacuation of the chamber. In this regard, the system must be very slowly evacuated; since a rush of gas by the wafer faces can also establish turbulence which pulls the wafer partially (sometimes completely) out of the susceptor depressions.

The results shown in Table I for samples which have been very carefully placed in the susceptor depressions, for which slow evacuation was used and the susceptor rotated at 5 rpm illustrate that very uniform samples can be

obtained. The mean values of uniformity and the deviation of the sample uniformity for the three runs noted in Table I are presented in Table II.

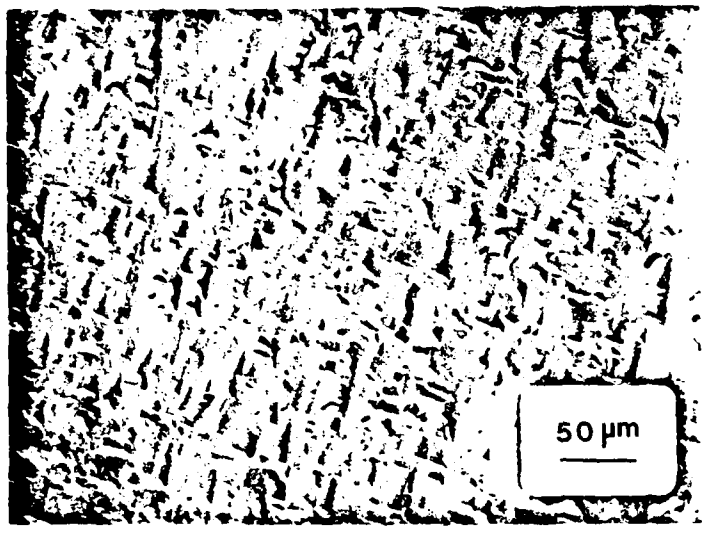


Figure 1. Optical micrograph of the final surface of a 16.4 µm thick undoped β-SiC film (sample #850513 (3)) produced using the standard growth procedure coupled with a 5 rpm rotation of the susceptor. This surface character is typical of films grown under these conditions.

Table I. Film Thickness and Resistivity Data for Growth Runs 851030, 851101 and 850620.

| RUN # | ROTATION (RPM) | SAMPLE # | FILM THICKNESS (μm) | RESISTIVITY (Ω-cm) |
|---|---|---|---|---|
| | | 1 | 15.6 | 0.67 |
| | | 2 | 16.1 | 0.88 |
| | | 3 | 14.5 | 0.90 |
| 851030 | 2.5 | 4 | 12.5 | 0.58 |
| | | 5 | 14.3 | 0.61 |
| | | 6 | 15.9 | 0.67 |
| | | 7 | 19.1 | 0.66 |
| | | 1 | 18.2 | 0.63 |
| | | 2 | 17.2 | 0.80 |
| | | 3 | 13.6 | 0.46 |
| 851101 | 2.5 | 4 | 14.5 | 0.73 |
| | | 5 | 14.1 | 0.69 |
| | | 6 | 14.1 | 0.60 |
| | | 7 | 16.3 | 0.62 |
| | | 1 | 11.4 | 0.34 |
| | | 2 | 6.1 | 0.51 |
| | | 3 | 8.2 | 0.63 |
| 850620 | 0 | 4 | 12.0 | 0.35 |
| | | 5 | 20.0 | 0.57 |
| | | 6 | 21.4 | 0.42 |
| | | 7 | 16.8 | 0.28 |

Table II. Statistical Data for the Thickness and Resistivity of the several SiC Films grown in the Runs noted in Table I.

| RUN # | FILM THICKNESS (μm) | | RESISTIVITY (Ω-cm) | |
|---|---|---|---|---|
| | Mean | Deviation | Mean | Deviation |
| 851030 | 15.4 | 1.9 | 0.71 | 0.12 |
| 851101 | 15.4 | 1.7 | 0.64 | 0.11 |
| 850620 | 13.8 | 5.5 | 0.44 | 0.12 |

The important point which is deduced from this data is that, although such good uniformity as that obtained for runs 851030 and 851101 is not achieved in every growth, it is never achieved without susceptor rotation. In addition, the bottom of the depressions in all future susceptors must be machined very flat and the intitial evacuation must be very slow in order to maintain the

wafer/susceptor interface.

C. In situ Doping of N using $N_2$ as the Dopant Source

1. Background

Amonia ($NH_3$) was originally employed as the dopant source of N in this program. However, it is difficult to obtain this gas with low concentrations of $O_2$ and other impurities. Furthermore when $NH_3$ is used, a heavy coating occurs on the inner quartz wall of the chamber. In addition, a rough surface morphology my be obtained.

Our initial concentrations of ≅50ppm $N_2$ in highest purity $H_2$ was insufficient to dope the β-SiC films at or above the ≅$10^{17}/cm^3$ minimum detectable level of the ion microprobe. Furthermore, increases in either the conductivity of the n-type carrier concentration were not detected. As such, the $N_2$ concentration in $H_2$ was increased to ≅1% which proved to be appropriate for doping the films. The $N_2$ (in $H_2$) was mixed with the $SiH_4$, $C_2H_4$, and $H_2$ carrier gas prior to its introduction into the growth chamber. Standard 1 atm. growth runs described in earlier reports were used in all cases. The following subsections describe the results of this research.

2. SIMS Data

The amount of introduction of N into the β-SiC films has been analyzed quantitatively as a function of depth using the CAMECA ims-3f ion microprobe. Oxygen was used as the primary ion with a beam size of 250 μm. The operation of this system allows the simultaneous evaluation of the concentrations of several elements; in this study both Si and N were determined. Comparison of the N/Si ratios in samples which had been grown using 1.0, 5.0, 10.0, 30.0, 50.0, 70.0 and 90.0 sccm of the N-in-$H_2$ gas mixture with standard N implanted samples allowed the atomic concentration of this element to be determined for each flow rate. These values were subsequently plotted as a function of the

partial pressure of $N_2$ in the gas stream. The resulting curve, shown in Figure 2, can be used in future studies where a particular N doping level is desired.

3. Theoretical Considerations of N in β-SiC

Using the equilibrium solubility considerations of Rai-Choudhuy and Salkovitz (), the dopa t species, when dissolved but not electrically activated (ionized) in the silicon carbide, is presumed to follow Henry's law for a dilute solute, i.e.,

$$P_D^{1/y} = K_D N_D \tag{1}$$

where $P_D$ is the gas phase partial pressure of the dopant species in equilibrium with the solid; Y is the number of dopant atoms per molecule of the above species; $K_D$ is the Henry's law constant of the dopant in the solid solution, and $N_D$ is the concentration of unionized dopant in the solid solution. The activity coefficient, $_D$, may be defined as follows:

$$\gamma D = \frac{N_D \; K_D}{N_D \; K_D} \tag{2}$$

where $\gamma_D$ is the ratio of the unionized dopant atom concentration at some actual $N_D$ to that at infinite dilution; $N_D$ is the total chemical concentration of the dopant and $K_D$ is a new Henry's law constant for total dopant concentration.

Combining equations (1) and (2), one gets

$$P_D^{1/y} = K_D \gamma_D N_D \tag{3}$$

This last equation predicts that a plot of log $N_D$ vs log $P_D$ should be linear with a slope 1/y, for $N_D$ 1 x $10^{18}$ $cm^{-3}$ at typical epitaxial deposition temperatures. At higher concentrations, where a significant fraction of the donor or acceptor atoms in the solid are ionized, the activity coefficient becomes larger than one.

Although there is some scatter, the data in Figure 2 show an essentially linear relationship between log $N_D$ and log $P_D$ where $P_D$ is the partial pressure

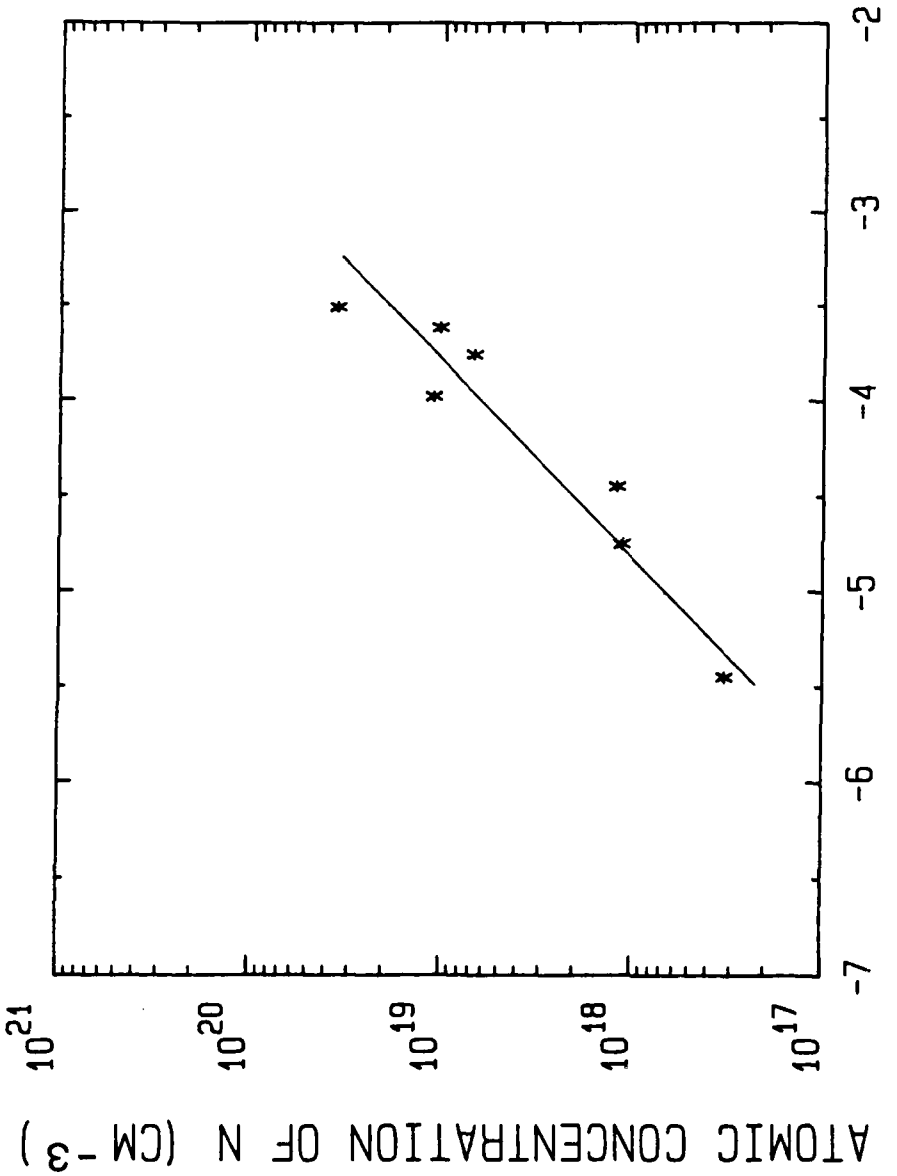


Figure 2. Atomic concentration of N in situ doped (using various flow rates of 1.0% $N_2$ in $H_2$) into β-SiC films vs. the partial pressure of $N_2$ in the input gas stream. The linear curve was obtained using a least squares relationship.

(of $N_2$) in the gas stream. The slope of this line is 0.97; however, equation (3) predicts a slope (=1/y) equal to 0.5 for $N_2$. This implies that N or other species containing one N atom is the actual dopant source for the incorporation of this species into β-SiC. This result is not unexpected even though $N_2$ is difficult to decompose.

4. Advantages in the use of $N_2$

A most important aspect is that $N_2$ can be obtained in much higher purities,including the vapor from above a liquid source, than can $NH_3$. Furthermore, essentially no coating occurred on the inner quartz wall even during an eight hour growth. Finally, the smoothness of the surface is improved to a point where it is essentially that shown in Figure 1 for the pure β-SiC films.

D. Growth of Large Area β-SiC Thin Films

1. Potential Advantages of Large Area Beta SiC Thin Film Growth

(a) Formation of a larger amount of useful material. A single standard growth run at NCSU entails the simultaneous use of up to 8 wafers each having a 1.1 cm diameter and a maximum total area of 7.6 $cm^2$. Since the thickness of the deposited β-SiC film at the very edge of each wafer is less than the remainder of the sample because the Si substrates sit in a depression during growth, this edge region is frequently of little value for characterization. However, in a single substrate having an area equal to or larger than the sum of the smaller wafers, the total edge length and thus loss of useful material is considerably reduced. Thus the growth process becomes more efficient.

(b) Enhanced uniformity of the β-SiC Films. As noted above, the use of the vertical (barrel-type) susceptor makes it necessary to place the 1 cm diameter samples in depressions in this susceptor. Although we have learned that extreme care must be taken in the initial placement of the wafers in

these depressions and in the evacuation of the chamber, for various reasons some of the wafers will become incorrectly situated and thus heated nonuniformly. In the use of large area wafers, "ears" machined into the susceptor hold the wafer(s) flat against the susceptor thus insuring a more uniform heat distribution and deposited films.

(c) Improved process and property characterization data. Improvements in deposition uniformity, as noted in (1), will allow both improved studies of the deposition rate and growth mechanisms as a function of deposition rate as well as more accurate photo-optical and electrical characterization where a uniform thickness and the thickness values are necessary to accurately calculate the desired parameter from the measured data.

In the initial portion of this reporting period, design, fabrication and employment of SiC-coated susceptors capable of holding larger wafers have been conducted. The results are given in the next section.

2. Growth Procedures

The initial step in this process involved the design and fabrication of the graphite susceptor illustrated in Figure 3. The barrel-type susceptor is capable of accepting two 2.4 cm (0.95 inch) x 1.65 cm (0.65 inch) Si substrates which are held in place by three pins on each face. Following machining, the graphite is purified in a $Fl_2$- and $Cl_2$-containing atmosphere at 2400K and coated via CVD at 1450K with a nominal 125 micron thick layer of high purity SiC to prevent C (or other impurities) from surface diffusing onto the Si substrate. As noted above, the three pins noted in Figure 3 are used to prevent the substrate from falling during evacuation of the CVD reactor.

Polished and etched rectangular Si wafers of somewhat lesser quality than normally employed (they contained a moderate concentration of pits) were used for the initial runs. The time used to convert the Si surface to SiC via

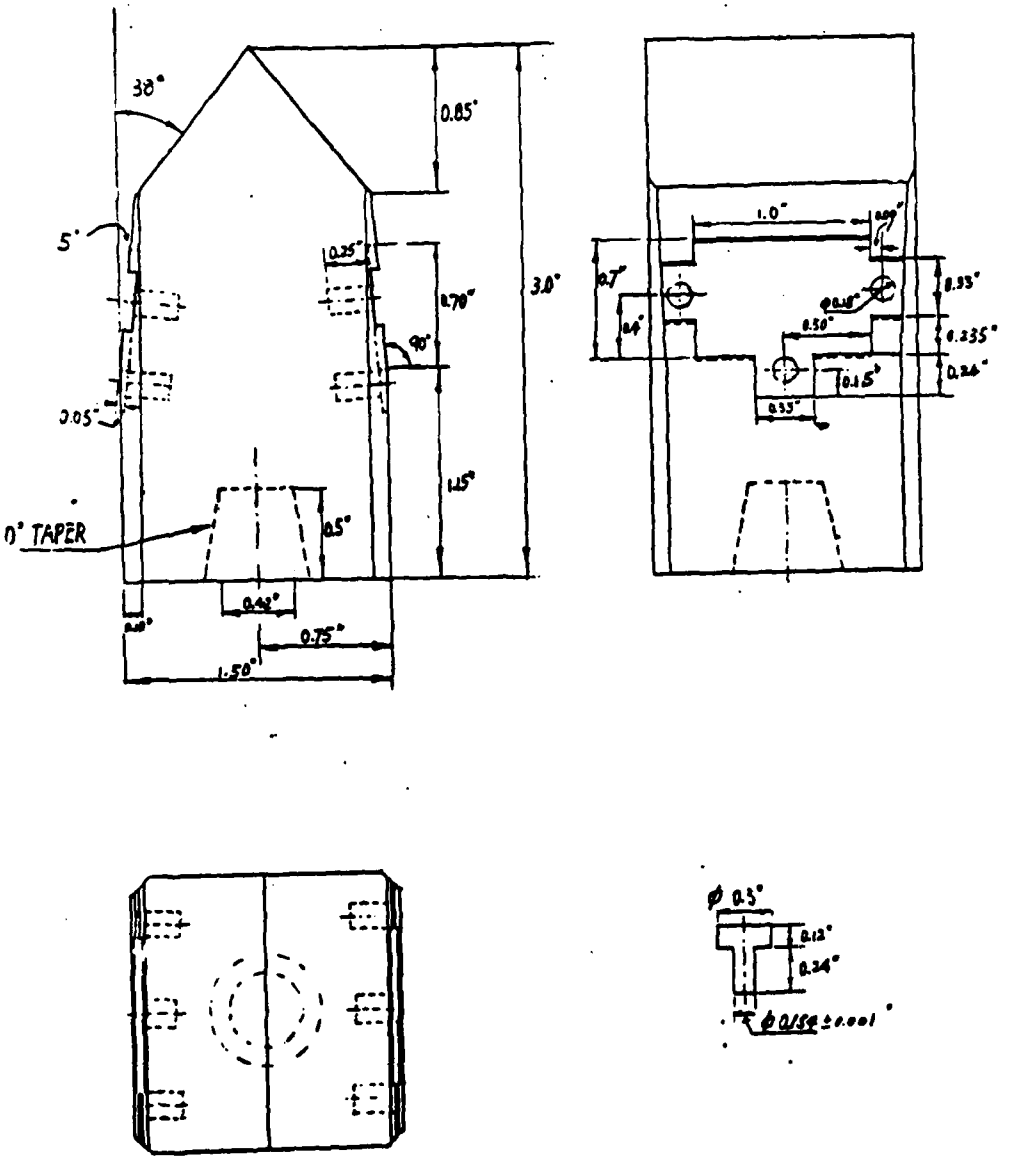


Figure 3. Schematic of graphite susceptor used for the growth of large area β-SiC thin films on rectangular Si substrates. The pins used to prevent the wafers from falling from the susceptor during evacuation of the chamber are also shown.

reaction with $C_2H_4$ was increased from the normal 150s to 170s because of the longer time required to heat the modified susceptor to ≅1590K.

It was also necessary to alter the optimum Si/C ratio in the reactive gases. The use of the standard ratio of 0.89 resulted in many black particles on the as-grown surface as shown in Figure 4a. However, changing the ratio to 1.05 resulted in the elimination of these particles as revealed by the optical micrograph of Figure 4b.

E. Characterization of the Large Area Films

1. X-ray Diffraction

Both transmission Laue and diffractometer patterns show that the large area film of Figure 4b is single crystal with the same [100]orientation of the Si wafer.

2. Thickness Uniformity

The uniformity of deposition across the large area wafers was determined as a check on the efficacy of the growth process to produce films of better uniformity than achieved with the smaller wafers. The thickness was measured in two directions: (a) from the center of the top edge (see Figure 5) to the bottom of the sample and (b) from the center of the left edge to the center of the sample (see Figure 6). As revealed by these two figures, the variation in thickness is small although there is a tendency for a slight reduction in thickness as one approaches the bottom of the sample. This phenomenon is probably due to the loss of the amount of reactant gas due to reaction at the top of the sample. The mean thickness of this film is 16.9 μm with a root mean square deviation of 1.15 μm. This and measurements on similar films reveals the growth rate to be 4.5 μm/hour.

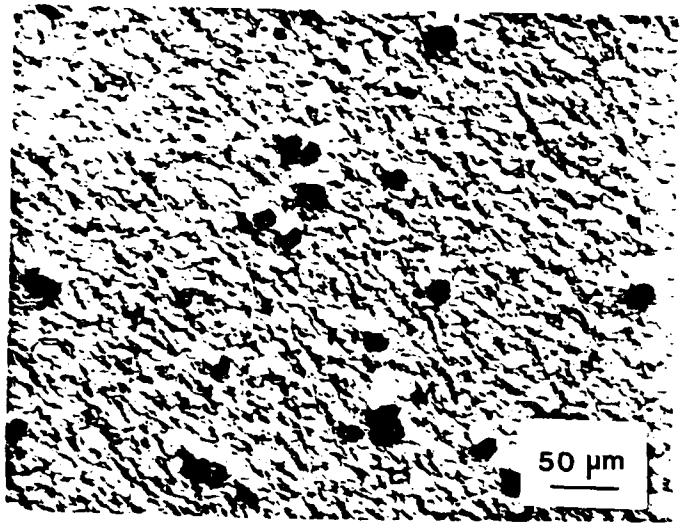


(a)

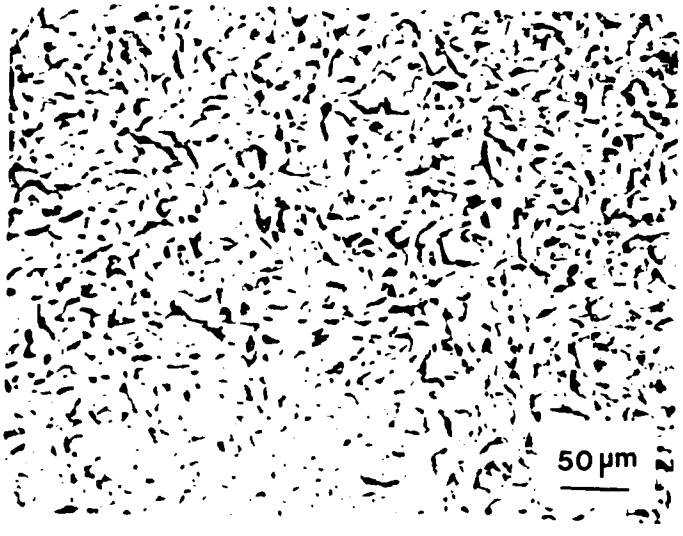


(b)

Figure 4. Optical micrographs of the final β-SiC surface of the large area samples produced under the Si/C gas flow ratios of (a) 0.89 and (b) 1.05. The black particles shown in (a) are believed to be SiC formed by homogeneous nucleation in the gas phase.

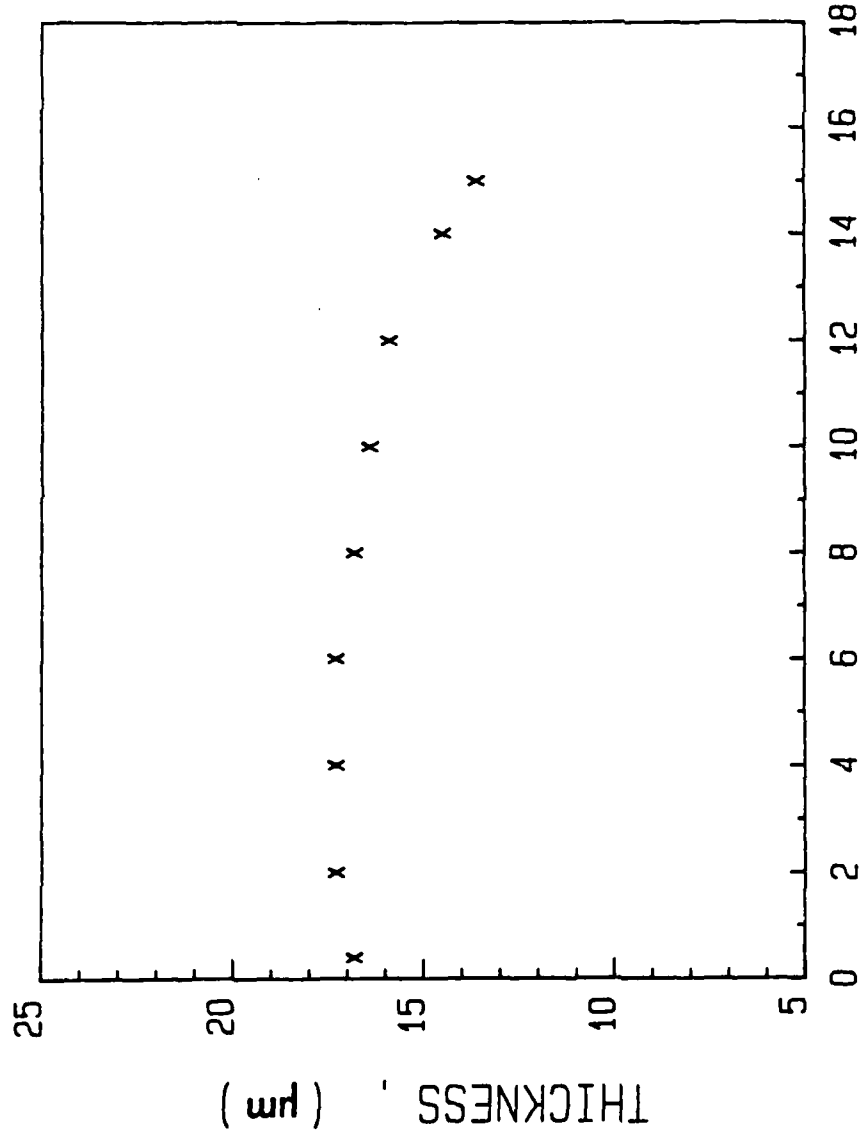


Figure 5. The thickness of a large area film and changes in this thickness from the center top edge to the bottom of sample #850522.

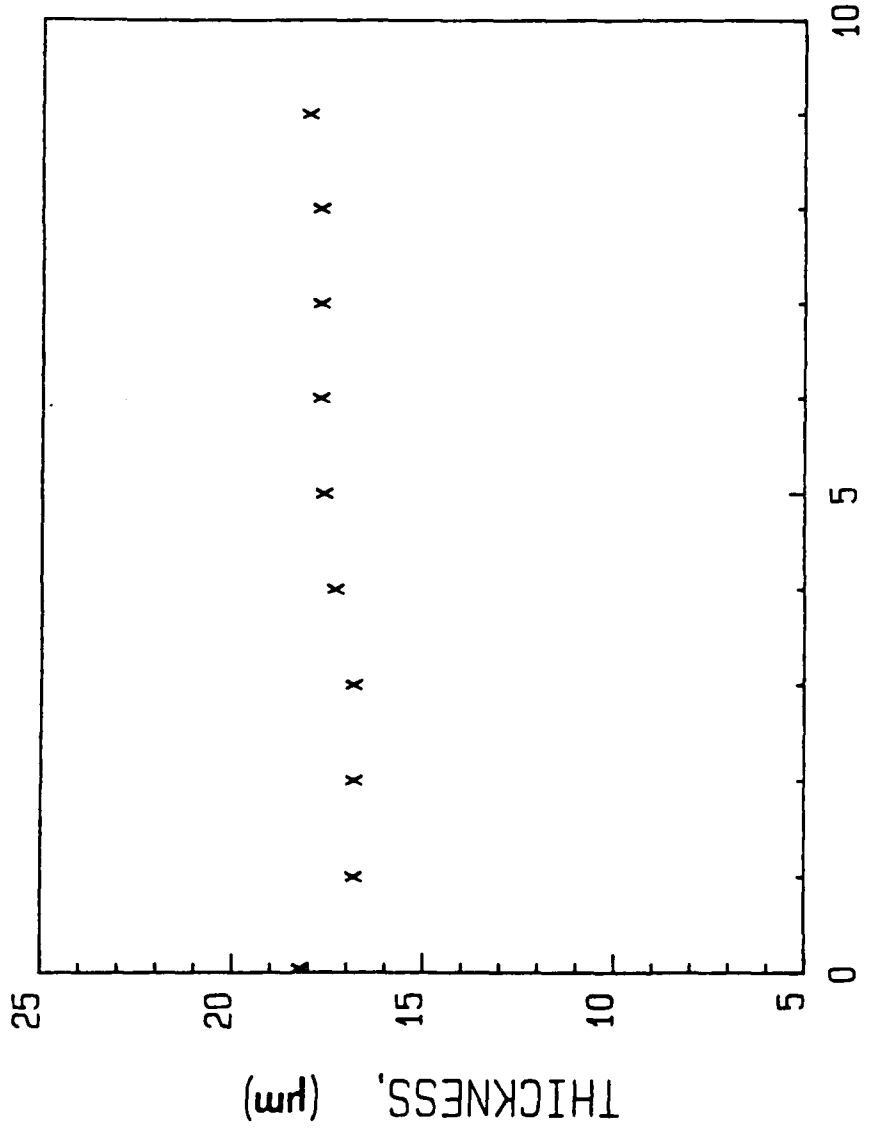


Figure 6. The thickness of a large area film and changes in this thickness from the center of the left edge to the center of sample #850522.

3. Sheet Resistivity and Its Uniformity

Four point probe measurements were used to measure the sheet resistivity along the same lines and sample positions used for the uniformity measurements. The values obtained for the two directions are given in Figures 7 and 8. They have not been corrected for the dimensions of the sample. As noted in these figures, the resistivity in this sample increases from the top edge to the bottom of the sample and also from the center edge to the center of the sample. The mean value is 69.4 ohms/□ with a root mean square deviation of 17.4 ohms/□ . The reasons for these deviations are a combination of physical events: the slight thickness variation across the sample and possible gradients in the defect population and Si/C ratios across the near surface region.

F. Future Research

Future research regarding growth of large area β-SiC films will include the use of higher quality Si wafers and the slight modification of the susceptor to make it more compatible with our CVD reactor.

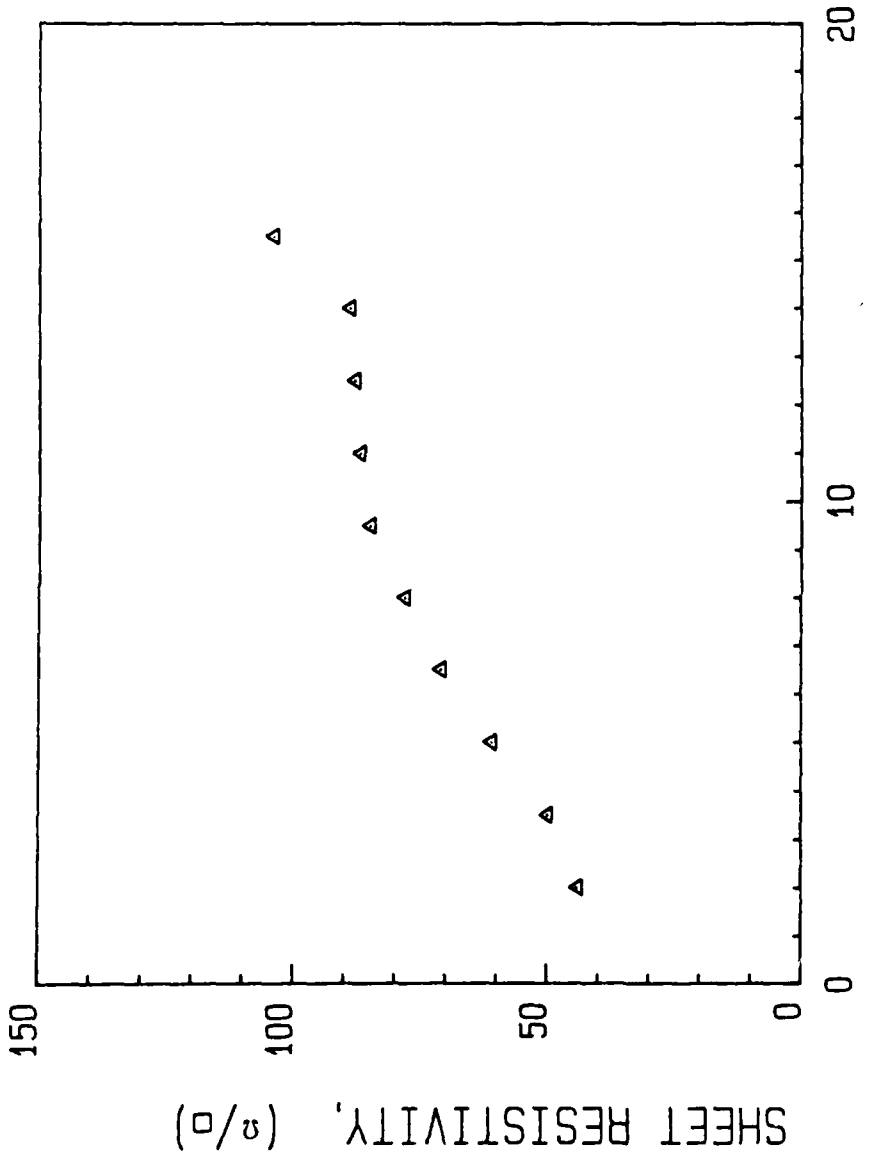


Figure 7. Sheet resistivity in sample #850522 as a function of position along a line from the center top edge to the bottom of the sample. Values have not been corrected for the dimensions of the sample.

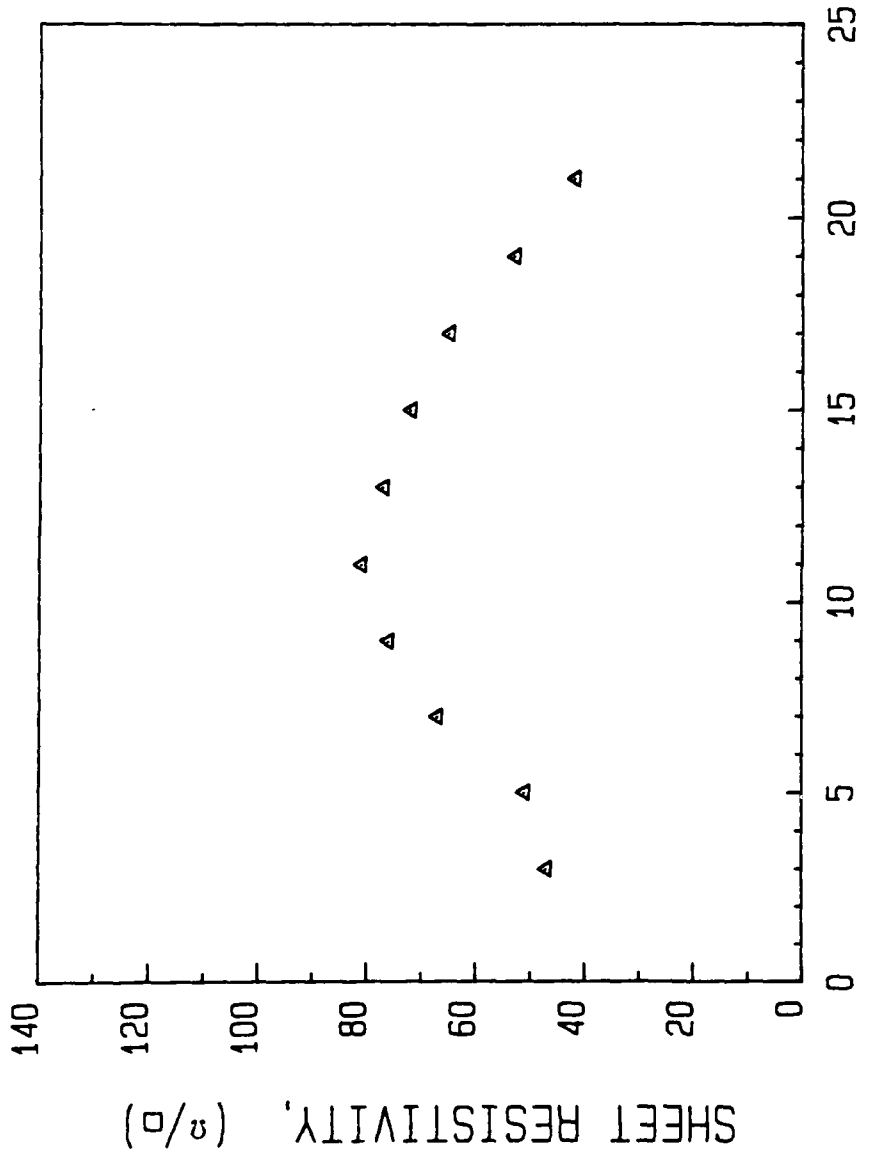


Figure 8. Sheet resistivity in sample #850522 as a function of position along a line from the edge center (left or right) to the center of the sample. The values have not been corrected for the dimensions of the sample.

## III. ADDITIONAL RESEARCH

The following five papers describe in concise form the additional research of this reporting period. The topics of this research are given in the titles of these papers which are noted below in order of the occurrence in this document:

| | PAPER TITLE | AUTHORS |
|---|---|---|
| 1. | "Amorphization and Recrystallization Processes in Monocrystalline Beta Silicon Carbide Thin Films" | Edmond, Withrow, Kong, Davis |
| 2. | "Rapid Thermal Annealing of Al and P Implanted Single Crystal Beta Silicon Carbide Thin Films" | Edmond, Kim, & Davis |
| 3. | "Rapid Thermal Annealing of B or N Implanted Monocrystalline β-SiC Thin Films and its Effect on Electrical Properties and Device Performance" | Ryu, Kim, & Davis |
| 4. | "Wet and Dry Oxidation of Single Crystal β-SiC: Kinetics and Interface Characteristics | Palmour, Kim, & Davis |
| 5. | "Dry Etching of β-SiC in $CF_4$+$O_2$ Mixtures | Palmour, Davis, Wallett & Bhasin |

# AMORPHIZATION AND RECRYSTALLIZATION PROCESSES IN MONOCRYSTALINE BETA SILICON CARBIDE THIN FILMS

J.A. EDMOND, S.P. WITHROW*, H.S. KONG, AND R.F. DAVIS
Department of Materials Engineering, North Carolina State University, Raleigh, NC 27695-7907
*Solid State Division, Oak Ridge National Laboratory, Oak Ridge, TN 37831

## ABSTRACT

Individual, as well as multiple doses of $^{27}Al^+$, $^{31}P^+$, $^{28}Si^+$, and $^{28}Si^+$ plus $^{12}C^+$ were implanted into (100) oriented monocrystaline β-SiC films†. A critical energy of ≈ 16 eV/atom required for the amorphization of β-SiC via implantation of Al and P was determined using the TRIM84 computer program for calculation of damage-energy profiles coupled with results of RBS/ion channeling analyses. In order to recrystallize amorphized layers created by the individual implantation of all four ion species, thermal annealing at 1600, 1700, or 1800°C was employed. Characterization of the recrystallized layers was performed using XTEM. Examples of SPE regrown layers containing; 1) precipitates and dislocation loops, 2) highly faulted- microtwinned regions, and 3) random crystallites were observed.

## INTRODUCTION

The processing steps leading to the development of selected electronic devices in cubic (beta) silicon carbide (β-SiC) thin films involve ion implantation to introduce electrically active dopants. As the dose of the implanted specie is increased, the near surface region of this compound semiconductor becomes progressively damaged; atomic disorder and eventual amorphization of the structure occurs. Early work by Hart et al. [1] utilized Rutherford Backscattering (RBS)/channeling techniques in order to study both disorder production in monocrystalline α-SiC by ion implantation and the subsequent thermal annealing of that damage. Williams et al. [2] have previously considered structural alteration in monocrystalline (0001) α-SiC as a result of Cr and N implantation. These authors have made direct comparisons of the theoretical damage profiles calculated using the computer codes E-DEP-1 [3] and TRIM [4] with those determined by RBS/channeling on experimentally implanted SiC samples. From the N implant results, it was determined that the critical energy density (CED) for randomization in their material was between 10 and 20 eV/atom (randomized regions refer to depths in the crystal where the aligned spectra coincide with the rotating random spectra).

The first objective in our investigation was to employ RBS ion channeling and Monte Carlo computer simulations together with the CED model [5] for implantation induced damage production in order to quantify, by a more novel approach, the disordering process during ion implantation of Al and P in β-SiC.

Solid-phase-epitaxial (SPE) regrowth during the thermal annealing of amorphous layers in compound semiconductors has been and continues to be the subject of a host of studies throughout the world [see, e.g.6] and also comprises our second objective in the present research. The quality of SPE regrown layers is generally very poor even when taking the utmost precautions. The two major problems are that nonstoichiometry results during implantation [7] and that dissociation of the constituent elements of the compound semiconductor generally occurs at different temperatures during thermal annealing.

We have studied SPE regrowth of β-SiC in order to better characterize these two effects.

## EXPERIMENTAL

Thin films of monocrystalline (100) β-SiC were epitaxially grown in-house on (100) silicon wafers via chemical vapor deposition [8]. Each sample was then mechanically polished, oxidized, and etched in HF in order to obtain a clean, undamaged and smooth surface. After mounting in ultra high vacuum, samples were implanted at room temperature with either P or Al at energies of 110 keV and 130 keV, respectively. The implants were made at an incident angle $7^{o}$ off normal to avoid channeling effects. Following implantation, in situ He backscattering analysis of the samples was obtained using 2.5 MeV $^{4}He^{+}$ ions incident along the <110> axial direction. The dosimetry was stepwise increased and additional ion scattering analyses made in order to measure the incremental increase in lattice damage as a function of implantation dose. Data were obtained until the backscattering yield from the damaged region was the same as that expected from a sample amorphous to the surface. Theoretical damage energy deposition profiles have been obtained for implantation of both species using the TRIM84 code [9]. These calculations were executed using a threshold displacement energy of 16 eV for SiC. However, it was determined that this parameter could be increased as high as 65 eV for SiC and have little effect on changing the CED for amorphization value.

Amorphous layers were also produced in β-SiC by implanting Al, P, Si and Si plus C in order to study SPE regrowth upon annealing. The former two species were implanted in order to dope β-SiC p-type and n-type, respectively; the latter two were used for preamorphization prior to subsequent dopant introduction at concentrations below which amorphization occurs. A summary of implant species and conditions is given in Table I. Solid-phase-epitaxial regrowth of amorphized layers was achieved by thermally annealing samples in 1 atm. of Ar at 1600, 1700, or $1800^{o}C$ for 300 s. Annealing in this temperature range is necessary for optimizing electrical characteristics of implanted p-type and n-type layers in β-SiC [10]. Residual lattice damage in the surface implanted regions before and after annealing has been visually evaluated using cross-sectional transmission electron microscopy (XTEM). The procedure for XTEM sample preparation is discussed in Ref. 11.

Table I. Summary of ion implantation conditions for SPE regrowth study. All implants performed using an offset angle of 7°.

| FIGURE NO | ION SPECIES | ENERGIES(keV) | DOSES ($cm^{-2}$) | * PEAK CONC.($cm^{-3}$) | IMPLANT TEMP. |
|---|---|---|---|---|---|
| 3 | $^{27}Al^{+}$ | 110,190 | 6E14,9E14 | 1E20 | RT |
| 4 | $^{31}P^{+}$ | 110,220 | 6E14,1E15 | 1E20 | $LN_2$ |
| 5 | $^{28}Si^{+}$ | 80,160,320 | 6E14,1E15,2E15 | 1E20 | $LN_2$ |
| 6 | $^{28}Si^{+}$ | 120,160,320 | 2.3E14,3.2E14,5.1E14 | 3E19 | $LN_2$ |
| | $^{12}C^{+}$ | 50,67,141 | 2.7E14,3.2E14,4.8E14 | 3E19 | $LN_2$ |

* Peak concentration values determined by LSS calculation.

## RESULTS AND DISCUSSION

### RBS/Channeling and TRIM84 Analyses

The RBS spectra in Fig. 1a illustrate the accumulation of damage in β-SiC as a result of P implantation. Prior to implantation, both an aligned spectrum from the undamaged sample, labeled 'virgin', and a random spectrum, obtained by rotating the sample around its normal axis to approximate the spectrum expected from amorphous SiC, were measured. As can be seen in the figure, damage accumulated in the sample with increasing implant dose until the scattering yield from the damaged region of the aligned spectrum was coincident with the yield from random rotation and thus indicative of an amorphous crystal. This condition initially occured at a depth of approximately 90 nm for a dose between 3.0 (not shown) and 5.0 x $10^{14}$ $cm^{-2}$. At the latter dose a buried amorphous layer ranging in depth between 55 nm and 118 nm was observed. The width of the amorphous region increased with increasing implant dose, until at the highest dose measured, 3.0 x $10^{15}/cm^2$, a surface amorphous layer 154 nm deep resulted, as indicated in the figure. The theoretical TRIM84 damage energy deposition profile for P implantation into SiC is shown in Figure 1b as a solid curve. The ordinate represents the energy deposition in eV/A. In order to determine the CED value for amorphization in β-SiC, the experimental minimum and maximum depths over which the P implant amorphized the crystal were measured as a function of dose from backscattering spectra like shown in Fig. 1a. These depths are plotted in Fig. 1b with the

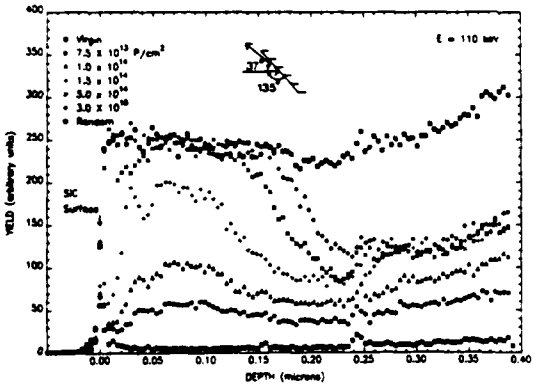


Fig. 1a. 2.5 MeV He RBS/channeling spectra for RT P-implanted β-SiC showing the accumulation of damage along the <110> axial direction with an increasing P dose.

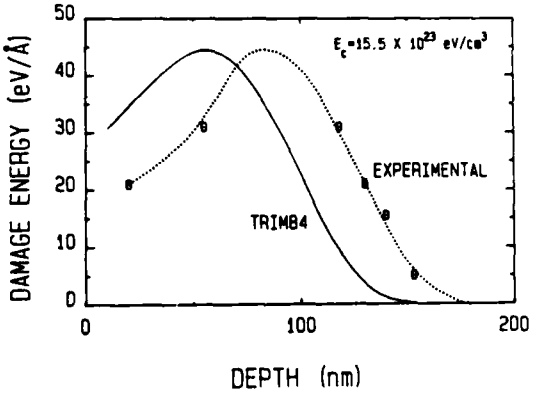


Fig. 1b. Comparison between theoretical (TRIM84) and experimental damage-energy profiles for 110 keV P-implanted β-SiC.

corresponding ordinate representing $k_{CED}$/dose, where $k_{CED}$ is a scaling factor that produces a curve through the data with the same maximum value and shape as the theoretical profile. This curve is shown dashed in Fig. 1b. For P implantation at room temperature, $k_{CED}$, which refers to the CED value, is 15.5 x $10^{23}$ $eV/cm^3$, or 16 eV/atom.

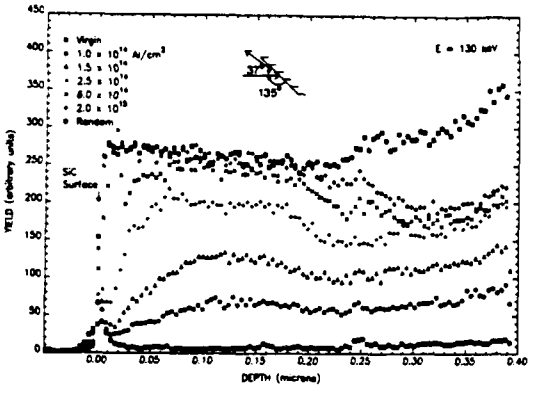


Fig. 2a. MeV He RBS/channeling spectra for RT Al-implanted β-SiC showing the accumulation of damage along the <110> axial direction with an increasing P dose.

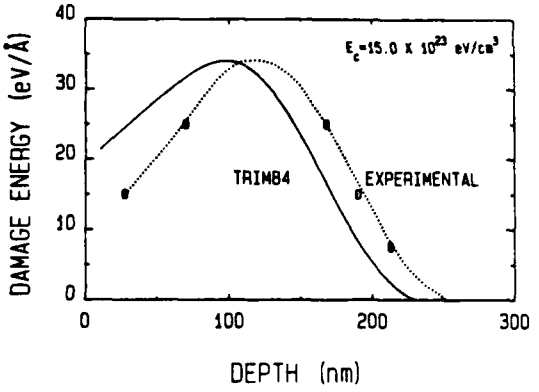


Fig. 2b. Comparison between theoretical (TRIM 84) and experimental damage-energy profiles for 130 keV Al-implanted β-SiC.

Fig. 2a shows the RBS spectra for damage accumulation as a result of room temperature implantation of Al in β-SiC. The measured lattice damage increased rapidly for doses greater than 1 x $10^{14}$ cm$^{-2}$. The sample first became amorphous at a depth of approximately 120 nm for a dose between 4.0 and 6.0 x $10^{14}$ cm$^{-2}$. For the 6.0 x $10^{14}$ cm$^{-2}$ implant, a buried amorphous layer ranging in depth from 70 to 168 nm resulted. A surface amorphous layer 213 nm in depth resulted from implanting with a dose of 2 x $10^{15}$ cm$^{-2}$.

The theoretical and experimental damage versus energy profiles for Al in β-SiC are compared in Fig. 2b using the same method as for the P implant described above. For Al, the CED value for amorphization is 15.0 x $10^{23}$ eV/cm$^3$, or 15.5 eV/atom. As expected, the amorphizing energy obtained from both analyses is nearly identical.

Deviation between the theoretical and experimental profile depths was very significant for both implanted species, possibly indicating a need for revision of parameters in the TRIM84 code for the implantation of SiC. However, a more likely source of deviation may be in the method in which the program computes damage production from recoils. The recoils are not individually followed in the program but rather the amount of damage they produce is approximated through the use of theoretical calculations. For that reason, the authors are presently investigating another Monte Carlo program that tracks damage production from recoils as well as from the primary ions.

## Solid-Phase-Epitaxial Regrowth

Figure 3 shows an XTEM micrograph of an Al double implant region having a peak concentration of 1 x $10^{20}$ Al/cm$^3$. A buried amorphous layer having a crystalline cap of 10 nm resulted after implantation (Fig. 3a). The lower amorphous/crystalline (a/c) interface located at a depth of ≈170 nm is very diffuse as a result of implanting at room temperature. After annealing at 1600°C for 300 s in Ar, the amorphous layer had regrown (Fig. 3b) by SPE. However, a high concentration of defects was observed. Precipitates and/or dislocation loops formed where the upper and lower a/c interfaces were initially located. A broad band of defects (40 nm - 110 nm) resulted where the two a/c interfaces converged during SPE regrowth. In contrast, by annealing a

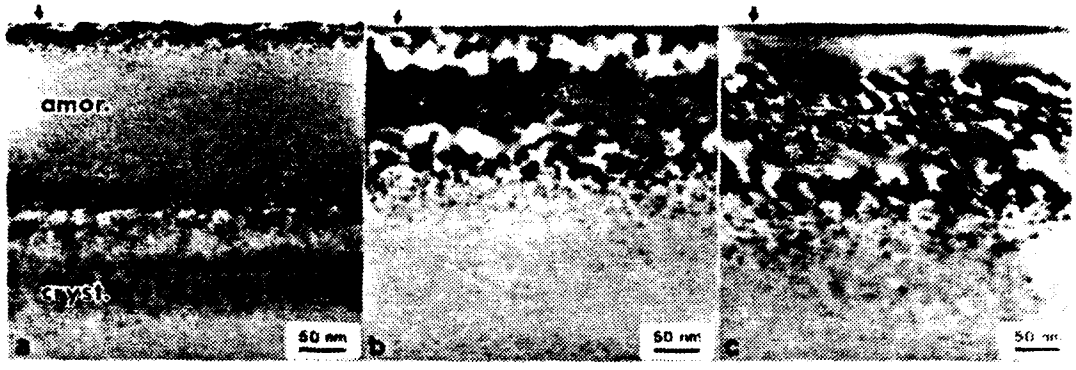


Figure 3. XTEM micrographs showing the surface of a sample which has been double implanted with Al to a peak concentration of $1 \times 10^{20}$ Al/cm$^3$. (a) As-implanted; (b) annealed at 1600°C; (c) annealed at 1800°C for 300 s.

like sample at 1800°C (see Fig. 3c) many of the precipitates did not appear. In this instance, a virtually defect free surface region (0-50 nm) resulted. Additionally, a band containing loops and stacking faults formed at the regrowth convergence as well as small loops where the lower a/c interface was initially located.

Figure 4 illustrates the regrowth properties of a P double implant with a peak concentration (as calculated by LSS) of $1 \times 10^{20}$ P/cm$^3$. The annealing temperature was 1700°C. Clearly, the supersaturation of P in the SiC matrix became sufficiently high to cause the layer to regrow in a polycrystalline condition after the first 100 nm of regrowth. However, within the first 100 nm, many small precipitates and loops formed. The regrowth properties of amorphous layers obtained using a lower atomic concentration of P is presently being investigated.

Figure 4. XTEM micrograph of a sample which has been double implanted with P to a peak concentration of $1 \times 10^{20}$ P/cm$^3$ and subsequently annealed at 1700°C for 300 s. The surface appears rough as a result of polycrystalline regrowth.

In order to preamorphize β-SiC for subsequent dopant introduction, implantation of Si and Si plus C was conducted. Figure 5 shows an XTEM micrograph of a Si triple implant region prior to and after thermal annealing. The peak concentration of Si is $1 \times 10^{20}$ Si/cm$^3$. After implantation, an amorphous surface layer 440 nm in depth was observed. After annealing at 1700°C for 300 s in Ar, the layer regrew epitaxially. The first 70 nm regrew moderately defect free. Thereafter, severe microtwinning and faulting occurred resulting in a polycrystalline layer (Fig. 5b) with a highly preferred orientation.

The XTEM micrographs in Fig. 6 directly compare the structural regrowth properties of implanted and amorphized layers created using Si and Si plus C. Figure 6a shows the amorphous layer which was formed by the Si triple implant with a peak concentration of $3 \times 10^{19}$ Si/cm$^3$. The a/c interface is located 400 nm below the sample surface. After annealing at 1700°C for 300 s in Ar, the layer regrew epitaxially without severe faulting and/or microtwinning as was observed in Fig. 5b. However, a high concentration of precipitates and/or loops formed throughout the regrown bulk. In an attempt to eliminate these defects, a triple C implant was superimposed on the triple Si implant thus simulating implantation of SiC into SiC. The projected range peaks were

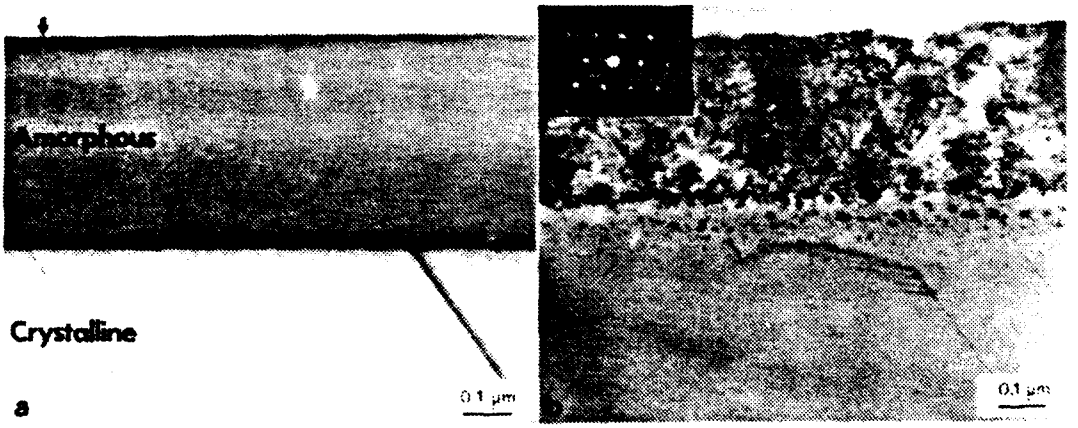


Figure 5. XTEM micrographs and diffraction pattern of (100) β-SiC which has been triple implanted with Si to a peak concentration of $1 \times 10^{20}$ Si/cm$^3$. (a) As-implanted; (b) annealed at 1700°C for 300 s. (The diffraction pattern is near [011] and from the microtwinned and highly faulted layer).

matched (1:1) SiC in order to obtain the correct stoichiometry using LSS theory. Fig. 6c shows an XTEM micrograph of the regrown layer previously implanted and amorphized with SiC at a peak concentration of $3 \times 10^{19}$ implanted SiC/cm$^3$. The annealing conditions were the same as described for the sample shown in Fig. 6b. Quite clearly, implanting Si plus C did not structurally improve the quality of the regrown layer. In fact, microfaulting and microtwinning occurred upon regrowth from 140 nm to the sample surface. However, a recent investigation using SIMS has revealed that implants of $^{30}Si^+$ and $^{13}C^+$ in SiC do not follow LSS theory and in fact, the above $^{28}Si^+$ and $^{12}C^+$ implant profiles may have deviated significantly. Therefore, the authors are further investigating the implantation of both $^{30}Si^+$ and $^{13}C^+$ in SiC in an attempt to subsequently improve the character of the regrown implanted layer.

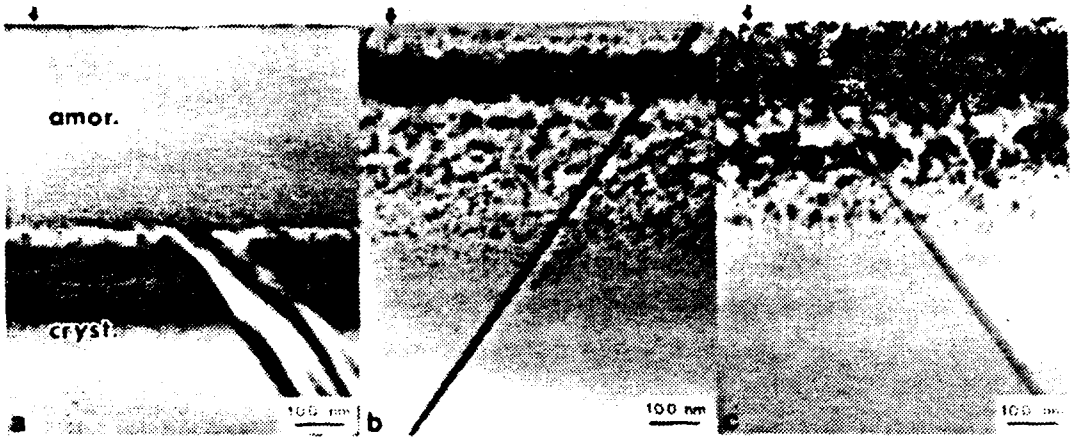


Figure 6. XTEM micrographs comparing the regrowth properties of samples implanted with equal atom concentrations ($3 \times 10^{19}/cm^3$) of Si (b, center) and Si + C (c, right). The as-implanted amorphous layer is also shown (a). Samples were annealed at 1700°C for 300 s.

## CONCLUSIONS

Using RBS/channeling and the TRIM84 computer code it has been determined that the critical energy for amorphization of β-SiC at room temperature is ≈ 16 eV/atom. Furthermore, it has been shown that amorphous SiC undergoes SPE regrowth upon thermal annealing at a temperature as low as 1600°C. For the case of amorphous layers created by P implants, polycrystalline regrowth was observed. Layers implanted with Al and Si regrew as single crystals but with residual line and planar defects. Initial attempts have shown that overlaying implants of C on Si does not improve the regrowth properties of amorphous SiC.

## ACKNOWLEDGEMENT

The authors gratefully acknowledge the support of this program by the Office of Naval Research under contract N00014-82-K-0182 P005 and to the ONR Fellowship program for support of one of the authors (Edmond). Work at Oak Ridge was sponsored by U.S. D.O.E. Division of Materials Sciences under contract DE-AC05-840R21400 with Martin Marietta Energy Systems, Inc.

## REFERENCES

[1] R.R. Hart, H.L. Dunlap, and O.J. Marsh, Rad. Effects 9, 261 (1971).

[2] J.M. Williams, C.J. McHargue, and B.R. Appleton, Nucl. Instr. and Meth. 209/210,317 (1983).

[3] I. Manning and G.P. Mueller, Comp. Phys. Comm. 7, 85 (1974).

[4] J.P. Biersack and L. G. Haggmark, Nucl. Instr. and Meth. 174, 257 (1980).

[5] J.R. Dennis and E.B. Hale, J. Appl. Phys. 49, 1119 (1978).

[6] J.P. Donnelly, Nucl. Instr. and Meth. 182/183, 553 (1981).

[7] L.A. Christel and J.F. Gibbons, J. Appl. Phys. 52, 5050 (1981).

[8] H.P. Liaw and R.F. Davis, J. Electrochem. Soc. 132, 642 (1985).

[9] J.P. Biersack and W. Eckstein, J. Appl. Phys. A34, 73 (1984).

[10] J.A. Edmond, H.J. Kim, and R.F. Davis, to be published in 1985 MRS Symposia Proceedings on Rapid Thermal Processing, Boston, MA 1985.

[11] C.H. Carter, Jr., J.A. Edmond, J.W. Palmour, J. Ryu, H.J. Kim, and R.F. Davis, to be published in MRS Symposia Proceedings on Microscopic Identification of Electronic Defects in Semiconductors, San Francisco, CA, 1985.

[12] W. Maszara, G.A. Rozgonyi, L. Simpson, and J.J. Wortman, to be published in 1985 MRS Symposia Proceedings on Beam-Solid Interactions and Phase Transformations, Boston, MA, 1985.

† These isotopes were used throughout this study unless otherwise noted.

# RAPID THERMAL ANNEALING OF Al AND P IMPLANTED SINGLE CRYSTAL BETA SILICON CARBIDE THIN FILMS

J.A. EDMOND, H.J. KIM AND R.F. DAVIS
Department of Materials Engineering, North Carolina State University, Raleigh, NC 27695-7907

## ABSTRACT

Ion implantation of $^{27}Al^{+}$ and $^{31}P^{+}$ ions into monocrystalline β-SiC films was conducted in order to acquire p-type and n-type conducting layers, respectively. Implant energies ranging from 110 to 190 keV and fluences from $7 \times 10^{13}$ to $9 \times 10^{14}$ $cm^{-2}$ were used. In order to activate each dopant specie, rapid thermal annealing (RTA) was employed. A decrease in sheet resistance with increasing annealing temperature for both type layers was observed up to 1800°C. After annealing at this highest temperature for 300 s in 1 atm. Ar, the percent of activated and ionized n-type and p-type dopant was ≈20% and ≈0.5%, respectively, as determined by room temperature capacitance-voltage measurements. Recrystallization of both heavily damaged and amorphized layers occurred as a result of the use of the aforementioned annealing process. Unlike SPE regrowth in other compound semiconductors, no microtwins were present in the regrown bulk as observed by XTEM. SIMS analyses also showed that there was essentially no redistribution of P and moderate redistribution of Al from the corresponding as-implanted profiles after annealing.

## INTRODUCTION

Cubic (beta) silicon carbide is a wide band gap (Eg=2.3 eV) semiconductor having a high melting temperature, high thermal conductivity, low dielectric constant, high breakdown electric field and high saturated electron drift velocity. Thus, β-SiC is a principal and perennial candidate material for use in high temperature device operations as well as for high power and high speed switching devices.

As an alternative to in situ doping, diffusion and ion implantation provide means of controllably introducing impurities into semiconductor materials. In SiC, diffusion processes require both temperatures greater than 1800°C and relatively long times [1] to accomplish the mass transport required for device fabrication. Under these conditions, masking oxide layers essential for selective doping vaporize, and SiC decomposition occurs. A viable solution to the difficulties in doping and fabrication techniques inherent with diffusion processes is ion implantation.

Few results on the formation of n-type conducting layers using $^{31}P^+$ implants in SiC have been reported. The most complete work which concerns implantation of $^{31}P^+$ in p-type hexagonal (6H) α-SiC, was published by Marsh and Dunlop [2] in 1970. They were successful in achieving p- to n-type conversion upon thermal annealing of these implanted samples at 1500°C for 120 s in vacuum. Phosphorous implantation in β-SiC has not been previously investigated.

Ion implantation of $^{27}Al^+$ in α-SiC has also been investigated. Kalinina et al. [3] were successful in producing p-n junctions in α-SiC using a wide range of $^{27}Al^+$ implant doses and annealing temperatures. Addamiano et al. [4] reported n- to p-type conversion in α-SiC using a minimum Al peak concentration of $1 \times 10^{21}$ Al/cm$^3$. The existance of p-type layer formation as a result of $^{27}Al^+$ implantation in β-SiC was also reported by Marsh et al. [2]. However, it was an isolated case and could not be reproduced.

The research of the present authors (and the focus of this paper) involves $^{31}P^+$ and $^{27}Al^+$ implantation in monocrystalline β-SiC thin films and the subsequent determination of the proper RTA procedures to achieve regrowth of the SiC and activation of the dopants. The results of the electrical, structural, and chemical evaluation of the implanted material prior to and following RTA are presented and discussed below.

## EXPERIMENTAL

The thin films of (100) β-SiC used in this research were epitaxially grown in-house on (100) silicon wafers via chemical vapor deposition [5]. Prior to implanting each sample was mechanically polished, oxidized, and etched in HF in order to obtain a clean, undamaged and smooth surface. Initial electrical measurements were also made before implanting for baseline reference. Ion implantation of $^{27}Al^+$ and $^{31}P^+$ ions was conducted in order to acquire layers having p-type and n-type conductivity, respectively. The phosphorus implant was conducted at a dose of $7.7 \times 10^{13}$ cm$^{-2}$ and an energy of 110 keV. The aluminum dual implant was performed at $6 \times 10^{14}$ cm$^{-2}$-110 keV and $9 \times 10^{14}$ cm$^{-2}$-190 keV. All implants were conducted at room temperature using an offset angle of 7° from the sample surface in order to ameliorate channeling of the implantation beam. After implanting, each sample was sectioned into 3 pieces; 1 half and 2 quarter pieces, respectively. The 2 quarter pieces from each sample were used, one as an implant standard and one as a subsequently annealed specimen, for secondary ion mass spectroscopy (SIMS) analyses. The remaining half of each sample was used for the stepwise annealing and electrical characterization experiment described below.

In order to activate each dopant specie and structurally anneal damaged regions created by implantation, RTA was employed. The RTA system utilizes a resistance heated ultra high purity SiC-coated graphite strip heater containing a shallow cup into which one sample is placed. Before annealing, each β-SiC thin film was separated from the Si substrate on which it was grown via etching in an (1:1) $HF:HNO_3$ solution until the Si was dissolved. The thickness of each film was approximately 15 μm. Upon loading a sample, the annealing chamber was evacuated to a pressure of $10^{-5}$ Torr and backfilled with Ar to a pressure ≈1 atmosphere argon was used in order to help reduce the rate of Si loss during the heating of SiC. A heating rate of 35°C/sec was employed. Sample halves were annealed in 100°C increments from 1000°C to 1900°C for period of 300 s each. The use of longer annealing times (up to 900 s) was previously shown to have no measureable effect on further reducing the sheet resistance or increasing the carrier concentration of implanted samples. Prior to electrical measurements, samples annealed at 1400°C or higher were oxidized at 1200°C for 90 minutes in dry oxygen (oxide thickness=100 nm) and then etched in HF in order to remove a remaining C-rich surface layer. Electrical characterization was accomplished using room temperature 4-point probe and differential capacitance-voltage (C-V) measurements. A mercury probe with a contact area ratio of 32:1 was used in order to provide electrical contacts for the latter measurements.

To evaluate residual lattice damage in the surface implanted regions before and after annealing, cross-sectional transmission electron microscopy (XTEM) was used. The procedure for XTEM sample preparation is discussed in Ref. 6. SIMS was also employed in order to determine the extent of dopant diffusion during annealing.

## RESULTS AND DISCUSSION

In order to obtain the optimum annealing schedule and thus maximize dopant activation, sheet resistance ($R_s$) data were collected as a function of annealing temperature for both types of implant layers. As shown in Fig. 1a, $R_s$ for the P implanted sample remained constant (40 Ω/□) up to 1300°C. This was also the value of $R_s$ for this sample prior to implantation. At annealing temperatures higher than 1300°C $R_s$ decreased, most rapidly between 1600°C and 1800°C. The value of $R_s$ stabilized at 1800°C at 18 Ω/□. Annealing at temperatures higher than 1825°C resulted in excessive surface decomposition of the SiC. As for the Al implanted layer, $R_s$ also remained at a constant value (42 Ω/□) over a wide range of annealing temperatures (1000°C - 1600°C) and likewise decreased rapidly above 1600°C (Fig. 1b). In this case an $R_s$

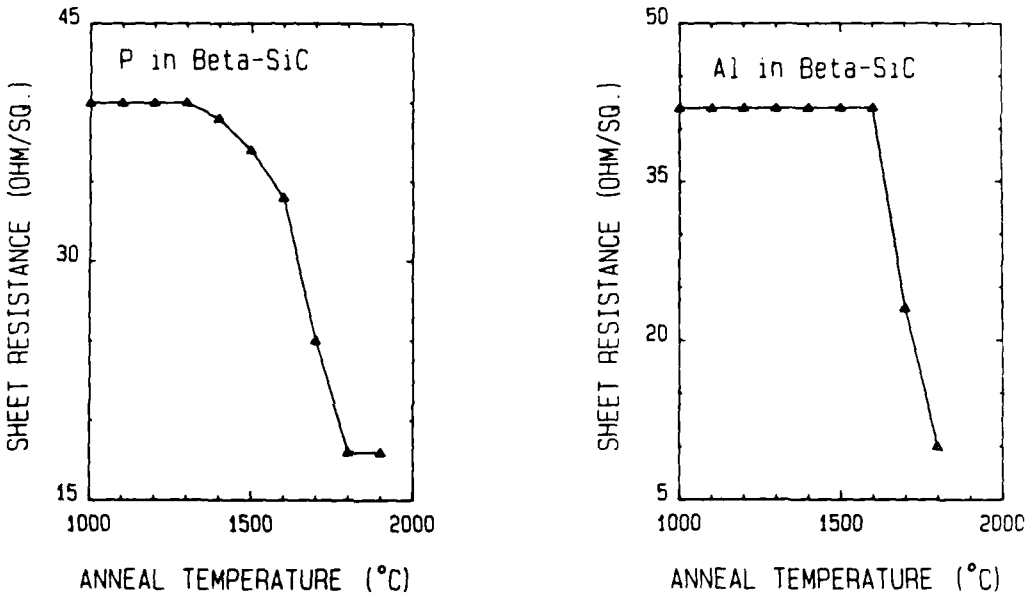


**Figure 1. Sheet resistance as a function of annealing temperature for (a) P-implanted and (b) Al-implanted β-SiC.**

value of 10 Ω/□ was obtained at the highest annealing temperature of 1800°C. From these results an 1800°C-300 s annealing schedule was established.

To observe the extent of dopant redistribution resulting from the use of the above annealing schedule, SIMS was utilized. Figure 2a compares the atomic concentration of P versus depth profiles of the as-implanted and 1800°C annealed samples. The annealed profile became marginally depressed and widened. Clearly, diffusion of P during annealing was insignificant. Figure 2b shows the comparison between the depth profiles for the as-implanted and 1800°C annealed Al implanted sample. In this case, there is a decrease in the concentration of this specie by a factor of two-to-four throughout most of the profile depth as a result of annealing. However, the concentration of Al is slightly increased at the sample surface. (This specie is also believed to have diffused into the bulk of the sample, though evidence for this is not available.)

Figures 3a and 3b are XTEM micrographs showing the P implanted surface prior to and following an 1800°C-300 s anneal, respectively. As shown in Figure 3a, a 160 nm surface layer best characterized as point defect-rich is evident. The first 20-30 nm appears to be moderately defect free, as the higher energy electronic scattering events dominate the incident ion displacement. The center of the adjacent darker band is approximately 90 nm from the sample surface. This coincides very well with the implanted P ion range value of 90.4 nm obtained from SIMS analyses. No amorphization occurred,

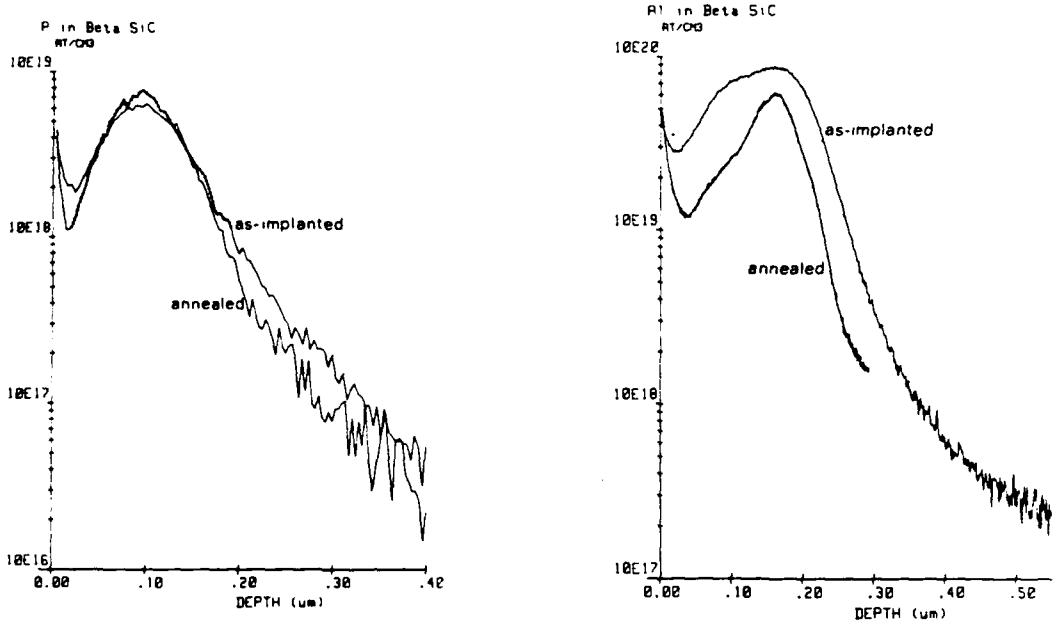


Figure 2. Comparison of SIMS profiles for (a) P-implanted and (b) Al-implanted β-SiC before and after thermal annealing at 1800°C for 300 s.

as indicated by the extension of stacking faults from the unimplanted region through the implanted region to the surface. Figure 3b shows the implanted surface after annealing. Clearly, the defect-rich surface appears to have structurally recovered to a large degree after the 1800°C anneal. However, there is also a fairly high concentration of small precipitates in the first 100 nm of the sample surface as a result of apparently exceeding the solubility limit of P in SiC. The presence of the precipitates are believed to cause a high surface leakage current as will be shown in the C-V measurement results.

Likewise, Figures 4a and 4b are XTEM micrographs showing the Al implanted surface prior to and following an 1800°C-300 s anneal, respectively. As shown in Figure 4a, a buried amorphous layer resulted. However, the amorphous-crystalline (a-c) interfaces appear very diffuse. This occurs as a result of dynamic annealing effects during room temperature implantation. Figure 4b shows the Al implanted surface after being annealed at 1800°C-300 s. During solid-phase-epitaxial (SPE) regrowth of this amorphized layer, precipitates and loops formed at the lower regrown a-c interface and along the boundary where the regrowth fronts from the upper and lower a-c interfaces converged. However, unlike other compound semiconductors, SPE regrowth occurred without the formation of twins. As expected from the existence of precipitates and loops, a high leakage current was also observed during C-V measurements for the p-type layer.

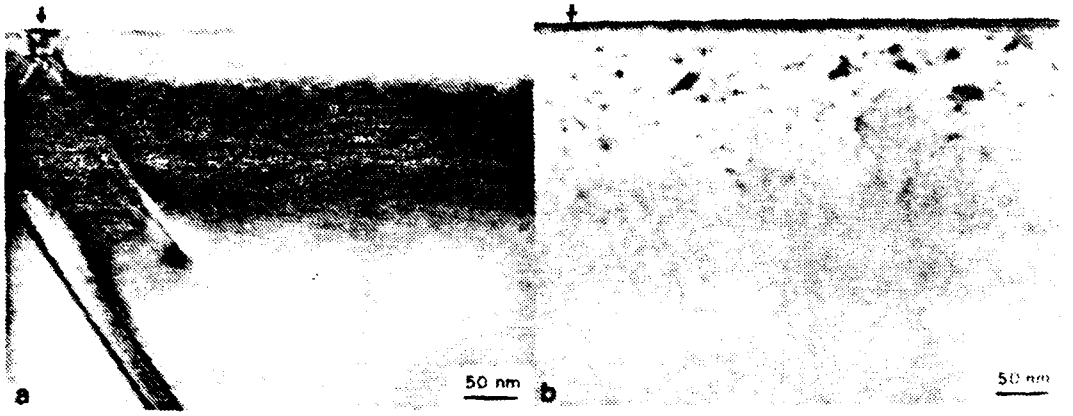


Figure 3. Cross-sectional TEM micrographs of the surface region of a P-implanted β-SiC single crystal thin film (a) prior to and (b) after thermal annealing at 1800°C for 300 s.

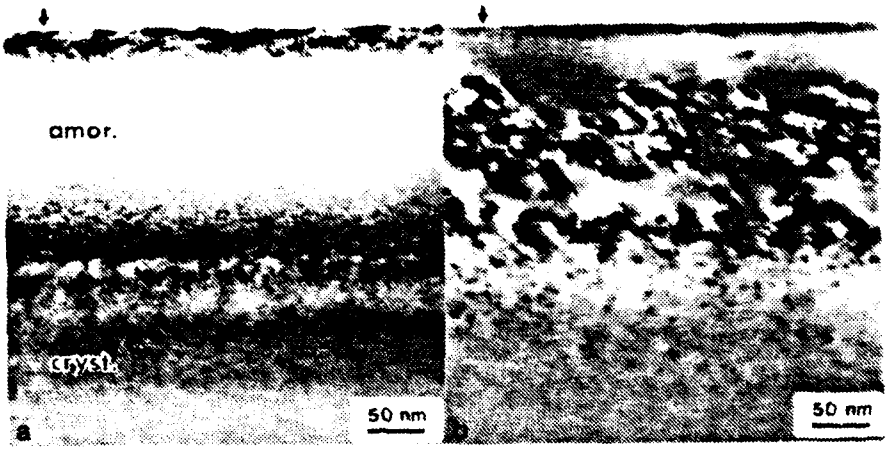


Figure 4. Cross-sectional TEM micrographs of the surface region of an Al-implanted β-SiC single crystal thin film (a) prior to and (b) after thermal annealing at 1800°C for 300 s.

Figure 5a shows the C-V profile of the P implanted layer in terms of the ionized carrier concentration as a function of depth in the sample. The implant profile for the annealed material obtained using SIMS and the intrinsic carrier concentration curve of the sample prior to implantation are shown for reference. The C-V profile for the annealed (1800°C-300 s) sample was obtained by increasing the reverse bias from 0 to -2.5 volts whereupon the leakage current exceeded 200 μA. Quite clearly, the shape of this curve closely mimicks the SIMS profile with the peak being near the 90 nm value previously determined. The effective carrier concentration value at this peak is, however, approximately one-fifth of the atomic concentration of P. Thus, it may be concluded that at room temperature, the activation combined with

ionization of P in this sample previously annealed at 1800°C-300 s is ≈ 20% of the maximum 6 x $10^{18}$ value. Furthermore, the presence of precipitates added to the increase in leakage current and to the loss of activated dopant.

Similarily, C-V measurements were also conducted at room temperature on the Al-containing samples previously annealed at 1800°C-300 s. Again, the implant profile obtained from SIMS and intrinsic carrier concentration curves are plotted in Figure 5b. After implantation and annealing, a p-type signal was recorded from 0 to -1.0 volt, where again the leakage current exceeded 200 μA. The resulting p-type peak concentration was 3 x $10^{17}/cm^3$. When compared to the atomic concentration of Al in the material after annealing, an ionized activation ≈ 0.5% is realized at room temperature. Again, the presence of precipitates added to the increase in leakage current and loss of activated Al dopant.

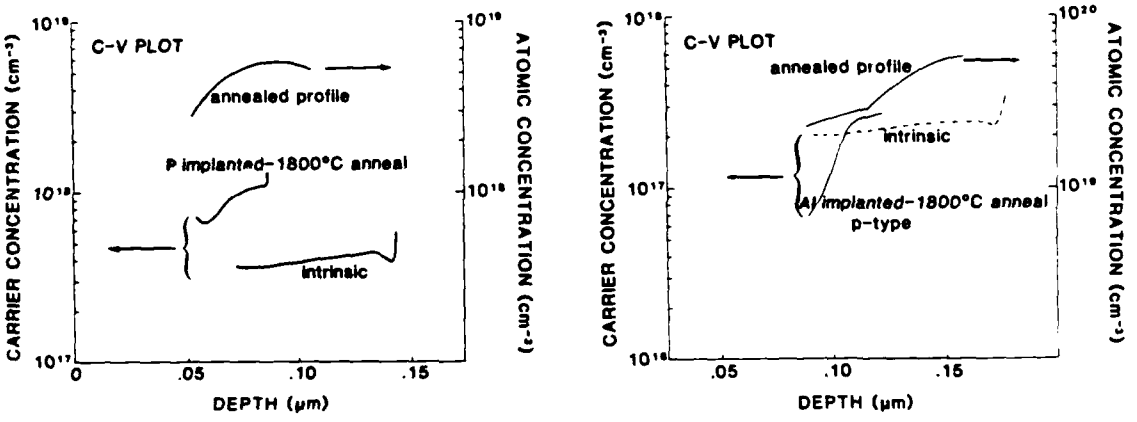


Figure 5. Carrier concentration and atomic concentration determined by C-V and SIMS measurements, respectively for (a) P-implanted and (b) Al-implanted β-SiC.

## CONCLUSIONS

Layers having p-type or n-type conductivity in monocrystalline β-SiC films were obtained by implantation of $^{27}Al^+$ or $^{31}P^+$, respectively, and subsequently exposing them to a 1800°C-300 s anneal in 1 atm. argon. As a result of using this annealing schedule, the percent of the activated and ionized n- and p-type dopants were ≈ 20% and ≈ 0.5%, respectively. Additionally, there was essentially no redistribution of P dopant and moderate loss of Al. It was also determined that precipitates and/or loops result when recrystallizing both damaged and amorphized layers upon annealing; however, no microtwins form during SPE regrowth.

ACKNOWLEDGEMENT

The authors gratefully acknowledge the support of this program by the Office of Naval Research under contract N00014-82-K-0182 P005 and to the ONR Fellowship program for support of one of the authors (Edmond). Appreciation is also expressed to Dr. D. Griffis and S. Bryan for the ion microprobe studies.

REFERENCES

1. Y.A. Vodakov and E.N. Mokhov, in Silicon Carbide 1973, edited by R.C. Marshall, J.W. Faust, Jr. and C.E. Ryan (University of South Carolina Press, Columbia, SC, 1973), pp. 508-519.

2. O.J. Marsh and H.L. Dunlap, Rad. Effects 6, 301 (1970).

3. E.V. Kalmina, A.V. Suvorov, and G.F. Kholuyanov, Sov. Phys. Semicond. 14, 652 (1980).

4. A. Addamiano, G.W. Anderson, J. Comas, H.L. Hughes, and W. Lucke, J. Electrochem. Soc. 119, 1355 (1972).

5. H.P. Liaw and R.F. Davis, J. Electrochem. Soc. 132, 642 (1985).

6. C.H. Carter, Jr., J.A. Edmond, J.W. Palmour, J. Ryu, H.J. Kim, and R.F. Davis, to be published in MRS Symposia Proceedings on Microscopic Identification of Electronic Defects in Semiconductors, San Francisco, CA 1985.

# RAPID THERMAL ANNEALING OF B OR N IMPLANTED MONOCRYSTALLINE β-SiC THIN FILMS AND ITS EFFECT ON ELECTRICAL PROPERTIES AND DEVICE PERFORMANCE

Jae Ryu, H. J. Kim and R. F. Davis
North Carolina State University
Materials Engineering Dept.
Box 7907, Raleigh, NC 27695-7907

## ABSTRACT

The annealing behavior of B or N dual implants in β-SiC thin films has been studied using cross-sectional TEM, SIMS, and four point probe electrical measurements. A high resistivity layer was produced after annealing the B implanted-amorphous layer in the temperature range from 1000°C to 1500°C for 300 s; however, the resistivity rapidly decreased as a result of annealing at higher temperatures. The reasons for these changes in resistivity and the lack of p-type conduction at all annealing temperatures in these B implants include: (1) possible compensation of the native n-type carriers, (2) reduction in the B concentration via formation of B-containing precipitates between 1300°C and 1600°C and out diffusion of this species at and above 1600°C, and (3) creation of additional n-type carriers.

No precipitates or defect structure was observed in N implanted-annealed samples. The resistivity of this non amorphous n-type layer decreased with increasing annealing temperatures from 700°C to 1800°C. Furthermore n-p junction diodes were fabricated for the first time in β-SiC via N implantation into samples previously in situ doped with $8 \times 10^{18}/cm^3$ Al coupled with rapid thermal annealing at 1200°C for 300 s. A typical diode ideality constant and a saturation current for these diodes was 3.4 and $9 \times 10^{-10}$ $A/cm^2$, respectively.

## INTRODUCTION

Fabrication of junction devices in SiC by diffusion or growth processes generally involves high temperatures and long periods of time. The more commonly employed epitaxial solution growth method also requires long process times(≅8 hrs.) at temperatures of around 1700°C. Thus, the ion implantation technique is very attractive, because it permits the control of both impurity levels and profiles at much lower temperatures.

In hexagonal 6H SiC, p-n junctions have been successfully produced by several investigators(1-4) via implantation of column V elements into in situ doped p-type layers. By contrast, the implantation of column III elements into n-type 6H SiC has resulted in high resistivity layers but not p-type conduction(5). One reason for this lack of p-type conductivity may be out-diffusion of the implanted species such as that observed for B(4) and Al(6). However, Marsh(5) found via backscattering studies that implanted In did not out-diffuse from 6H-SiC when annealed in the range of 1200-1700°C. He concluded that the absence of p-type conductivity was caused by the presence of deep donor-type defects. As a results of this lack of p-type conductivity in annealed samples implanted with group III elements, essentially all previous implanted junctions in 6H SiC have been produced by implanting donor impurities into in situ doped p-type layers; the one exception is noted in Ref. 7.

In cubic β-SiC, ion implantation and annealing studies have been very restricted because of difficulties in obtaining sufficiently large crystals. Recently, however, moderate area and high quality monocrystalline β-SiC thin films have been successfully produced by CVD techniques at NCSU(8) and in other laboratories(9,10). In the present research, B and N has been implanted into these films in order to produce p- or n-type layers, respectively. The

microstructural and chemical changes in these implanted layers have been examined as a function of annealing temperature using cross sectional transmission electron microscopy (XTEM) and secondary ion mass spectroscopy (SIMS). The changes in the electrical characteristics of the implanted and annealed layers and the associated junctions were also analyzed via four point probe, current-voltage (I-V) and capacitance-voltage (C-V) techniques. Both a Hg probe and a probe station were used for the latter two measurements. The following sections describe the procedures used and the results obtained in this research.

## EXPERIMENTAL PROCEDURES

The acceptor species of B was twice implanted into liquid nitrogen cooled β-SiC films under the conditions of energy and dose of 200 kev, $2 \times 10^{15}/cm^2$ and 100 kev, $1.5 \times 10^{15}/cm^2$. The atomic concentration of B at the peak was $10^{20}/cm^3$. This amount was calculated to be sufficient to produce a p-type layer in the unintentionally doped n-type SiC having a carrier concentration of $5 \times 10^{16}/cm^3$; however, p-type conduction was not obtained at room temperature even after annealing. The donor species of N was also twice (200 kev, $1.5 \times 10^{14}/cm^2$; 100 kev, $1.1 \times 10^{14}/cm^2$) or three times (200 kev, $3.6 \times 10^{15}/cm^2$; 100 kev, $2.5 \times 10^{15}/cm^2$; 50 kev, $1.6 \times 10^{15}/cm^2$) implanted into similar samples under the same conditions of cooling. Samples containing the individual implanted species were annealed in Ar at a single temperature between 1000°C and 1800°C (100°C intervals) using a specially designed rapid thermal annealing system and a very high purity SiC-coated graphite heating strip containing a 1 cm dia. sample cavity. Each annealing period was 300 s.

The microstructures of both the implanted and the annealed samples were examined using XTEM(11). Dopant distribution profiles were determined using SIMS (ion microprobe). Sheet resistance measurements were conducted using a conventional four point probe. Prior to the electrical characterization of the annealed samples, a 200 A layer was removed from the surface by dry oxidation (1200°C-1 hr.) and etching in buffered HF in order to remove a C-rich surface layer which resulted from the preferential evaporation of Si during annealing.

Implanted n-p junction diode were developed via the dual implantation of the N into p-type β-SiC which had previously been in situ doped with $8 \times 10^{18}/cm^3$ Al. The implantation conditions in terms of dose and energy were $1.5 \times 10^{14}/cm^2$ at 200 kev and $1.1 \times 10^{14}/cm^2$ at 100 kev, respectively. This implant was annealed at 1200°C for 300 s; from previous research it was predicted that $3 \times 10^{18}$ N/cm$^3$ would be ionized under these conditions. Reactive ion etching (RIE) in 40 mTorr of $CF_4$ at a power of 150 watts was employed to produce a mesa structure. A 91-Au/2-Ta/7-Al alloy and rf sputtered $TaSi_2$ were applied to obtain ohmic contacts for the p- and n-type layers, respectively. The fabricated n-p junctions were characterized via I-V and C-V measurements.

## RESULTS AND DISCUSSION

### B-implant

The results of the sheet resistance measurements as a function of annealing temperature for the B-implanted samples are shown in Fig. 1. The as-received and the as-implanted films showed a resistance of 96 and 116 ohm/□, respectively. However, after annealing in the temperature range of 1000-1600°C, the resistance of the implanted films increases to a higher value of 170 ohm/□. This increase in resistance implies either a compensation effect from the ionized implanted B or the interference with charge transport caused by the presence of new structural, non electrically active defects generated by the implantation and annealing processes. Complementary C-V

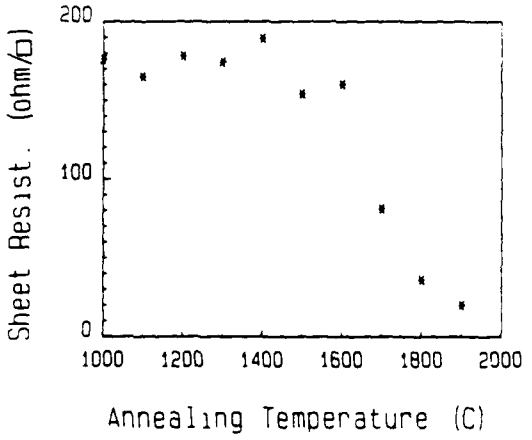


Fig. 1. Sheet resistance as a function of annealing temperature for B dual implanted samples. The annealing time was 300 s at each temperature.

measurements via Hg probe indicated no apparent p-type conduction at room temperature after annealing in the same temperature range.

A rapid decrease in resistance was observed after annealing above 1700°C. In fact, the 1800°C annealed sample has a lower resistivity than the as-grown, unimplanted film. However these samples showed strong n-type conduction. The formation of a low resistivity n-type sample as a result of annealing above 1700°C was also observed in the as-grown, undoped ß-SiC(12). The creation of electrically active n-type point defects during the high temperature anneal(T>1700°C) was suggested as a reason for this phenomenon. Thus, the rapid decrease in resistance of the B implanted samples may be caused by the creation of additional n-type point defects throughout the entire volume of the films rather than by a change in the electrical character of the implanted layer.

A buried amorphous layer extending from 0.1 to 0.44 µm beneath the surface is revealed in the XTEM microstructure of the as-implanted samples shown in Fig. 2. A heavily damaged region extends an additional 0.11 m into the film. Annealing at 1300°C caused solid phase epitaxial(SPE) regrowth of the amorphous layer which began at both crystalline/amorphous interfaces. Two distinct bands of B-containing precipitates, corresponding in position to the two peak maxima of the dual implants, occurred as a result of this heat treatment, as is evident in the associated XTEM micrograph of Fig. 2. No detectable diffusion of B occurred as a result of annealing at 1300 C, as shown by the essentially identical SIMS profiles of the as-implanted and this sample. Annealing at 1600°C caused the formation of coarse precipitates near the sample surface and dislocation loops near the center of the original amorphous layer. The corresponing SIMS profile(see Fig. 2, 1600°C) shows that the B concentration peaks became less defined and moved closer to the surface. Annealing at 1800°C also produced SPE regrowth but without residual defects. However, SIMS analysis shows that the B had diffused into and perhaps out of the sample such that the concentration profile was essentially flat to at least 0.6 µm into the sample.

N Implant

The results of sheet resistance measurements on N dual implants, as a function of annealing temperature are shown in Fig. 3. The resistance of the as-received and the as-implanted films was 68 and 78 ohm/□, respectively. A perusal of this figure reveals that the sheet resistance slowly decreased from the 900°C annealing temperature up to 1600°C, but rapidly decreased when the implanted film was annealed at 1700°C and higher. This decrease in sheet resistance in the temperature range from 1000°C to 1600°C results from both an increase in the carrier concentration of the ionized N atoms and from an increase in the carrier mobility as a result of the annealing of the implanted

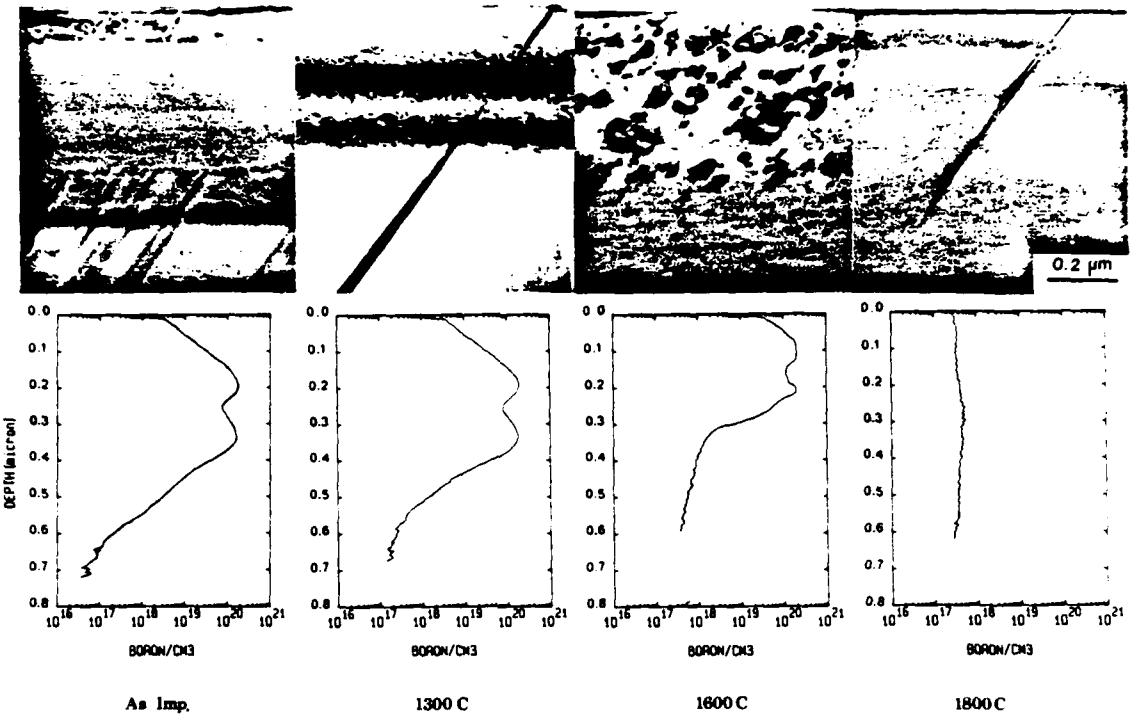


Fig. 2. XTEM and complementary SIMS profiles of B dual implanted samples after annealing at various temperatures. The annealing time at each temperature was 300 s. (Each sample was subjected to only one temperature.)

damage (see below). The measured value of the n-type carrier concentration was $3 \times 10^{18}/cm^3$ in the 1200°C annealed samples. This represents ≅40% ionization. The rapid decrease in resistance after annealing above 1700°C results again from the creation of additional n-type point defects.

A heavily damaged but crystalline layer is revealed in the XTEM structure of the dual as-implanted layer(peak concentration $8 \times 10^{18}/cm^3$), as shown in Fig. 4. Annealing of this sample at temperatures above 1300°C caused structural rearrangement. No visible damage was observed. The results of SIMS anlysis on N triple implanted and annealed samples are shown in Fig. 5. A small amount of N redistribution was observed as a result of annealing at 1300°C . Annealing at 1600° or 1800°C (curves (c) and (d)) caused considerable out diffusion of N which resulted in a high concentration in the near-surface region. However, the concentration of this element diminished rapidly beyond 1800°C profile for this species and the similarly annealed B implant is the more rapid diffusion of the latter species in SiC.

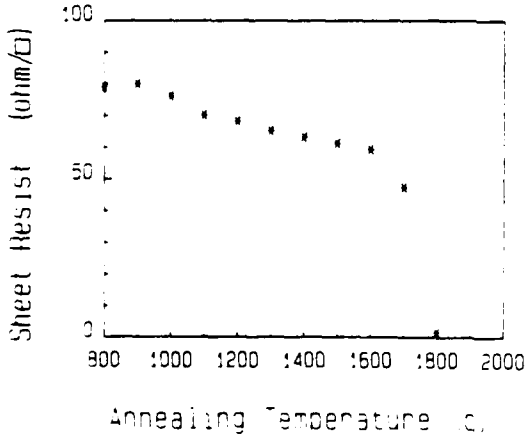


Fig. 3. Sheet resistance as a function of annealing temperature for N dual implanted samples. The annealing time was 300 s at each temperature.

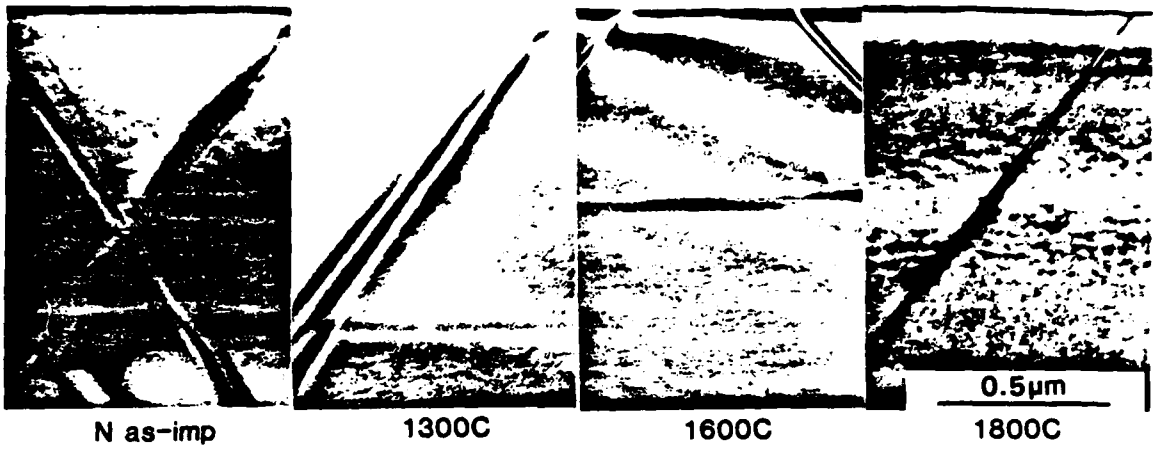


Fig. 4. XTEM of N dual implanted samples after annealing at various temperatures. The annealing time at each temperature was 300 s. Each sample was subjected to only one temperature. Note the stacking faults in all micrographs.

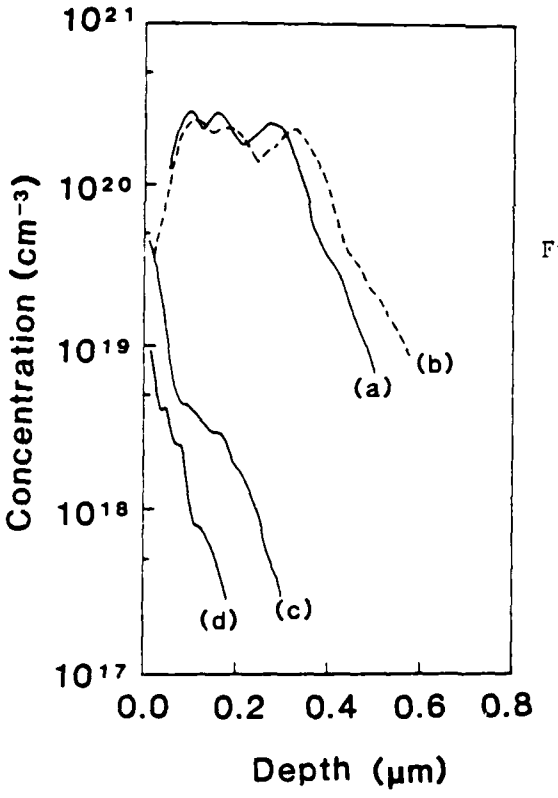


Fig. 5. Nitrogen concentration profiles, for (a) unannealed N triple implant and for samples annealed at (b) 1300°C, (c) 1600°C, and (d) 1800°C. The annealing time at each temperature was 300 s.

Implanted n-p junctions

Typical I-V characteristics of fabricated n-p junction diodes are shown in Fig. 6. Following mesa structure formation via RIE, a high leakage current caused by a C-rich layer on the surface(13) was observed by I-V measurements, as shown in Fig. 6(a). Values of this parameter were greatly reduced by oxidizing this surface, as shown in Fig. 6 (b). Typical values of the ideality factor and saturation current for these diodes were 3.4 and $9 \times 10^{-10}$ A/cm$^2$,

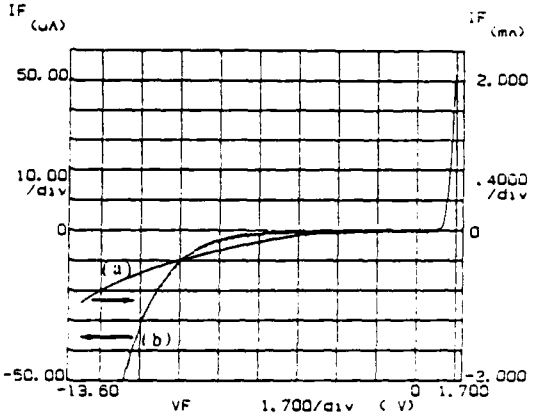


Fig. 6. Typical I-V characteristics of n-p junction diodes produced by dual N implantation into Al-containing β-SiC films: (a) before oxidation, (b) after oxidation. Note that the leakage current was greatly reduced from 400 μA to 10 μA at -10 volts by oxidation, as shown by the two different scales for current (IF).

respectively. The leakage current of this diode in the final structure is negligible up to -5 volts, the breakdown voltage is -12 volts. This unexpected low breakdown voltage could indicate the existence of defects which were not observed in the XTEM of the N implanted and annealed samples. An abnormal $1/C^2$-V relationship (not shown in this paper) of this diode indicate the presence of a thick "i-layer" in the implanted junction boundary. The presence of a semi-insulating layer in the implanted junctions was also reported in 6H SiC(3) and in GaAs(14). This "i-layer" has been attributed to the presence of trapping levels introduced by defects. Its effects can be dissipated in SiC by high temperature annealing above 1500°C as shown by Marsh(5).

## CONCLUSIONS

A high resistivity layer was produced by ion implantation of B into undoped n-type β-SiC films coupled with subsequent annealing to 1600°C. But p-type conduction was not observed. The reasons for these phenomena are: (1) possible compensation of the native n-type carriers, (2) formation of B-containing precipitates at temperatures between 1300°C and 1600°C, (3) out diffusion of B during high temperature annealing above 1600°C, and (4) creation of electrically active n-type point defects above 1700°C. By contrast, no precipitates or defect substructure have been observed in N implanted and annealed samples. Furthermore, the resistivity of this crystalline n-type layer decreased with increasing annealing temperature. Almost 40% of implanted N are ionized after annealing at 1200°C for 300 s. Increasing the annealing temperature above 1600°C caused out diffusion implanted N.

Implanted n-p junction diodes have been fabricated for the first time in β-SiC via N implantation into P-type samples previously in situ doped with Al coupled with rapid thermal annealing at 1200°C for 300 s. The values of the ideality factor and the saturation current for these diodes were typically 3.4 and $9 \times 10^{-10}$ A/cm$^2$, respectively. The leakage current of this diode is negligible up to -5 volts and the breakdown voltage is around -12 volts.



## ACKNOWLEDGMENTS

The authors acknowledge the support of the Office of Naval Research for this research under contract N00014-82-K-0182 P0005. Appreciation is also expressed to D. Griffis and J. Palmour for the SIMS research and the oxidation and RIE, respectively.

REFERENCES

1. F.A. Leith, W.J. King and P. McNally, Air Force Contract AFCRL-67-0123, Ion Physics Co., (1967).

2. H.L. Dunlap and O.J. Marsh, Appl. Phys. Lett. 15, 311 (1969).

3. O.J. Marsh and H.L. Dunlap, Rad. Effects 6, 301 (1970)

4. A. Addamiano, G.W. Anderson, J. Comas, H.L. Hughes and W. Lucke, J. Electrochem. Soc. 119, 1355 (1972).

5. O.J. Marsh, in Silicon Carbide-1973, R.C. Marshall, J.W. Faust and C.E. Ryan Eds., §University of South Carolina Press, Columbia, SC, 1974† p. 471.

6. J. Comas, W. Lucke and A. Addamiano, Bull. Am. Phys. Soc. 18, 606 (1973).

7. E.V. Kalinina, A.V. Suvorov, and G.F. Kholuyanov, Sov. Phys. Semicon. 14, 652 (1980).

8. H.P. Liaw and R.F. Davis, J. Electrochem. Soc., 132, 642 (1985).

9. S. Nishino, J.A. Powell and H.A. Will, Appl. Phys. Lett. 42, 460 (1983).

10. S. Nishino, Y. Hazuki, H. Matsunami and I. Ianaka, J. Electrochem. Soc. 127, 2674 (1980).

11. C.H. Carter,Jr., J.A. Edmond, J.W. Palmour, J. Ryu, H.J. Kim and R.F. Davis, presented at 1985 Spring Meeting of MRS, San Francisco; to be published in the MRS Symposia Proc.

12. J.S. Ryu and R.F. Davis, presented at the AIME Electronic Materials Conference, Boulder, CO, June, 1985, paper in preparation.

13. J.W. Palmour, R.F. Davis, T.M. Wallett and K.B. Bhasin, submitted to the J. Am. Vacuum Soc.

14. R. Hunsperger, O. Marsh and C. Mead, Appl. Phys. Lett. 13, 295 (1968).

# WET AND DRY OXIDATION OF SINGLE CRYSTAL β-SiC: KINETICS AND INTERFACE CHARACTERISTICS

JOHN W. PALMOUR, H. J. KIM, AND R. F. DAVIS
North Carolina State University, Materials Engineering Dept., Box 7907, Raleigh, NC 27695-7907

## ABSTRACT

Silicon dioxide layers were grown on single crystal (100) β-SiC between 1000°C and 1200°C, in wet $O_2$, dry $O_2$, and wet Ar. All processes demonstrated a linear-parabolic relationship with time. Both wet processes had a slower rate than dry oxidation at 1050°C and below. The activation energies of the linear and parabolic rate constants were calculated for each process. The activation energy of the parabolic rate constant for wet oxidation was found to be inversely dependent on the amount of oxygen present as a carrier gas.

The dry oxides exhibited a very flat surface; in contrast, SEM and XTEM reveal that wet oxidation preferentially oxidizes dislocation bands, causing raised lines on the oxide and corresponding grooves in the SiC. It is proposed that the much higher solubility of $H_2O$ in $SiO_2$ as compared with that of $O_2$ ($10^3$ at 1000°C), allows wet oxidation to be preferential.

## INTRODUCTION

Because of its wide band gap, short carrier lifetime, and high thermal conductivity, cubic (zincblende structure) β-SiC is a promising semiconductor material for high temperature, high frequency, and high power electronic devices [1,2]. In order to fabricate devices, thermal oxidation is needed to produce both passivating layers and gate dielectrics for MOS devices. Oxidation can also be used as one of the few non-damaging methods for etching SiC. In order to understand the oxidation behavior of monocrystalline β-SiC, the kinetics and interface characteristics of both wet and dry oxidation processes have been investigated.

Silicon carbide can be thermally oxidized, albeit at a slower rate, in the same manner and temperature range that is employed for Si. Most of the previous studies on the oxidation of SiC concerns polycrystalline materials [3], which are most often comprised of hexagonal 6H α-SiC. It has been shown that the (0001) face of single crystals of 6H SiC oxidizes [4,5] according to the same linear-parabolic equation reported for Si by Deal and Grove [6]:

$$x_0^2 + Ax_0 = B(t + \tau) \qquad (1)$$

where $x_0$ is the oxide thickness, t is the time of oxidation, B is the parabolic rate constant, B/A is the linear rate constant, and τ is a constant that allows for any initial oxide present or peculiarities in the initial stages of oxidation. This model states that the initial stage of oxidation is reaction rate limited and linear, but becomes parabolic as the diffusion of the oxidant through the oxide becomes the rate limiting factor. Fung and Kopanski [7] found that wet oxidation of single crystal cubic (β) SiC also obeys the linear-parabolic law. The rate constants for dry oxidation of this material have not been reported, nor have they been compared with those of wet oxidation. As such, these topics, as well as the interfacial phenomena during oxidation, have been addressed in this research and are reported below.

Mat Res Soc Symp Proc Vol 54 - 1986 Materials Research Society

## EXPERIMENTAL

The oxidation system used high purity $O_2$ or Ar introduced into a fused quartz tube furnace containing the β-SiC films. The $O_2$ was either dry (150 ccm) or saturated with $H_2O$ vapor. The latter condition was produced by bubbling the $O_2$ (60 ccm) through a heated (98°C) three liter flask containing deionized water. Both wet and dry processes were conducted at temperatures from 1000°C to 1200°C for times up to 50 hours. The samples were loaded in an Ar atmosphere and the temperature was allowed to stabilize before introducing the oxidizing atmosphere. After the desired amount of time, the samples were quickly pulled from the furnace hot zone.

The (100) β-SiC thin films used in these experiments were epitaxially grown on Si substrates via chemical vapor deposition [8], polished with 0.1 μm diamond paste to remove the inherent surface roughness, oxidized in dry $O_2$ at 1200°C for 1.5 hours to remove the 20 nm of material damaged during polishing, and etched clean in HF. The carrier concentrations of the samples were measured by capacitance voltage techniques; those in the range of $2 \times 10^{15}$ to $5 \times 10^{16}$ $cm^{-3}$ (n-type) were used. Before any oxidation step, the samples were degreased in organic solvents and cleaned in heated $H_2SO_4$, then heated $NH_4OH:H_2O_2$ (1:1 volume ratio), dipped in HF to remove any residual oxide, and rinsed in deionized water.

All oxide thicknesses were determined by measuring an etched step in the oxide with a profilometer. In order to obtain this step, the oxide layer was partially masked with wax, the exposed oxide etched off in buffered HF, and the wax removed with acetone. The XTEM samples were made using standard sample preparation techniques [9].

## KINETICS

The results of the dry oxidation experiments are shown in Fig. 1. The solid black lines are the theoretical curves calculated from eq. (1) using the constants A, B, and τ that were determined from the data at each temperature. It can be seen that the experimental results and the theoretical curves closely correspond, indicating that the linear-parabolic model is correct. The constant τ is the negative of the t intercept when the data is plotted linearly and the curve is extrapolated to $x_o = 0$. The constants B and A were calculated by plotting the thickness, $x_o$, versus $(t + \tau)/x_o$. The slope of this line is the constant B and the negative of the Y-intercept is the constant A. The values of the slopes and intercepts were determined by the least squares method.

The results of the wet oxidation experiments, for both wet $O_2$ (60 ccm) and wet Ar (60 ccm), are shown in Fig. 2. A comparison of the data for wet and dry $O_2$ shows that dry oxidation at 1200°C is, as expected, much slower than wet oxidation. However, as temperature is reduced, the rates come closer together with dry oxidation becoming faster at 1050°C and 1000°C. This a somewhat surprising result in that, for Si, the dry process is always slower than the wet. Since the rate of oxidation in $H_2O$ is slower than in its carrier gas alone (dry $O_2$) at 1050°C and below, it was reasoned that the $O_2$ was enhancing the wet oxidation rates in this range. Thus, the wet Ar experiments were performed in order to separate any combined effect of $O_2$ and $H_2O$.

When Deal and Grove [6] replaced $O_2$ with Ar in their experiments on wet oxidation of Si, they found that the rate constants A and B remained essentially the same. This indicated that the effect of oxygen in the wet $O_2$ atmosphere was negligible, and that the oxidizing species was $H_2O$. When $O_2$ is replaced with Ar for wet oxidation of β-SiC, the rate at 1200°C was also essentially unchanged. However at 1000°C, wet Ar was markedly slower than wet $O_2$, as shown in Fig. 2, reducing the parabolic rate constant by almost 80%. Clearly, the presence of $O_2$ in this lower temperature range enhanced the wet oxidation rates. It can also be seen in Fig. 2 that the data for wet Ar at

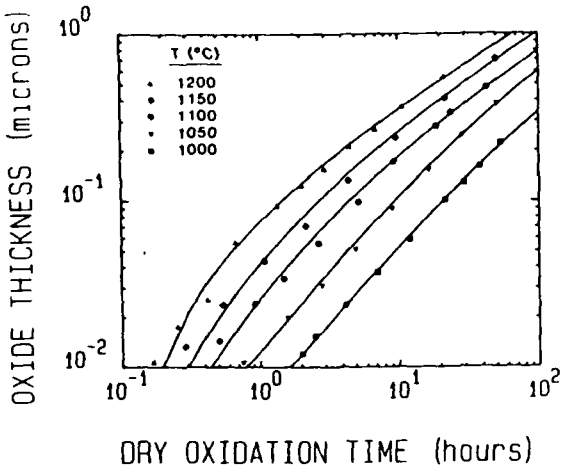


Fig. 1. $SiO_2$ thickness as a function of growth time on (100) β -SiC in dry $O_2$ in the temperature range of 1000°C-1200°C. The solid lines are theoretically calculated with eq. (1).

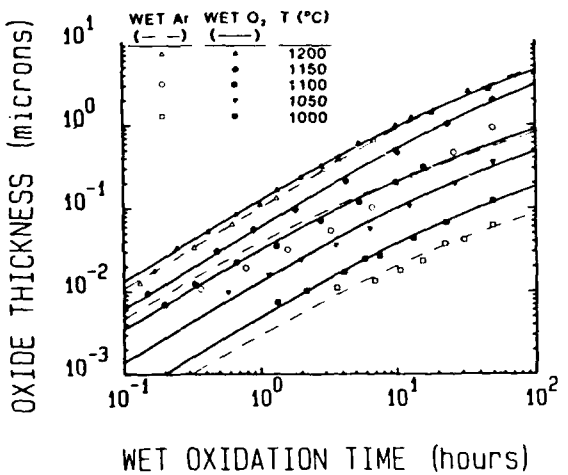


Fig. 2. $SiO_2$ thickness as a function of growth time of on (100) β -SiC in wet $O_2$ (black symbols and solid theoretical lines) and wet Ar (open symbols and dashed theoretical lines).



1200°C and 1000°C fit the theoretical curves well, but the data at 1100°C do not. This phenomenon cannot be explained at present.

The linear rate constants (B/A) are plotted as a function of the reciprocal of the absolute temperature in Fig. 3. The activation energies of the linear rate constants for each process were determined from the slope of each line. It can be seen that the temperature dependance is quite similar for each process, with the activation energies of the linear rate constants for dry $O_2$, wet $O_2$, and wet Ar having values of 58, 60, and 67 kcal/mol, respectively. These activation energies are related to the initial reaction rate limited regime of oxidation and correspond, as would be expected, to the 69.3 kcal/mol required to break a Si-C bond [10].

The activation energy of the parabolic rate constant is related to the oxidant diffusion rate controlled regime associated with longer times. The Arrhenius plot for the parabolic rate constants is shown in Fig. 4. For dry $O_2$, the parabolic rate constant has an activation energy of 34 kcal/mol, which is reasonably close to the accepted value of 27 kcal/mol for the diffusivity of oxygen through $SiO_2$ [11]. However, the parabolic rate constant for wet $O_2$ has an activation energy of 127 kcal/mol, which does not agree with the 18.3 kcal/mol for diffusion of $H_2O$ in $SiO_2$ [12]. In the case of wet Ar, as stated earlier, an even larger temperature dependence is seen with a value of 153 kcal/mol. It can be concluded that the activation energies for dry $O_2$ and wet Ar are valid for dry and truly wet oxidation and that the value for wet $O_2$ is a compromise between these extremes. This also explains the wide variance of values in previously published studies on the wet oxidation of SiC [5,7]. For instance, Fung and Kopanski reported an activation energy of 50 kcal/mol for the parabolic rate constant of wet oxidation of β-SiC, but their $O_2$ flow conditions were different than those used in this research. They obtained wet oxygen by burning $H_2$ (1000 ccm) and $O_2$ (700 ccm), which is equivalent to

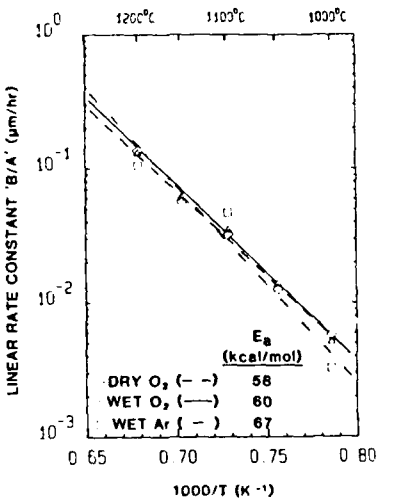


Fig. 3. Temperature dependence of the linear rate constants for oxidation in dry $O_2$, wet $O_2$, and wet Ar.

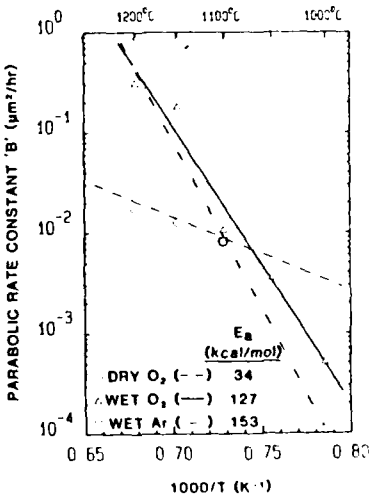


Fig. 4. Temperature dependence of the parabolic rate constants for oxidation in dry $O_2$, wet $O_2$, and wet Ar.

bubbling $O_2$ at 200 ccm through 95°C $H_2O$. Thus they would have less water vapor and more $O_2$ present in the atmosphere, causing the activation energy to be lower than the one obtained in this research. Thus it is proposed that the activation energy of the parabolic rate constant in wet oxidation is inversely proportional to the amount of $O_2$ present as the carrier gas.

The fact that none of the aforementioned activation energies for wet oxidation agree with the 18.3 kcal/mol for diffusion of $H_2O$ in $SiO_2$ has been noted by other authors as well [5,7]. It is commonly thought that, in the case of SiC wet oxidation, the activation energy of the parabolic rate constant reflects the outward diffusion of the by-product CO [13] and not the inward diffusion of $H_2O$, meaning that the out-diffusion of CO is the parabolic rate controlling factor.

## INTERFACE CHARACTERISTICS

During profilometer measurements, dry oxides always exhibited a very smooth surface while wet oxides always had a roughened surface. When these oxides were examined by scanning electron microscopy (SEM) it could be seen that the wet oxides had a mosaic arrangement of raised lines on a flat surface and the underlying SiC-$SiO_2$ interface contained corresponding grooves. This phenomenon is shown in Fig. 5(a). A higher magnification view is shown in Fig. 5 (b), showing a groove on the SiC side running into its corresponding raised line on the $SiO_2$ side. This behavior has been seen in all wet oxidation experiments regardless of the carrier gas (although it appears to be more severe in the case of wet Ar).

Cross-sectional transmission electron microscopy (XTEM) revealed that these lines occur where the wet atmosphere preferentially oxidizes the higher energy dislocation bands that are present in the sample, as shown in Fig. 6(a). Dry oxidation does not exhibit any preferential oxidation at these defects (Fig. 6(b)).

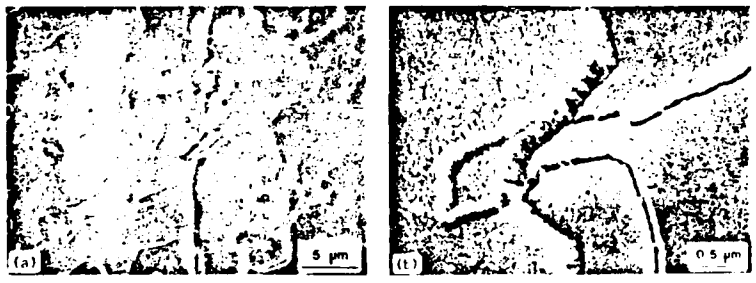


Fig. 5. SEM micrographs of (a) SiC oxidized in wet Ar at 1200°C for 80 mins. (0.1325 μm thick) and (b) the same sample at higher magnification. On both micrographs, the left side is the oxide surface and the right side is the SiC surface where the oxide has been removed by etching.



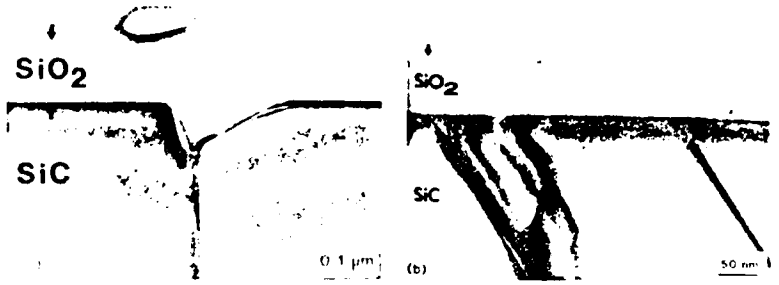


Fig. 6. XTEM micrographs of β-SiC oxidized in (a) wet $O_2$ at 1200°C for 58 mins., showing preferential oxidation at a dislocation band, and (b) dry $O_2$ at 1200°C for 60 mins., revealing no preferential oxidation.

It is proposed that the much higher solubility of $H_2O$ in $SiO_2$ ($3.4 \times 10^{19}$ $cm^{-3}$ at 1000°C) [12] as compared with that of $O_2$ ($5.5^2 \times 10^{16}$ $cm^{-3}$ at 1000°C) [11], causes the flux of $H_2O$ to be much higher than the flux of $O_2$. Therefore, in wet oxidation, the dislocation bands are allowed to preferentially oxidize because they are exposed to a large amount of $H_2O$. In dry oxidation, there is a limited amount of $O_2$ available and the dislocation bands are not allowed to oxidize faster than the unfaulted material.

## CONCLUSIONS

Thermal oxide layers were grown on the (100) face of β-SiC in dry $O_2$, wet $O_2$, and wet Ar atmospheres in the temperature range of 1000°C to 1200°C. The oxidation rates of all processes were found to obey the linear-parabolic equation that is accepted in the case of Si oxidation. The dry oxidation rate was found to surpass that of wet oxidation at 1050°C and below. The activation energies of the linear rate constants for all processes were quite similar and reasonably close to the 69.3 kcal/mol required to break a Si-C bond. While the 34 kcal/mol activation energy of the parabolic rate constant for dry $O_2$ agrees with the value for diffusion of $O_2$ in $SiO_2$ (27 kcal/mol), the values for wet $O_2$ and wet Ar did not agree with the value for diffusion of $H_2O$ in $SiO_2$ (18.3 kcal/mol). It is proposed that the out-diffusion of the by-product CO is actually the rate controlling factor. Because the wet $O_2$ oxidation rate in an $H_2O$ atmosphere is slower than that of its carrier gas (dry $O_2$) at 1050°C and below, the activation energy of the parabolic rate constant for wet oxidation is inversely proportional to the amount of $O_2$ present in the atmosphere. The two extremes of these values should be 34 kcal/mol (dry $O_2$) and 153 kcal/mol (wet Ar) with the value for wet $O_2$ lying somewhere in between, depending on the $O_2$ flow conditions. For the wet $O_2$ conditions used in this study, the activation energy of the parabolic rate constant was 127 kcal/mol.

Wet oxidation has been found to preferentially oxidize at dislocation bands that are present in the samples. SEM and XTEM show humps in the oxide and corresponding cuts in the underlying SiC. It is proposed that the higher solubility of $H_2O$ in $SiO_2$ causes a much higher flux for $H_2O$. This allows wet oxidation to be preferential, while the limited amount of $O_2$ available in dry oxidation does not allow the dislocations to oxidize faster.

ACKNOWLEDGEMENTS

The authors express their appreciation to Dr. C. Carter Jr., Mr. J. Ryu, and Mr. J. Edmond for their assistance in the XTEM sample preparation and microscopy, and to Mr. R. Kunz for assistance in the SEM work. The authors also wish to thank Dr. B. Deal for his valuable comments. This work was supported by the Office of Naval Research under contract N00014-82-K-0182 P0005.

REFERENCES

1. R.W. Keyes, Silicon Carbide-1973, edited by R. C. Marshall, J. W. Faust, Jr., and C. E. Ryan, (University of South Carolina Press, Columbia, S.C., 1974), p.534.

2. C.E. Ryan, ibid., p.651.

3. E. Fitzer and R. Ebi, ibid., p. 320.

4. R.C.A. Harris and R.L. Call, ibid., p.329.

5. A. Suzuki, et al., Jap. J. Appl. Phys. 21, 579 (1982).

6. B.E. Deal and A.S. Grove, J. Appl. Phys. 36, 3770 (1965).

7. C.D. Fung and J.J. Kopanski, Appl. Phys. Lett., 45, 575 (1984).

8. P. Liaw and R. F. Davis, J. Electrochem Soc., 132, 642 (1985).

9. C.H. Carter, et al., "Cross-Sectional Transmission Electron Microscopy of Defects in Beta Silicon Carbide Thin Films," presented at 1985 Spring Meeting of MRS, San Francisco; to be published in the MRS Symposia Proc.

10. L. Pauling, The Nature of the Chemical Bond and the Structure of Molecules and Crystals, 3rd Ed., Cornell University, New York, 85 (1960).

11. A.J. Moulson and J.P. Roberts, Trans. Faraday Soc. 57, 1208 (1961).

12. F.J. Norton, Nature 171, 701 (1961).

13. R.W. Kee, et al., J. Vac. Sci. Technol., 15 1520 (1978).

# DRY ETCHING OF β-SiC IN $CF_4$ AND $CF_4$+$O_2$ MIXTURES

J. W. PALMOUR and R. F. DAVIS
Materials Engineering Department, North Carolina State University
Raleigh, NC 27695-7907

and

T. M. WALLETT and K. B. BHASIN
National Aeronautics and Space Administration, Lewis Research Center
Cleveland, Ohio 44135

## Abstract

Dry etching of cubic (100) β-SiC single crystal thin films produced via CVD has been performed in $CF_4$ and $CF_4$+$O_2$ mixtures, in both the reactive ion etching (RIE) and plasma etching modes. The latter process yielded measurable etch rates, but produced a dark surface layer which appears, from the results of secondary ion mass spectrometry, to be residual SiC. The RIE samples had no residual layer, but Auger electron spectroscopy did reveal a C-rich surface. The optimal RIE conditions were obtained with 10 sccm of pure $CF_4$ at 40 mTorr and a power density of 0.548 W/cm$^2$, giving an etch rate of 23.3 nm/min. Neither the increase of temperature between 293K and 573K, nor the incremental addition of $O_2$ to $CF_4$ to 50%, produced any strong effect on the etch rates of SiC during RIE. Pictorial evidence of fine line structures produced by RIE of β-SiC films are also presented.

## I. Introduction

Because of its wide band gap, short carrier lifetime, and high thermal conductivity, β-SiC is a promising semiconductor material for high temperature, high frequency, and high power electronic devices.[1,2] It has been reported that this material is also resistant to radiation damage.[3] Blue light-emitting diodes[4] and bipolar transistors[5] have been fabricated using 6H SiC; pn junctions[6] have also been produced using β-SiC. In order to fabricate devices, a method of surface removal and mesa etching is needed. Because the

only suitable wet etchants for SiC are molten salts at 1173K-1273K,[7] dry etching techniques have also been investigated.

The majority of studies concerned with the dry etching of SiC has been conducted on sputter deposited material which is presumed to be amorphous (a-SiC). Winters has shown that $XeF_2$ vapor combined with $Ar^+$ bombardment from a differentially pumped ion gun readily etches a-SiC[8], while the use of $XeF_2$ alone does not.[9] The major Si-containing product from this reaction was found to be $SiF_4$, while the major C-containing product was proposed to be either $CF_4$ or $CF_2$, although it could not be identified. Reactive ion etching of a-SiC using $CF_4$ has also yielded good etch rates.[10] Finally, plasma etching of hydrogenated a-SiC films[11] using $CF_4$+$O_2$ has been studied, but the mixing ratios were not reported.

Monocrystalline β-SiC has been dry etched using reactive ion-beam techniques[12] with $CF_4$ and $CF_4$+$O_2$ mixtures as the reactive gases. This study found that the maximum etching rate was obtained when the amount of $O_2$ was 40%. It was proposed that in the case of pure $CF_4$, the Si etched away as $SiF_4$, while the C remained on the surface to be removed by sputtering. When $O_2$ was added to the system, the cause of the enhanced etch rate was theorized to be the reaction of C and O to form CO or $CO_2$.

The principal objective of the present research was to examine non-beam techniques of dry etching, namely plasma and reactive ion processes, and their effect on the removal of material from cubic (100) monocrystalline β-SiC thin films under various conditions. In both techniques, $CF_4$ and $CF_4$+$O_2$ mixtures were employed as the reactant gases.

## II. Experimental

The (100) β-SiC thin films used in these experiments were epitaxially grown on Si substrates[13] via chemical vapor deposition and subsequently

polished with 0.1 μm diamond paste. In order to remove the top 20 nm of material damaged during polishing, the wafers were oxidized in dry $O_2$ at 1473K for 90 mins.[14] and the oxide layer removed in HF. Positive photoresist was used as the mask material in the plasma etching experiments while Cr and Al were used as the mask materials in the RIE etch rate and fine line lithography experiments, respectively.

Plasma etching was performed on the grounded, water cooled plate of a small, conventional parallel plate system using an RF power supply at 30 kHz, pressures from 0.5 to 2 Torr and power densities from 0.081 to 0.326 $W/cm^2$ (on an 11 in. electrode). Reactive ion etching was performed on a 6 inch diameter driven electrode in a conventional parallel plate RIE system using a 2 inch plate separation and a 13.56 MHz power supply, at a variety of power densities (0.274 to 1.92$W/cm^2$).

All etch rates were obtained by measuring steps, which were etched for 10 minutes, with a profilometer. The etched and unetched surfaces were also studied with Scanning Electron Microscopy (SEM), Auger Electron Spectroscopy (AES), and Secondary Ion Mass Spectrometry (SIMS).

Fine line patterns were produced using the standard "lift off" photolithographic technique. The Al patterned sample was then reactive ion etched with 10 sccm $CF_4$ at a pressure of 40 mTorr and 0.548 $W/cm^2$ power density for 50 minutes.

## III. Results and Discussion

### A. Plasma Etching

High pressure plasma etching in varying mixtures of $CF_4$ and $O_2$ yielded measurable etch rates in the range of 15 to 55 nm/min. However, these rates were inconsistent and non-reproducible because of poor gas flow and pressure control. More importantly, this process produced a dark surface layer with a

thickness in the range of 20 to 150 nm, depending on the etch time and power used. The composition of this layer was at first assumed to be C residue because the Auger spectra indicated mostly C with a very small Si peak. However, the layer would not quickly oxidize at 1473K, nor would it etch in hot $HNO_3$, as C would be expected to do. When the bulk of the dark layer was analyzed using SIMS, the layer was found to have a composition almost identical to that of unetched SiC. The only major difference between the spectra is that the surface layer had a substantially higher flourine content than unetched SiC; however this level was orders of magnitude below the levels of Si and C. Thus, it is assumed that the dark layer is actually residual SiC with a C-rich surface.

B. Reactive Ion Etching

When SiC was etched using RIE, no dark surface layer was formed under most of the conditions used. However, there was a slight discoloration of the sample surface. This phenomena was caused, in part, by surface roughening during etching, but also could again be attributed to the formation of a C-rich surface, which was detected by AES. The Auger spectra for a β-SiC surface which has been HF etched and sputter cleaned to remove the native oxide and for one which has been reactive ion etched (pure $CF_4$) are shown in Figs. 1(a) and (b), respectively. There is a definite weakening of the Si signal and strengthening of the C signal after reactive ion etching relative to that of the sample which had not undergone RIE. Also present in the spectra for the RIE sample, is a moderate amount of O, which most likely adsorbed onto the surface after removal from the etching chamber. The three small peaks from 590 to 700 eV on the same spectra are attributed to the presence of Fe sputtered from the electrodes which would overlap any F signal. The C content of the surface increases with etching power density. When the power is

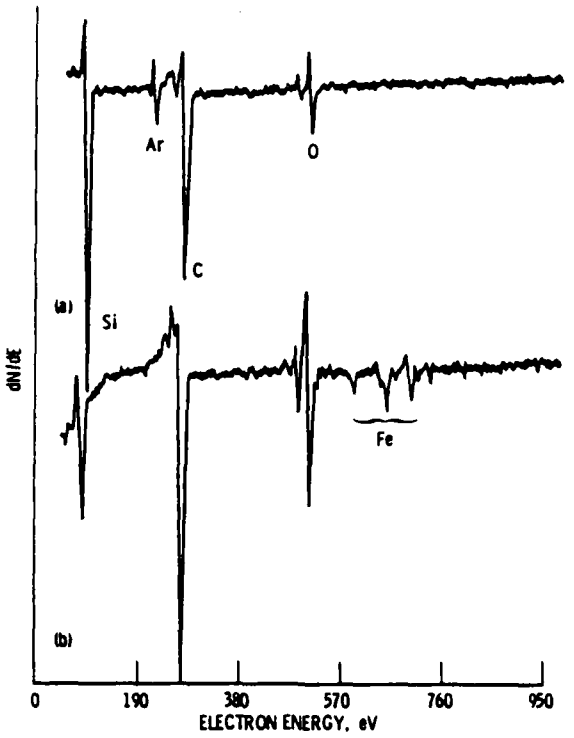


Fig. 1. Auger spectra obtained at 3kV and 5mA for (a) an $Ar^+$ sputter cleaned SiC surface, and (b) a SiC surface after RIE in $CF_4$ (40 mTorr, 0.548 $W/cm_2$). Note the decrease and increase in the intensities of Si and C, respectively, as a result of RIE. Both starting samples were sections derived from the same thin film.

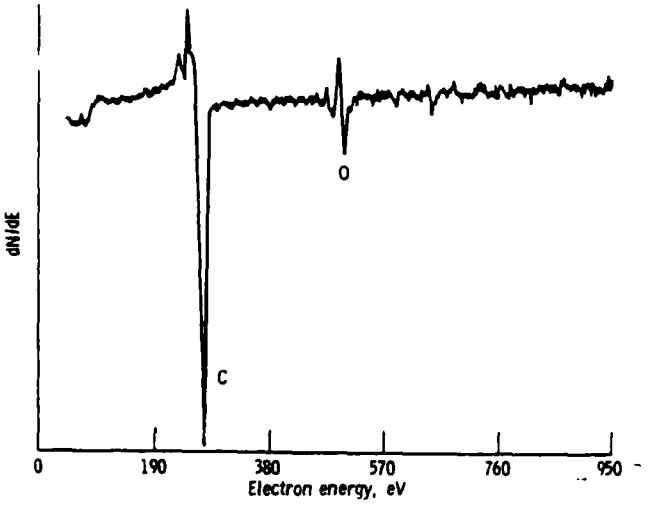


Fig. 2. Auger spectrum obtained at 3kV and 5mA for a sample surface which shows the absence of Si after RIE at high power in $CF_4$ (1.92 $W/cm^2$ 40 mTorr).

increased to 1.92 $W/cm^2$, the KLL peak for Si (87 eV) completely disappears, as shown in Fig. 2 (there was a small LMM Si peak at 1606 eV), leaving C as the principal constituent. This C-rich layer resulted in a large amount of leakage current on a SiC $n^+p$ junction diode[6] fabricated by mesa etching via RIE. The leakage current was greatly reduced by oxidizing the C-rich surface after etching. The physical and electrical effects of reactive ion etching of SiC will be the subject of future research.

It was originally thought that the addition of $O_2$ to $CF_4$ would enhance the etch rate of SiC, as seen in the reactive ion-beam studies mentioned previously. However, Fig. 3 shows that there was no significant effect of $O_2$ up to 50%. In fact, there was a steady decrease in the etch rate as more $O_2$ was introduced, presumably because of the decreased availability of free F atoms. The fact that $O_2$ did not affect the SiC etch rate suggests that the C does not etch away as CO or $CO_2$. Because of this trend it was decided that this study would concentrate on reactive ion etching of SiC in pure $CF_4$ plasmas.

The etch rates in pure $CF_4$ increased quite sharply with the RF power density, as would be expected. Fig. 4 shows that the etch rates at a pressure of 40 mTorr go from 6.8 nm/min at 0.274 $W/cm^2$ up to 62.2 nm/min at 1.92 $W/cm^2$. However, at the higher power densities the samples exhibited substantial surface roughening. The optimum power density was determined to be 0.548 $W/cm^2$, which maintained a suitable etch rate (23.3 nm/min) while reducing the surface roughening to a minimum.

The curve of the SiC etch rate versus $CF_4$ pressure is shown in Fig. 5. As can be seen, the etch rate decreases rapidly when the pressure goes below 20 mTorr because of the decrease in the free F concentration. The etch rate also falls above 40 mTorr because of the decrease in bias voltage, and thus a drop

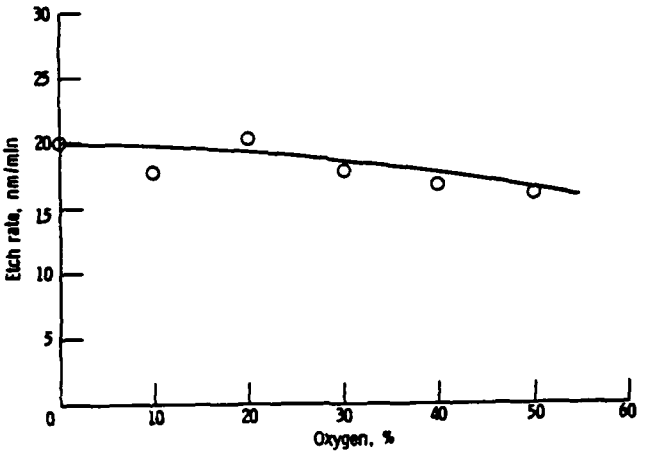


Fig. 3. RIE rates vs. % $O_2$ in $CF_4$ obtained at a pressure of 20 mTorr and a power density of 0.548 $W/cm^2$.

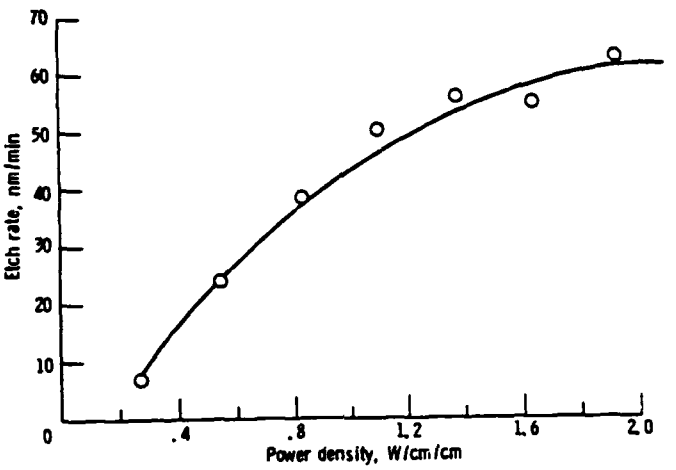


Fig. 4. RIE rates vs. RF power density in $CF_4$ at 40 mTorr and 10 sccm.

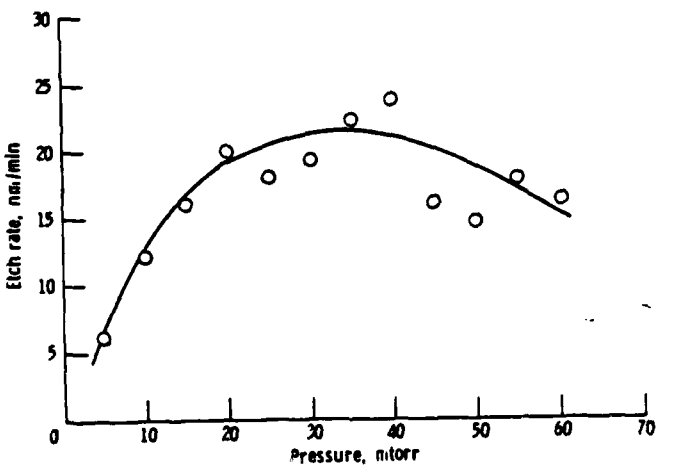


Fig. 5. RIE rates vs. $CF_4$ pressure at 10 sccm and 0.548 $W/cm^2$.

in ion energy[15], that is associated with higher pressures. The optimal etching pressure for SiC was determined to be 40 mTorr. Because of the scarcity of this material, it was not feasible to examine the loading effect of SiC on RIE rates. All etching experiments were performed with only one or two samples (0.25 $cm^2$ each) present in the chamber.

All of the aforementioned RIE experiments were performed on an uncooled electrode. As such, the measured electrode temperature was about 310K. The effect of temperature on the reactive ion etching rates in pure $CF_4$ was investigated from 293K to 573K (electrode temperature) using a power density and pressure of 0.548 $W/cm^2$ and 40 mTorr, respectively. While there was a slow increase in etch rate with increasing temperature, most likely caused by an increase in the reactivity of the sample, there was no dramatic increase that would indicate that any etch product remaining on the SiC surface was volatilized.

As stated earlier, fine line structures were fabricated on SiC using reactive ion etching. A 2 μm line pattern is shown in Fig. 6(a), along with a higher magnification view of the line's edge in Fig. 6(b). Both of these views show very good edge definition, with sharp vertical walls and no undercutting. One should note the short columns, or "spikes", that start to occur on the etched SiC surface away from the sidewalls. The origin and composition of these columns are unknown, but they have only been observed in the case of a deeper etch such as this (etched 5 times longer than the etch rate experiments). It is possible that this phenomenon, which darkened the surface, is related to the surface layer observed in the case of plasma etching. In future research, these spikes will be studied in more detail.

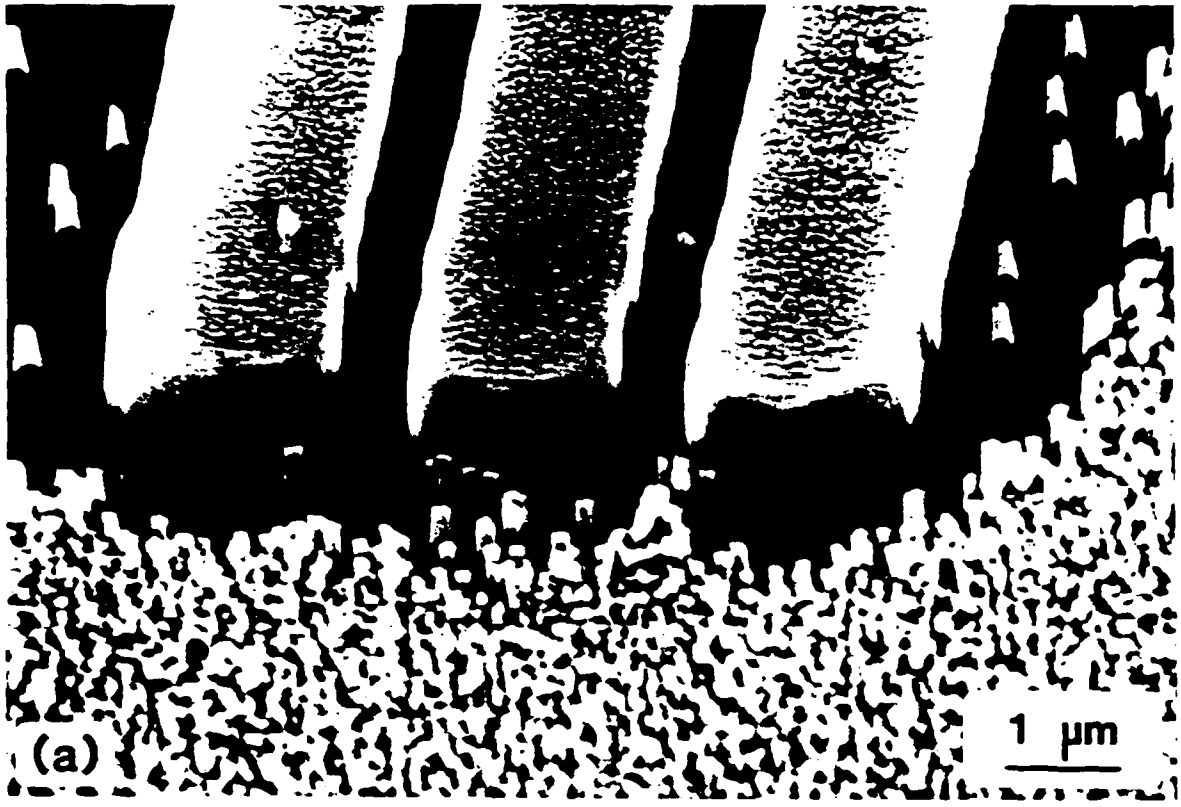


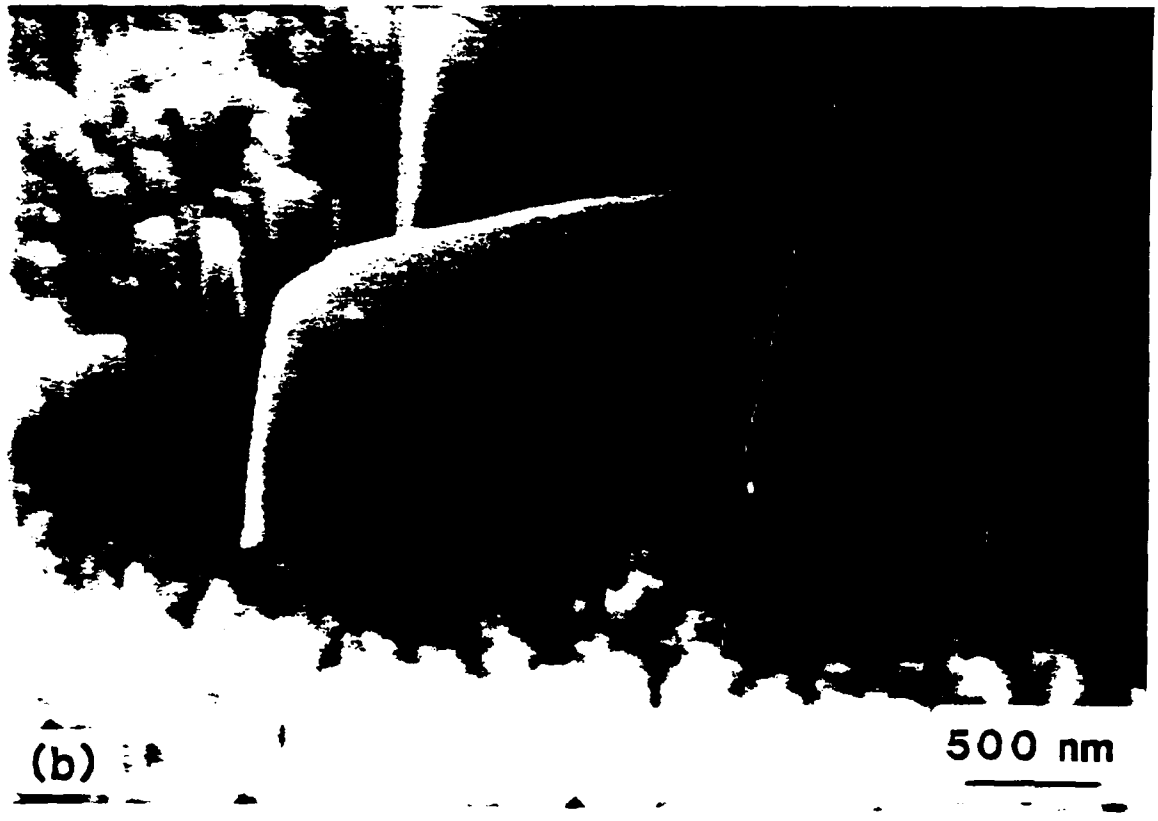


Fig. 6. (a) Fine line pattern (2 μm line width) on SiC obtained by RIE and (b) perspective view of the edge definition of the pattern.

## IV. Conclusions

Dry etching of single crystal thin films of β-SiC has been successfully performed in $CF_4$ and $CF_4$+$O_2$ plasmas. In the case of high pressure plasma etching, which does not employ ion bombardment, etch rates were desirably high (15 nm/min to 55 nm/min). However, a dark, relatively thick, surface layer was formed during etching which was determined to be residual SiC with a C-rich surface.

Reactive ion etching of SiC, which does utilize ion bombardment, yielded good etch rates without, in most cases, the formation of any residual layer. However, AES shows that a C-rich surface was also formed during this process and that the C content of the surface increased with power density. Furthermore, the presence of this surface layer caused high leakage current. Optimal RIE conditions were obtained using a flow of 10 sccm of pure $CF_4$, a pressure of 40 mTorr, and a power density of 0.548 W/cm$^2$. These conditions gave an etch rate of 23.3 nm/min and minimal surface roughening. This optimal etch rate was obtained at an electrode temperature of about 310K; however, positive and negative variations in the temperature from this point were found to have no strong effect on the etch rates. Using these conditions, high quality fine line structures were fabricated on SiC via RIE, but the deep etch produced surface roughness in the form of closely packed "spikes."

As determined by Winters[8], the major Si-containing etch product is $SiF_4$ (gas) when SiC is etched in the presence of $XeF_2$ and $Ar^+$ bombardment, and it is assumed that this is also true for the case of RIE with $CF_4$ and $CF_4$+$O_2$. In the present RIE research, the addition of $O_2$ to $CF_4$ did not affect the SiC etch rate which indicates that the C does not etch away as CO or $CO_2$. Furthermore, the yield of elemental C by physical sputtering of SiC is very small.[16] Thus, the major C-containing etch product is assumed to be $CF_4$ or $CF_2$

(although the presence of other fluorocarbon compounds is possible), as was also suggested by Winters' work.

Acknowledgments

The authors express their appreciation to Dr. W. D. Williams, Mr. C. Hulbert, and L. Hinkle for their assistance in the photolithography and SEM work, and to Dr. D. P. Griffis and Mr. M. Mantini for their help with the SIMS and Auger analysis, respectively. The authors also wish to thank Dr. J. Dickman for his helpful discussions. This work was partially supported by the Office of Naval Research under contract N00014-82-K-0182P0005.

References

1. R. W. Keyes, SiC-1973, University of South Carolina Press, S. C., 534 (1974).

2. C. E. Ryan, SiC-1973, University of South Carolina Press, S.C., 651 (1974).

3. E. H. Voice, SiC-1968, Permagon Press, New York, S331 (1969).

4. A. Suzuki, et al., J. Appl. Phys., 47,4546 (1976).

5. W. von Munch and P. Hoeck, Sol. State Electronics, 21,479 (1978).

6. J. S. Ryu and R. F. Davis, Accepted for publication in MRS Symposium Proceedings, Symposium B, Fall, (1985).

7. J. W. Faust, Jr., Silicon Carbide - A High Temperature Semiconductor, Permagon Press, New York, 403, (1960).

8. H. F. Winters, J. Vac. Sci. Technol. B, 1(4), 927 (1980).

9. H. F. Winters and J. W. Coburn, Appl. Phys. Lett., 34, 70 (1979).

10. S. Krongelb, IBM Tech. Discl. Bull., Vol. 23, 2, 828 (1980).

11. C. Y. Chang, et al, J. Electrochem. Soc., Vol. 132, 2, 418 (1985).

12. S. Matsui, et al, Jap. J. Appl. Phys., Vol. 20, 1, L38 (1981).

13. P. Liaw and R. F. Davis, J. Electrochem. Soc., 132, 642 (1985).

14. J. W. Palmour and R. F. Davis, Accepted for publication in MRS Symposium Proceedings, Symposium E, Fall (1985).

15. D. J. DiMaria, L. M. Ephrath and D. R. Young, J. Appl. Phys., Vol. 50, 4015 (1979).

16. L. Maissel, in Handbook of Thin Film Techn., L. Maissel and R. Glang, ed. McGraw Hill, N.Y., 3-1 (1970).

# APPENDIX I

## Report on the SiC National Review Meeting

### I. INTRODUCTION

The function of this report is to provide a summary of the second ONR-sponsored one day National Review Meeting concerned with "The Growth and Characterization of SiC and its Employment in Semiconductor Applications". The workshop was held on Monday and Tuesday, November 18-19, 1985 at the McKimmon Continuing Education Center on the campus of North Carolina State University. The primary objective of the workshop was the discussion and exchange of ideas regarding the current state of research aimed at developing SiC semiconductor devices. An overview of this workshop and suggestions for the future meetings to be held in subsequent years is given in the following section.

### II. CONDUCT AND ACCOMPLISHMENTS OF THE SiC WORKSHOP

The two-day workshop brought together persons from within the borders of the United States who are (1) currently conducting research on SiC for semiconductor applications, (2) planning research programs in SiC or (3) interested in following the development of this material and its applications.

A notice of the meeting and the call for papers (lectures) was broadcast via a memorandum to parties known to be working or interested in the field of SiC as a semiconductor material. This call resulted in the submission of twenty-two (22) abstracts which were accepted. These were arranged into a formal program which contained both a review of the previous SiC semiconductor research and papers concerned with current key issues on various program topics. A copy of the program and the abstracts of the papers in the order of their presentation are given in Sections V and VI, respectively. In addition, the notice of the meeting resulted in the attendance of 57 persons representing universities, government laboratories and corporations from all

over the United States. A list of attendees is presented in Section VII.

The formal program was opened by Dr. J. J. Hren, Head, Department of Materials Engineering who welcomed the guests and provided a brief review of the department. The review format was continued by W. J. Choyke, who described the previous growth and photo-optical research at the Westinghouse R and D Center.

Recent growth research at NASA-Lewis and NCSU was the next topic on the agenda. Powell (NASA) described their results of numerous runs in a horizontal reactor, Jackson et al. (Howard) detailed (poster paper) the use of Auger spectroscopy to optimize the growth and Kim (NCSU) reported the effects of changing the Si/C ratio on the physical character of the films. These papers were followed by the reports of infrared reflectance evaluations and ESR studies on the NCSU films by Holm et al. and Carlos et al., respectively, of the Naval Research Laboratory.

The following papers described the research by Bellina et al. regarding the effects of heating and ion bombardment on the stoichiometry of β-SiC and the TEM studies of Chorey et al., particularly in regard to the defects at the Si/SiC interface. Additional TEM studies combined with electrical property measurements on films implanted with B or N and annealed were described by Ryu. The electrical property theme was continued in a poster paper by Spencer et al. and by Matus with a formal presentation which ended this first session.

The initial papers in the next session were concerned with metal contact/SiC studies. Formal presentations by Messick et al. Ioannou and Papanicolaou and Zeller, as well as a poster paper by Kelner and Binari, discussed this theme from variety of avenues. The first portion of this session was concluded with a presentation which described a variety of characterization studies recently conducted on in situ doped β-SiC films

produced at NCSU.

The final half of the second session included papers on the theoretical and experimental aspects of P and Al doping amorphization and rapid thermal annealing by Edmond, a somewhat similar study for Band N doping by Ryu and photoluminescence spectroscopy studies on Al implanted material by Freitas et al. The last two papers of the meeting were oriented toward the fabrication of devices. Specifically, the fabrication of p-n junction diodes was discussed by Kopanski and a paper regarding the inversion layer behavior of MOS structures on β-SiC was presented by Avila.

For a more complete review of the content of the papers noted above, the reader's attention is directed to the abstracts in Section VI.

## III. ARRANGEMENTS AND FINANCE

The meeting was arranged by the staff of the McKimmon Center. Sponsorship was derived from a grant from ONR. This covered the cost of space, secretarial, copies of abstracts and letters, postage and communications and staff time. The attendees paid a registration fee of $30.00 to cover the cost of a dinner, a luncheon and coffee breaks.

## IV. FUTURE MEETINGS

Similar or enlarged meetings will be held at NCSU in each of the years of 1986 and 1987. Support will again be derived from ONR. Notes derived from discussions with several attendees indicate that the two-day format with an "in-house" dinner and discussion period was suitable and useful for the discussion of ideas.

SECTION V

PROGRAM

# Second National Review Meeting on Growth and Characterization of SiC and its Employment in Semiconductor Applications

Jane S. McKimmon Center for Extension and Continuing Education
North Carolina State University
Corner of Western Boulevard and Gorman Street
Box 7401
Raleigh, NC 27695-7401

Monday, November 18
and
Tuesday, November 19

SECOND NATIONAL SIC REVIEW MEETING
NOVEMBER 18-19, 1985

Monday, November 18

| | | |
|---|---|---|
| 12:30 p.m. and 12:45 p.m. | Bus leaves Quality Inn Mission Valley for Jane S. McKimmon Center | |
| 12:30 p.m. | Registration - Lobby, McKimmon Center | |
| 1:00 p.m. | Introduction to NCSU<br>Overview of Workshop and Remarks | J. J. Hren<br>R. F. Davis |
| 1:15 p.m. | "SiC Studies at the University of Pittsburgh and the Westinghouse R&D Center" | W. J. Choyke |
| 1:45 p.m. | "Growth and Characterization of Cubic SiC Single Crystal Films on Si" | J. A. Powell<br>L. G. Matus<br>M. A. Kuczmarski |
| 2:10 p.m. | "Theoretically Predicted and Experimentally Determined Effects of the Si/C Phase Ratio on the Growth and Character of Monocrystalline Beta Silicon Carbide Films" | H. J. Kim<br>R. F. Davis |
| 2:35 p.m. | "Infrared Reflectance Evaluation of CVD SiC Films Grown of Si Substrates" | R. T. Holm, P.H. Kle<br>P.E.R. Nordquist, Jr |
| 3:05 p.m. | "ESR Studies of Doped Cubic SiC" | W. E. Carlos, J. Ryu<br>R. Kaplan, R.F. Davi |
| 3:30 p.m. | Break - see also Poster "Newspaper" | |
| 4:00 p.m. | "On the Stoichimoetry of (100) 3C-SiC after Heating & Ion Bombardment as observed by Angle-Resolved Auger Electron Spectroscopy" | Joseph J. Bellina, J<br>Stephen V. Pepper<br>Mary V. Zeller |
| 4:25 p.m. | "A TEM Investigation of Beta-SiC grown Epitaxially on Silicon Substrate by Chemical Vapor Deposition" | C. M. Chorey<br>P. Pirouz, J.A. Powe<br>T. E. Mitchell |
| 4:50 p.m. | "Structural and Electrical Characterization of Beta Silicon Carbide Thin Films" | J. S. Ryu<br>R. F. Davis |
| 5:15 p.m. | "Electrical Properties of Cubic SiC Epitaxial Films" | L. G. Matus<br>J. A. Powell |
| 5:35 p.m. | "Discussion of Future Directions for Growth and Characterization of Beta-SiC | R. F. Davis |
| 6:00 p.m. | Social and Dinner at McKimmon Center | |
| 8:00 p.m. | Bus leaves McKimmon Center for Hotel | |

Tuesday, November 19

| | | |
|---|---|---|
| 7:30 a.m. and 7:45 a.m. | Bus leaves Quality Inn Mission Valley for Jane S. McKimmon Center | |
| 8:00 a.m. | "Characterization, MOS/C-V Structures and Ohmic Contact Studies on Beta-SiC Epilayers" | L. Messisk, D.I. Elc<br>C. R. Zeisse,<br>M. J. Taylor<br>K. Moazed<br>D. P. Mullin<br>H. H. Caspers |
| 8:30 a.m. | "Metal Contacts of Beta-SiC" | D. E. Ioannou<br>N. A. Papanicolaou |
| 8:50 a.m. | "Continuation Studies of M/SiC Interfaces-Carbide Formers" | M. V. Zeller |
| 9:10 a.m. | "Oxidation and Dry Etching of Beta-SiC Single Crystal Thin Films" | J. W. Palmour<br>R.F. Davis<br>T. M. Wallett<br>K. B. Bhasin |
| 9:30 a.m. | "Characterization of n- and p- type Beta-SiC Monocrystalline Thin Films in Situ Doped via Chemical Vapor Deposition Process" | H. J. Kim<br>R. F. Davis |
| 9:50 a.m. | Break - see also Poster "Newspapers" | |
| 10:10 a.m. | "Amorphization and Recrystallization Processes in Monocrystalline Beta Silicon Carbide Thin Films" | J. A. Edmond<br>R. F. Davis |
| 10:30 a.m. | "Rapid Thermal Annealing of B or N Implanted Monocrystalline Beta-SiC Thin Films and its Effect on Electrical Properties and Device Performance" | J. S. Ryu, R.F. Dav |
| 10:50 a.m | "Photoluminescence Spectroscopy of Ion Implanted Cubic SiC Grown by Chemical Vapor Deposition" | J. A. Freitas, Jr.<br>S. G. Bishop<br>J. A. Edmond, J. Ryu<br>R. F. Davis |
| 11:10 a.m. | "Ion-Implanted Planar SiC p-n Junction Diodes" | J. J. Kopanski<br>R. E. Avila<br>C. D. Fung |
| 11:30 a.m. | "Inversion Layer Behavior of MOS Structures on 3C Silicon Carbide" | R. E. Avila<br>J. J. Kopanski<br>C. D. Fung |
| 11:50 a.m. | Wrap-up and adjournment of Session | |
| 12:00 noon | LUNCH | |

SECTION VI - ABSTRACTS

# SiC Studies at the University of Pittsburgh and the Westinghouse R&D Center

W.J. Choyke
University of Pittsburgh and Westinghouse R&D
Pittsburgh, PA

## Abstract

A short historical review will be given of the developments of SiC in Western Pennsylvania since the turn of the 20th Century. The fundamental studies on SiC initiated at the Westinghouse Research Laboratories over 30 years ago will round out the background phase of this discussion.

Current programs that will be briefly touched upon are the following:

1. Damage profiles and annealing studies of hydrogen implanted 6HSiC using RBS/Channeling and XTEM.
2. Surface modification of SiC by ion implantation.
3. Plasma deposition of SiC thin films.
4. U.H.V. studies of SiC synthesis.
5. A comparison study using low temperature luminescence and Raman scattering of 3C SiC single crystal films grown at NASA-Lewis and a variety of Hexagonal/ Rhombohedral polytypes grown at (W) R&D.

# Growth and Characterization of Cubic SiC Single Crystal Films on Si

J. A. Powell, L. G. Matus, and M. A. Kuczmarski

NASA Lewis Research Center
Cleveland, Ohio 44135

## ABSTRACT

Single crystal cubic SiC films, up to 40 um thick, have been grown by chemical vapor deposition on single crystal Si substrates. A morphological study has been made of films produced in several hundred growth runs. Results show that films can be produced that are smooth and featureless. However, many films exhibit a variety of features that include film/substrate warpage, ridges, regular-shaped bumps, and irregular-shaped depressions. The electrical properties of the films seem to be independent of the presence of most of these morphological features. In addition to the above results, various factors that can affect the film growth will also be discussed.

# THEORETICALLY PREDICTED AND EXPERIMENTALLY DETERMINED EFFECTS OF THE Si/C GAS PHASE RATIO ON THE GROWTH AND CHARACTER OF MONOCRYSTALLINE BETA SILICON CARBIDE FILMS*

H. J. Kim and R. F. Davis
Department of Materials Engineering
North Carolina State University
Raleigh, NC 27695-7907

## ABSTRACT

The effects of the Si/C ratio in the reaction gas stream on the growth and properties of monocrystalline β-SiC films grown on the Si (100) substrates via chemical vapor deposition have been theoretically and experimentally studied. The amounts of the condensed phases of β-SiC and Si, and the partial pressures of the Si- and C-containing gases as a function of the Si/(Si+C) ratio in the source gases have been initially obtained from thermodynamic calculations using the "SOLGASMIX-PV" computer program. This was followed by the experimental study of growth rate, microstructure, carrier concentration and resistivity of monocrystalline β-SiC thin films as a function of the Si/(Si+C) ratio in the source gases.

The highest growth rate, a minimum value of resistivity and a maximum value of carrier concentration of the β-SiC films were obtained near Si/(Si+C) = 0.5. Inclusion-free β-SiC films were also produced near the same range of the Si/C ratio.

* Sponsored by the Office of Naval Research under Contract No. N00014-82-K-0182 P0005, Max Yoder, monitor.

# INFRARED REFLECTANCE EVALUATION OF CVD SiC FILMS GROWN ON Si SUBSTRATES

R. T. Holm, P. E. R. Nordquist,Jr. and P. H. Klein

Naval Research Laboratory
Washington, DC 20375

Infrared reflectance from 400 to 4000 $cm^{-1}$ provides a routine, non-destructive evaluation of SiC films immediately after growth. Our SiC crystals are grown on (100) Si substrates by chemical vapor deposition. First, a buffer layer is grown at about 1350C in a propane-hydrogen mixture. Layer growth then follows in a silane-propane-hydrogen mixture with C/Si typically 1.5.

Film thickness and film-thickness uniformity can be determined from the interference fringes beyond 2000 $cm^{-1}$. Surface roughness becomes evident in the reststrahlen region between 800 and 950 $cm^{-1}$. Mechanical polishing produces a damaged layer which is also seen in this region. Interfacial roughness is revealed by a decreasing fringe envelope beyond 2000 $cm^{-1}$.

Films with low carrier concentrations have deep minima in their spectra near 1000 $cm^{-1}$. These minima shift to higher wavenumbers for carrier concentration greater than $10^{18}$ $cm^{-3}$. The concentration can be estimated from the size of the shift.

While IR reflectance spectra can be used for selection of "good" specimens, they do not differentiate among smooth layers with carrier concentrations less than $10^{18}$ $cm^{-3}$. Concentrations below $10^{18}$ $cm^{-3}$ could be estimated from spectra recorded below 250 $cm^{-1}$.

# ESR Studies of Doped Cubic SiC

W.E. Carlos and R. Kaplan
Naval Research Laboratory, Washington, DC.

J. Ryu and R.F. Davis
North Carolina State University, Raleigh, NC.

Electron Spin Resonance measurements on unintentionally doped Beta-SiC films grown on Si(100) reveal a three line isotropic spectrum characteristic of nitrogen. Subtle changes in this spectrum with annealing are observed which may indicate defect migration and complexing. The binding energy of the donor may be estimated from the strength of the hyperfine interaction or an activation energy analysis of the intensity. These yield a binding energy of about 0.05 eV which agrees fairly well with ESR results on nitrogen-doped bulk material as well as results from transport and cyclotron resonance measurements. The ESR results will be compared with transport measurements on these films. The spectra of films which have been implanted with boron show similar amounts of nitrogen. In addition, a much weaker structure which may be due to boron is also apparent.

# On the Stoichiometry of (100) 3C-SiC after Heating and Ion Bombardment as observed by Angle-Resolved Auger Electron Spectroscopy

Joseph J. Bellina, Jr
Saint Mary's College, Notre Dame, IN 46556 and
NASA Lewis Research Center, Cleveland, OH 44135

Stephen V. Pepper
NASA Lewis Research Center, Cleveland OH 44135

and
Mary V. Zeller
University of Notre Dame, IN 46556

The changes of the stoichiometry of the (100) surface of 3C-SiC was monitored during, and after, heating or Argon ion sputtering in situ in ultra-high vacuum. The Auger Electron Spectroscopy (AES) derivative line shapes and peak-to-peak heights of the Si LVV and C KLL transitions indicated changes in surface stoichiometry, bonding, and short range order. To improve sensitivity to the surface, angle-resolved AES spectra were obtained from electrons which leave the surface at a grazing angle, and for comparison from electrons which leave normal to the surface.
Heating above about 1050 Celsius depleted the surface of silicon with an activation energy of 120 kcal/mole, resulting eventually in an disordered graphitic layer several atomic layers thick. Bombardment by Ar ions of energies greater than 500 eV enhanced the Si to C ratio of the surface and changed the C KLL line-shape-fine-structure. Subsequent annealing at a less than 600 Celsiius restored the fine structure.
The results of the angle-resolved AES measurements indicate that under all conditions of ion bombardment and heating which were observed, the C to Si ratio in the spectra obtained from grazing exit is greater than previously observed by conventional AES or from that obtained with normally exiting electrons. This suggests that the free surface is ordinarily enriched with carbon.

# A TEM Investigation of beta-SiC grown epitaxially on silicon substrate by Chemical Vapor Deposition

C. M. Chorey(1), P. Pirouz[(1)], J. A. Powell[(2)] & T. E. Mitchell[(1)]
(1) Department of Metallurgy & Materials Science, Case Western Reserve University, Cleveland, OHIO 44106
(2) NASA-Lewis Research Center, 2100 Brookpark Road, Cleveland, OHIO 44135

Single crystals of beta-SiC were grown epitaxially on a {001} silicon substrate using the technique of Chemical Vapor Deposition (CVD). Using Transmission Electron Microscopy (TEM) as the primary means of investigation preliminary studies have been made on these crystals. Observations in plan view showed a large density of stacking faults in the SiC lying on the {111} planes . The Burgers vectors of dislocations bounding a number of the stacking faults were analysed and were all found to be of the Shockley type $a_o/6$ <112> where $a_o$ is the lattice parameter of the cubic silicon carbide. Most of the stacking faults proved to be intrinsic in nature although the results on a few of them were inconclusive. High Resolution Electron Microscopy (HREM) has also been used to look at cross-sectional specimens in order to study the Si/SiC interface. Preliminary results show that the interface is sharp with lattice fringes on both sides running to the interface, albeit with a high density of misfit dislocations. However, there may be small amorphous regions of nanometer size dispersed at the interface. There is also a large density of twins on the SiC side of the interface.

# STRUCTURAL AND ELECTRICAL CHARACTERIZATION OF BETA SILICON CARBIDE THIN FILMS*

J. S. Ryu and R. F. Davis
Department of Materials Engineering
North Carolina State University
Raleigh, NC 27696-7907

## ABSTRACT

Differential capacitance-voltage and Hall effects measurements as well as cross sectional transmission electron microscopy (XTEM) have been employed to characterize high purity, unintentionally doped beta SiC thin films grown on a chemically converted Si surface by chemical vapor deposition. XTEM of all SiC films grown in this manner reveals a 3 μm - 3.5 μm thick strained interface region having a high density of misfit dislocations. Although some of the dislocations thread to the surface, the overall density decreases rapidly beyond this near-interface region.

Capacitance-voltage measurements show that the carrier concentration in the SiC is uniform to a point which is approximately 4.5 μm from the Si/SiC interface. Additional profiling reveals that the active carrier concentration decreases continuously to this interface. This steady decrease is essentially an inverse function of the dislocation density. It is thus postulated that this decrease in concentration is caused by the gettering of impurities by the dislocations and/or pipe diffusion of these impurities to the Si/SiC interface.

The carrier concentration as a function of temperature has also been measured from 100K to 700K using the Van der Pauw method. Two distinct impurity energy levels have been noted in the SiC films as a function of temperature. The first level is at ~20 mev in the temperature range from 100K to 300K, while the second is at 50 mev in the range from 300K to 700K. The source of these impurity levels is also the reason for the n-type character in the undoped material. The possible sources for this phenomenon as well as the information noted above will be discussed at the conference.

*Sponsored by the Office of Naval Research Contract No. N00014-82-K-0182 P0005, Max Yoder, monitor.

# Electrical Properties of Cubic SiC Epitaxial Films

L.G. Matus and J.A. Powell

NASA Lewis Research Center

Cleveland, Ohio 44135

## ABSTRACT

Resistivity and Hall coefficient measurements of cubic SiC heteroepitaxially grown on silicon have been made using the van der Pauw technique. Room temperature measurements have been made on more than one hundred samples. A correlation was found for both resistivity and electron mobility as a function of electron carrier concentration. Measurements from 77 to 1000 K have also been made on selected samples. The measurement error associated with finite size electrical contacts was investigated by measuring cloverleaf-shaped samples. The influence of the silicon substrate on the measurements was also studied.

# Characterization, MOS/C-V Structures and Ohmic Contact Studies on beta-SiC Epilayers

L. Messick, C. R. Zeisse, D. I. Elder, M. J. Taylor
K. Moazed, D. P. Mullin, and H. H. Caspers

Electronic Material Sciences Division
Naval Ocean Systems Center
San Diego, CA 92152

Hall measurements were performed on an undoped beta-SiC epitaxial layer grown at NCSU on 100 Si both before and after removal of the substrate by etching which left a free standing 5 $\mu$m SiC layer. It was found that the substrate altered the Hall data by about 20%. Hall data at 300K show a carrier concentration of $6 \times 10^{16} cm^{-3}$ n-type and a mobility of 320 $cm^2 V^{-1} sec^{-1}$ and together with 77K data are consistent with a model of $6.4 \times 10^{16}$ uncompensated donors 50 meV below the conduction band edge. Auger electron spectroscopy results on these layers showed only Si and C below the surface while in addition oxygen was indicated at the surface. Optical transmission results on the free standing epilayer indicate the onset of strong absorption between 2.6 and 2.7 eV as compared with previously reported values for the energy band gap of beta-SiC ranging between 2.2 and 2.6 eV.

Device gate quality thermal oxides were grown on beta-SiC epitaxial layers by oxidation in dry $O_2$ at 1200°C. MOS structures were fabricated by evaporating Al dots on top of the oxide and ohmic contacts were made to the SiC layers by soldering with In. Capacitance versus voltage measurements performed on these structures yield curves exhibiting sharp transitions and very little hysteresis strongly suggesting that electrically stable FET devices could be fabricated on SiC using this thermal oxide as the gate dielectric. These results are in approximate agreement with the thermal oxidation results of Suyuki et al.[1]

The results of current ohmic contact studies on beta-SiC epilayers will also be reported.

Reference: [1] A. Suzuki, H. Ashida, N. Furui, K. Mameno and H. Matsunami, Japanese J. Appl. Phys., 21, 579 (1982).

# METAL CONTACTS TO β-SiC

D. E. Ioannou
Electrical Engineering Department
University of Maryland
College Park, MD 20742

and

N. A. Papanicolaou
Naval Research Laboratory
Washington, DC 20375

Metal contacts to β-SiC, both rectifying and ohmic, are expected to play an increasingly important role in the development of SiC material and device technology. In this report we present and compare results obtained from the study of such contacts, formed by the deposition of Au, Pt, W, and TiW. The deposition was done by sputtering and by resistive evaporation, and prior to metal deposition the surface was either chemically treated, or first oxidized and then chemically treated. Pt and W contacts obtained so far show ohmic behavior. TiW contacts show rectifying behavior, albeit they are rather poor rectifiers. Finally, Au contacts deposited by sputtering show ohmic behavior, whereas Au contacts deposited by resistive evaporation show good rectifier behavior.

# CONTINUATION STUDIES OF M/SiC INTERFACES-

# CARBIDE FORMERS

by

M.V. Zeller
College of Engineering
University of Notre Dame
Notre Dame, IN 46556

With β-SiC samples provided by NASA/Lewis Research, we have been investigating the chemical and electrical stability of various metals suitable for high temperature device applications. In our previous report, Ni and nichrome were examined as possible metallization materials. From these studies Ni was found to diffuse rapidly into SiC forming Ni silicide at temperatures above 500 C. Graphitic type carbon and Cr carbide, in the case of nichrome, were detected in the surface above the Ni silicide rich zone. In addition to diffusion, secondary phases consisting of a Ni rich material remained on the SiC surface after Ar ion etching through the metallization layer into the SiC substrate. Auger Electron Spectroscopy (AES) was the primary analytical tool employed to determine these chemical interactions.

During our current investigations, Ta, Cr, and Al have been deposited onto the SiC single crystals. A detectable amount of metal carbide formation occurs at the M/SiC interface upon deposition but does not react further upon thermal treatment up to 600 C for 5 hours. This report will summarize the data showing that the metal carbide formers tend to adhere well without diffusing into the SiC substrate.

# OXIDATION AND DRY ETCHING OF β-SiC SINGLE CRYSTAL THIN FILMS*

J. W. Palmour and R. F. Davis
Department of Materials Engineering
North Carolina State University
Raleigh, NC 27695-7907

And

T. M. Wallett and K. B. Bhasin
National Aeronautics and Space Administration
Lewis Research Center
Cleveland, OH 44135

## ABSTRACT

Silicon dioxide layers were thermally grown on single crystal (100) β-SiC at temperatures between 1273K and 1473K, in both wet and dry oxygen, and the activation energies of the linear and parabolic rate constants for each process were obtained. The parabolic rate constant for wet oxidation had an activation energy of 127 kcal/mol, which does not agree with the 18.3 kcal/mol for diffusion of $H_2O$ in $SiO_2$. Furthermore, if the carrier gas is switched from $O_2$ to Ar, an even larger temperature dependence is seen. These latter values of activation energy also differ from those reported in other studies using different $O_2$ flow conditions. Therefore, the activation energy of the parabolic rate constant for wet oxidation is proposed to be directly dependent on the amount of oxygen present as a carrier gas.

Scanning electron microscopy studies have revealed a mosaic-type surface for wet oxides, while dry oxides exhibited a moderately flat surface. Cross-sectional transmission electron microscopy has revealed that raised lines occur in a mosaic pattern where the wet atmosphere preferentially oxidizes dislocation bands present in the sample. There were also corresponding grooves in the SiC at the SiC-$SiO_2$ interface. This phenomenon does not occur during dry oxidation. It is proposed that the much higher solubility of $H_2O$ in $SiO_2$, as compared with that of $O_2$ ($10^3$ at 1273K), causes the flux of $H_2O$ to be much higher than the flux of $O_2$. Therefore, wet oxidation is not limited by $H_2O$ flux and is preferential; whereas, dry oxidation is limited by the oxygen flux and is non-preferential.

Dry etching of β-SiC single crystal thin films has been performed in $CF_4$ and $CF_4$+$O_2$ mixtures, in both the reactive ion etching (RIE) and plasma etching modes. The latter process yielded measurable etch rates, but produced a dark surface layer which appears, from the results of secondary ion mass spectrometry, to be redeposited SiC. The RIE samples had no redeposited layer, but Auger electron spectroscopy did reveal a C-rich surface. The optimal RIE conditions were obtained with 10 sccm of pure $CF_4$ at 40 mTorr and a power density of 0.548 W/cm$^2$, giving an etch rate of 23.3 nm/min. Neither the increase of temperature between 293K and 573K, nor the incremental addition of $O_2$ to $CF_4$ to 50%, produced any strong effect on the etch rates of SiC during RIE. Pictorial evidence of mesa structures produced by RIE of β-SiC films are also presented.

*Research sponsored by the Office of Naval Research under contract #N00014-82-K-0182 P0005, Max Yoder, monitor

# CHARACTERIZATION OF n- AND p-TYPE BETA-SiC MONOCRYSTALLINE THIN FILMS IN SITU DOPED VIA CHEMICAL VAPOR DEPOSITION PROCESS*

H. J. Kim and R. F. Davis
Department of Materials Engineering
North Carolina State University
Raleigh, NC 27695-7907

## ABSTRACT

The effect of electronically active dopants on the structure and the optical and electrical properties of beta-SiC monocrystalline thin films have been studied. The dopant elements used were phosphorus, nitrogen, boron and aluminum, which were introduced into the CVD reaction chamber during epitaxial growth of beta-SiC on Si substrates. The effects of these dopants on crystal quality were investigated and changes in absorption bands by IR and Raman spectroscopies. The atomic concentration and the carrier concentration of each of the dopants were measured as a function of the dopant partial pressure in the gas phase using SIMS and C-V techniques, respectively. From these results, the "conversion" factor, i.e. the degree of electronic activation, of each dopant was obtained. The structural changes caused by the heavy doping were also observed. Using electron diffraction, it was found that a high concentration of B resulted in the occurrence of twinning in beta-SiC and ultimately polycrystallization. From these structural changes, the solubility limits of B and P in beta-SiC were estimated.

* Sponsored by the Office of Naval Research Contract No. N00014-82-K-0182 P0005, Max Yoder, monitor.

# AMORPHIZATION AND RECRYSTALLIZATION PROCESSES IN MONOCRYSTALLINE BETA SILICON CARBIDE THIN FILMS*

John A. Edmond and Robert F. Davis
Department of Materials Engineering
North Carolina State University
Raleigh, NC 27695-7907

## ABSTRACT

Individual, as well as multiple doses of $^{27}Al^+$, $31P^+$, $^{28}Si^+$ and $^{12}C^+$ were implanted into (100) oriented $\beta$-SiC films. The critical energy required for the amorphization of $\beta$-SiC was determined using the TRIM 84 computer program for calculation of the damage energy profiles coupled with the results of RBS/ion channeling analyses. These calculations showed the energy necessary to amorphize $\beta$-SiC to be $\approx$ 16 eV/atom. In order to recrystallize the amorphized layers, rapid thermal annealing between 1973K and 2073K was employed. Characterization of the regrown layers was performed using cross-sectional TEM. Recrystallized layers were evaluated as a function of atomic concentration of each specie implanted. Examples of solid-phase-epitaxial (SPE) regrown layers containing: (1) precipitates and dislocation loops, (2) highly faulted-microtwinned regions, and (3) random crystallites have been observed. The results of this research as well as corresponding SIMS profiles showing the redistribution of aluminum and phosphorus upon annealing will be presented.

*Sponsored by the Office of Naval Research under Contract No. N00014-82-K-0182 P0005, Max Yoder, monitor.

# RAPID THERMAL ANNEALING OF B OR N IMPLANTED MONOCRYSTALLINE β-SiC THIN FILMS AND ITS EFFECT ON ELECTRICAL PROPERTIES AND DEVICE PERFORMANCE*

J. S. Ryu and R. F. Davis
Department of Materials Engineering
North Carolina State University
Raleigh, NC 27695-7907

## ABSTRACT

Dual ion implants of B or N have been produced in β-SiC thin films grown for microelectronic applications. In the B implanted films, cross-sectional TEM revealed a buried amorphous layer. Subsequent rapid thermal annealing at 1573K for 300s resulted in both solid phase epitaxy of the layer and the formation of B-containing precipitates in this region. Progressive increases in the annealing temperature to 1873K resulted in a reduction in the amount of second phase but the formation of larger precipitates as well as the appearance of dislocation loops in previously unannealed samples. SIMS profiles revealed a shift in the positions of the B peaks toward the sample surface as the annealing temperature was increased. A precipitate- and dislocation-free regrown layer was obtained at 2073K; however, most of the B had diffused out of the implanted region. A high resistivity p-type layer was produced after annealing at temperatures up to 1773K; however, the resistivity rapidly decreased as a result of annealing at higher temperatures. The material reverted to n-type character at $T \geq 1973K$ as a result of the out-diffusion of B.

No precipitates or defect substructure has been observed in N implanted and annealed samples. The resistivity of this n-type layer decreased with increasing annealing temperatures from 973K to 2073K. Furthermore, a p-n junction diode has been fabricated for the first time via N implantation into an in situ Al doped sample coupled with rapid thermal annealing (1573K, 300s). The results of these chemical, microstructural and electrical studies will be presented and correlated.

*Sponsored by the Office of Naval Research under Contract No. N00014-82-K-0182 P0005, Max Yoder, monitor.

# PHOTOLUMINESCENCE SPECTROSCOPY OF ION IMPLANTED CUBIC SiC GROWN BY CHEMICAL VAPOR DEPOSITION *

J.A. Freitas, Jr.** and S.G. Bishop
Naval Research Laboratory, Washington, D.C. 20375

J.A. Edmond, J. Ryu, and R.F. Davis
North Carolina State University, Raleigh, NC 27695

Low temperature (4.2-100K) photoluminescence spectroscopy has been carried out on thin films of CVD cubic SiC which were implanted with B, Al, or P ions and annealed for 5 min at temperatures up to 1800 C. In addition to nitrogen donor bound exciton PL spectra, the ion implanted samples exhibited the strong $D_1$ and $D_2$ bands (with zero phonon lines (ZPL) at 1.97 and 2.307 eV, respectively) reported previously[1,2] for implanted Lely-grown crystals of SiC and in some as-grown samples of the CVD films[3]. The rich spectral detail of these two defect bands as reported for the Lely material, i.e. ZPL splittings and one and two phonon spectra, is reproduced in every respect in the spectra obtained from the CVD films for each of the implantants studied. For annealing temperatures up to 1600 C the defect bands dominate the PL spectra; above 1600 C the $D_2$ band (tentatively attributed to carbon di-interstitials[2]) begins to anneal out and is reduced in intensity by a factor of ~100 in samples annealed at 1800 C. We have not observed donor-acceptor pair PL bands which can be attributed unambiguously to the implanted species. This is probably due to a combination of the dominance of the defect PL bands and to the low percentage activation of the implantants.

* Partially supported by an Office of Naval Research contract.
** Sachs-Freeman Associates, Landover, MD 20785

1. W.J. Choyke and L. Patrick, Phys. Rev. B 4, 1843 (1971).
2. L. Patrick and W.J. Choyke, J. Phys. Chem. Solids 34, 565 (1973).
3. J.A. Freitas, Jr., S.G. Bishop, A. Addamiano, P.H. Klein, H.J. Kim, and R. Davis, Proc. MRS Symposium on the Microscopic Identification of Electronic Defects in Semiconductors, San Francisco, CA, 15-18 April 1985, in press.

# ION-IMPLANTED PLANAR SiC p-n JUNCTION DIODES*

J. J. Kopanski, R. E. Avila and C. D. Fung
Department of Electrical Engineering and Applied Physics
Case Institute of Technology
Case Western Reserve University
Cleveland, Ohio 44106

The doping of n-type 3C SiC with B or Al has been studied. Multiple implants at energies from 30 to 200 KeV and doses from $10^{14}$ to $10^{15}$ $cm^{-2}$ were used. Annealing was carried out at 1365°C for 15 minutes in an Ar atmosphere. Both B and Al implanted layers exhibit p-type behavior revealed by the capacitance-voltage characteristics of the Hg-SiC Schottky diodes.

An array of p-n junction diodes was fabricated on an n-type 3C SiC layer deposited on the Si wafer. Ions were implanted on the SiC substrate through photolithographically defined windows in a thermally grown $SiO_2$ surface layer. Both contacts (Al for the p-type implanted regions and Au-Ta for the n-type substrate) were made to the front side of the substrate to form a planar diode structure. The n-type background concentration is $10^{17}$ $cm^{-3}$ and the multiple implantation condition is chosen to produce a surface region with approximately $10^{20}$ $cm^{-3}$ impurities and 0.4 micron thickness. Both the B and Al implanted diodes show good rectifying current-voltage (I-V) characteristics. Measurements of the I-V characteristics of the implanted diodes up to 400°C continue to show rectifying property. Detailed discussion on the cut-in voltage, breakdown voltage and reverse saturation current as a function of temperature will be presented.

* Work supported by NASA Lewis Research Center, Grants NAG 3-490 and NAG 3-389.

# INVERSION LAYER BEHAVIOR OF MOS STRUCTURES ON 3C SILICON CARBIDE*

R. E. Avila, J. J. Kopanski and C. D. Fung
Department of Electrical Engineering & Applied Physics
Case Institute of Technology
Case Western Reserve University
Cleveland, Ohio 44106

The field-induced surface-charge regions in 3C silicon carbide (SiC) are studied by 1 MHz capacitance-voltage (C-V) measurements. A double column mercury probe was used on oxidized SiC substrates to form metal-oxide-semiconductor (MOS) structures. These MOS structures were first qualified by using linear ramp and pulsed voltage biases to measure the doping profile, effective fixed oxide charge (4 to 7 x $10^{11}$ $cm^{-2}$) and interface trap density (4.3 x $10^{11}$ $cm^{-2}$ $ev^{-1}$ at 0.66 ev below the conduction band edge).

A unique feature of the inversion layer in the surface-charge region was revealed by C-V curves biased with a linear ramp at room temperature. In a forward measurement, where the bias voltage is swept from accumulation towards inversion, the capacitance curve enters deep depletion and then relaxes to its equilibrium value at inversion. This behavior is attributed to field ionization of interface traps followed by tunneling of electrons from the traps into the conduction band. In a reverse measurement, as the voltage is swept from inversion towards accumulation, the capacitance rises above the inversion level before coming to a plateau and subsequently joining the forward curve. This is explained by a stagnant inversion layer in response to the voltage ramp.

* Work supported by NASA Lewis Research Center, Grants NAG 3-490 and NAG 3-389.

# Cr/Ni Ohmic Contacts to n-Type β-SiC

G. Kelner and S. Binari

Several methods of making ohmic contacts to n-type β-SiC have been reported. In this work we report on Cr/Ni ohmic contacts.

The material used was β-SiC grown at NCSU by chemical vapor deposition on Si substrates and had a room temperature Hall mobility of 220 $cm^2/V\text{-}sec$ and a carrier concentration of $1.7 \times 10^{17}$ $cm^{-3}$. To prepare the surface of SiC for metal deposition the samples were polished with 0.1 μm diamond paste and cleaned with solvents. Multiple diameter dots, defined by photoresist lift-off, were deposited by thermal evaporation using Cr/Ni (300/1000Å). The I-V characteristics of the as-deposited contacts were non-linear. Sintering of the contacts in an Argon atmosphere at 960°C for 10 minutes produced ohmic contacts.

To determine the specific contact resistance, the silicon substrate was removed by etching in the mixture of $HNO_3$ and HF and a contact to the back side of the sample was deposited using Cr/Ni (300/1000Å). The samples were mounted on a metalized substrate with silver epoxy. Using the method of Cox and Strack[1], a specific contact resistance in the range of $3\text{-}9 \times 10^{-4}$ $\Omega\text{-}cm^2$ was determined.

---

1) R. H. Cox, H. Strack, Ohmic contacts for GaAs devices, Solid State Electronics, Vol. 10, pp 1213-1218.

# ELECTRICAL PROPERTIES OF REDUCED PRESSURE CVD OF SiC ON SILICON (100) AND (111) SUBSTRATES

M.G. Spencer, G.L. Harris, K. H. Jackson, G. Felton, K. Osborne, and K. Fekade
Howard University
Electrical Engineering Department
Washington, D.C. 20059

Paul Chu
Charles Evans Associates
San Mateo, California 94402

## ABSTRACT

The need for a high temperature semiconductors for use in harsh enivronments, such as, deep gas wells, gas turbine and piston engines has lead to an increasing interest is SiC. We will report on the electrical properties of reduced pressure CVD grown SiC. C-V, PL, SIMS, Auger, etc. techniques have been used to characterize the grown layers of SiC. The process has been used to produce 2 inch diameter SiC wafers with unintentionally n-type doping in the $10^{17}$ $cm^{-3}$ range with mobilities of several hundred $cm^2/V$-sec.

*Research Sponsored by: NASA-Lewis Research Center

POSTER SESSION PAPER



# AUGER SPECTROSCOPY OF REDUCED PRESSURE CHEMICAL VAPOR DEPOSITION OF SiC ON SILICON

K. H. Jackson, G. L. Harris, M. G. Spencer, V. Watt, and G. Felton

Solid State Electronics Group
Department of Electrical Engineering
Howard University
Washington D.C. 20059

## ABSTRACT

We report on the use of Auger electron spectroscopy, with sputter profiling, to optimise the growth, at reduced pressure of single crystal (beta) Silicon Carbide in the Howard University chemical vapor deposition reactor. Results will be presented on buffer layer growth by chemical conversion of the silicon substrate ( with $C_3H_8$ ), the effects of in situ HCL etching, and interface studies of oxidized SiC layers.

*Research Sponsored by: NASA-Lewis Research Center,and the Department of Defense University Research Instrumentation Program

REGISTRATION LIST
SILICON CARBIDE REVIEW MEETING
NOVEMBER 18-19, 1985



| NAME | TITLE / COMPANY / ADDRESS |
|---|---|
| RICARDO E. AVILA | GRAD STUDENT<br>CASE WESTERN RESERVE UNIV.<br>EEAP DEPT<br>CLEVELAND, OH 44106 |
| JOSEPH J. BELLINA, JR. | ASSOC. PROF.<br>SAINT MARY'S COLLEGE<br>DEPT OF CHEMISTRY & PHYSICS<br>NOTRE DAME, IN 46556 |
| DR. STEPHEN BISHOP | NAVAL RESEARCH LAB.<br>CODE 6822<br>WASHINGTON, DC 20375-5000 |
| JONATHAN CALDWELL | MGR, HUMAN RESOURCES<br>AVCO SPECIALTY MATERIALS<br>2 INDUSTRIAL AVENUE<br>LOWELL, MA 01740 |
| WILLIAM CARLOS | NAVAL RESEARCH LAB.<br>CODE 6816<br>WASHINGTON, DC 20375 |
| CALVIN CARTER | VISITING ASST PROF.<br>N. C. STATE UNIVERSITY<br>MATERIALS ENG-BOX 7907<br>RALEIGH, NC 27695-7907 |
| C. M. CHOREY | GRADUATE STUDENT<br>CASE WESTERN RESEVE UNIV.<br>DEPT METALLURGY & MAT. SCIENCE<br>CLEVELAND, OH 44106 |
| J. J. CHOYKE | ADJUNCT PROF<br>UNIV OF PITTSBURGH<br>DEPT OF PHYSICS<br>PITTSBURGH, PA 15260 |
| ROBERT F. DAVIS | PROF.<br>N. C. STATE UNIV.<br>BOX 7907 - MATERIALS ENG.<br>RALEIGH, NC 27695-7907 |
| JOHN A. EDMOND | GRAD RES ASST<br>N. C. STATE UNIV.<br>MATERIALS ENG-BOX 7907<br>RALEIGH, NC 27695-7907 |

| NAME | TITLE / COMPANY / ADDRESS |
|---|---|
| EDWARD HAUGLAND | NASA-LEWIS RES CTR.<br>21000 BROOKPARK RD.<br>CLEVELAND, OH 44135 |
| WILLIAM E. HOKE | SR SCIENTIST<br>RAYTHEON<br>131 SPRING ST.<br>LEXINGTON, MA 02173 |
| DR. JOHN HREN | NCSU-MATERIALS ENG.<br>BOX 7907<br>RALEIGH, NC 27695-7907 |
| C E. IOANNOU | ASST PROF.<br>UNIV OF MARYLAND<br>ELECTRICAL ENG DEPT<br>COLLEGE PARK, MD 20742 |
| DR. KEITH JACKSON | ASSISTANT PROFESSOR<br>HOWARD UNIVERSITY<br>2300 6TH ST. NW<br>WASHINGTON, DC 20059 |
| C LINA KELNER | NAVAL RESEARCH LAB.<br>WASHINGTON, DC 20375 |
| THOMAS A. KENNEDY | RES PHYSICIST<br>NAVAL RESEARCH LAB.<br>CODE 6871<br>WASHINGTON, DC 20375 |
| J. J. KIM | GRAD RES ASSOC.<br>N. C. S. U.<br>BOX 7907<br>RALEIGH, NC 27695-7907 |
| PHILIPP H. KLEIN | SECTION HEAD<br>US NAVAL RESEARCH LAB.<br>CODE 6822<br>WASHINGTON, DC 20375-5000 |
| JA-SHUANG KONG | RES ASST.<br>N. C. STATE UNIV.<br>MATERIALS ENG-BOX 7907<br>RALEIGH, NC 27695-7907 |

| NAME | TITLE / COMPANY / ADDRESS |
|---|---|
| JOSEPH KOPANSKI | ELECTRICAL ENG.<br>CASE WESTERN RESERVE UNIV.<br>10900 EVCLID AVE-ELECTRONICS<br>CLEVELAND, OH 44106 |
| 1 RIA KUCZMARSKI | ELECTRONICS ENG.<br>NASA-LEWIS RESEARCH CENTER<br>M.S. 77-1, 21000 BROOKPARK RD<br>CLEVELAND, OH 44135 |
| S. K. LAU | SOHIO ENGINEERED MATERIALS CO.<br>PO BOX 832<br>NIAGRA FALLS, NY 14302 |
| L WRENCE G. MATUS | RESEARCH SCIENTIST<br>NASA LEWIS RESERACH CTR.<br>MS 77-1/ 21000 BROOKPARK RD.<br>CLEVELAND, OH 44135 |
| JON M. MEESE | RESEARCH PHYSICIST<br>AMOCO RESEARCH CENTER<br>P O BOX 400, B-605, R-2510, 25<br>NAPERVILLE, IL 60566 |
| J. MESSICK | SCIENTIST<br>NAVAL OCEAN SYSTEMS CENTER<br>CODE 561<br>SAN DIEGO, CA 92152 |
| K. L. MOAZED | NAVAL OCEAN SYSTEMS CTR.<br>CODE 56<br>SAN DIEGO, CA 92152 |
| . ERIC NEEDHAM | DIR RES & DEV<br>ENGELHARD INDUSTRIES<br>RT 152, P. O. 1676A<br>PLAINVILLE, MA 02762 |
| PAUL E. R. NORDQUIST, JR. | RES CHEMIST<br>NAVAL RESEARCH LAB.<br>COE 6822-US NAVAL RES LAB.<br>WASHINGTON, DC 20375-5000 |
| RK OSBORNE | GRADUATE STUDENT<br>HOWARD UNIVERSITY<br>2300 6TH ST. NW<br>WASHINGTON, DC 20059 |

| NAME | TITLE / COMPANY / ADDRESS |
|---|---|
| JOHN W. PALMOUR | GRAD RES ASST.<br>N. C. STATE UNIV.<br>MATERIALS ENG-BOX 7907<br>RALEIGH, NC 27695-7907 |
| . JACQUES I. PANKOVE | SERI - UNIV COLORADO<br>2386 VASSAR DRIVE<br>BOULDER, CO 80303 |
| NICK PAPANICOLAOU | PHYSICIST<br>NRL CODE 6815<br>4555 OVERLOOK AVENUE<br>WASHINGTON, DC 20375 |
| M PARSONS | HUGHES RESEARCH LABORATORY<br>3011 MALIBU CANYON RD<br>MALIBU, CA 90265 |
| P. PIROUZ | ASSOC. PROF.<br>CASE WESTERN RESERVE UNIV.<br>METALLURGY & MATERIALS SCIENCE<br>CLEVELAND, OH 44106 |
| ANTHONY POWELL | PHYSICIST<br>NASA LEWIS RESEARCH CTR.<br>MS. 77-1/ 21000 BROOKPARK RD.<br>CLEVELAND, OH 44135 |
| JAE RYU | N. C. STATE UNIV.<br>MATERIALS ENG. BOX 7907<br>RALEIGH, NC 27695-7907 |
| RTIN V. SCHNEIDER | PH.D.<br>AT&T BELL LABS<br>P. O. BOX 400<br>HOLMDEL, NJ 07733 |
| GARY T. SENG | NASA-LEWIS RESEARCH CENTER<br>M.S. 77-1<br>CLEVELAND, OH 44135 |
| NG SHIH | DR.<br>US GOVERNMENT<br>1404 SOUTHWIND CT.<br>VIENNA, VA 22140 |

AD-A173 511 FUNDAMENTAL STUDIES AND DEVICE DEVELOPMENT IN BETA SILICON CARBIDE(U) NORTH CAROLINA STATE UNIV AT RALEIGH DEPT OF MATERIALS ENGINEERING R F DAVIS 31 JAN 85 2/2

UNCLASSIFIED 243-043-008 N00014-82-K-0182 F/G 20/12 NL

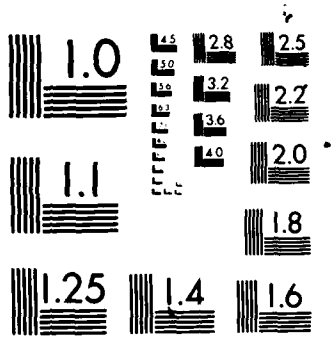

| NAME | TITLE / COMPANY / ADDRESS |
|---|---|
| KEN SLEGER | NAVAL RESEARCH LAB.<br>CODE 6811<br>WASHINGTON, DC 20375 |
| ARTER STINESPRING | AERODYNE RESEARCH<br>45 MANNING ROAD<br>BILLERICA, MA 01821 |
| SAM C. WEAVER | PRESIDENT<br>PHOENIX INTERNATIONAL<br>P. O. BOX 23556<br>KNOXVILLE, TN 37933 |
| . HERBERT WILL | ENGINEER<br>NASA<br>21000 BROOKPARK RD, M.S. 7701<br>CLEVELAND, OH 44135 |
| MAX YODER | OFFICE OF NAVAL RESEARCH<br>ELECTRONICS PROGRAM-CODE 1114<br>ARLINGTON, VA 22217 |
| RY V. ZELLER, PH.D. | DIR-SURFACE SCI LAB<br>UNIV OF NOTRE DAME<br>COLLEGE OF ENGINEERING<br>NOTRE DAME, IN 46556 |
| DAVID ZOOK | HONEYWELL<br>10701 LYNDALE AVENUE SOUTH<br>BLOOMINGTON, MN 55420 |

# APPENDIX II

## DISTRIBUTION LIST - ANNUAL LETTERS REPORT

Contract Number N00014-82-K-0182 P0005

| Address | No. of Copies |
|---|---|
| Mr. Max Yoder<br>Office of Naval Research<br>Electronics Program - Code 1114<br>800 North Quincy Street<br>Arlington, VA 22217 | 2 |
| Mr. Michael Karp<br>ONR Resident Representative<br>Georgia Institute of Technology<br>214 O'Keefe Building<br>Atlanta, GA 30332 | 1 |
| Director, Naval Research Laboratory<br>ATTN: Code 2627<br>Washington, DC 20375 | 6 |
| Defense Technical Information Center<br>Bldg. 5<br>Cameron Station<br>Alexandria, VA 22314 | 14 |
| Dr. G. L. Harris<br>Electrical Engineering<br>Howard University<br>Washington, D.C. 20059 | 1 |
| Dr. J. Anthony Powell<br>NASA Lewis<br>2100 Brookpark Road<br>Cleveland, OH 44135 | 1 |
| Dr. Ray Kaplan<br>Code 6834<br>Department of the Navy<br>Naval Research Laboratory<br>Washington, D.C. 20375 | 1 |
| Dr. P. Klein<br>Naval Research Laboratory<br>Code 6820<br>Washington, D.C. 20375 | 1 |

Distribution List (Con't)

| Address | No. of Copies |
|---|---|
| Dr. Steve Bishop<br>Naval Research Laboratory<br>Code 6870<br>Washington, D.C. 20375 | 1 |
| Dr. J. Parsons<br>Hughes Research Laboratory<br>3011 Malibu Canyon Road<br>Malibu, CA 90265 | 1 |


DATE
FILMED
2-8